

UTRECHT UNIVERSITY

MASTER'S THESIS

Non-unitary Isometric Quantum Mechanical Time Evolution in Cosmology

Author:
Konstantinos MANOS

Supervisor:
Dr. Stefan VANDOREN

*A thesis submitted in fulfillment of the requirements
for the Master's degree in - Theoretical Physics
in the*

Graduate School of Natural Sciences of Utrecht University

May 22, 2023

UTRECHT UNIVERSITY

*Abstract*Utrecht University
Graduate School of Natural Sciences

-

Non-unitary Isometric Quantum Mechanical Time Evolution in Cosmology

by Konstantinos MANOS

The past and the future are tightly linked in conventional quantum mechanics by unitary evolution. Perhaps too tightly in an expanding spacetime. A tweak to the theory could let quantum possibilities increase as space expands. The tweak corresponds in replacing unitary quantum mechanical time evolution with a non-unitary isometric one. Cosmological expansion points into this direction since new degrees of freedom arise during the time evolution. We motivate this hypothesis from two different approaches, all in $1 + 1$ spacetime dimensions: (i) the net entanglement entropy produced by toy and cosmological models is increasing in time, (ii) the Lorentzian path integral for a finite elements latticization gives non-unitary isometric time evolution for a scalar and possibly a fermionic field.

Acknowledgements

I would like to express my gratitude to my supervisor, Stefan Vandoren, who not only guided me throughout this thesis but most importantly kept me going with his constant enthusiasm. I would also like to thank my friends and family who supported me during the compilation of this project.

Contents

| | |
|---------------------------------------------------------|------------|
| Abstract | iii |
| Acknowledgements | v |
| 1 Introduction | 1 |
| 2 Preliminaries | 5 |
| 2.1 Path Integrals and Quantum states | 5 |
| 2.1.1 Transition Amplitudes | 5 |
| 2.1.2 Wavefunctions | 6 |
| 2.1.3 Cutting the Path Integral | 6 |
| 2.1.4 Euclidean vs. Lorentzian | 6 |
| 2.1.5 The Ground State | 7 |
| 2.1.6 Glueing Path Integrals | 7 |
| 2.1.7 Density Matrices | 8 |
| 2.1.8 Thermal Partition Function | 8 |
| 2.2 Basics of Entanglement Entropy | 9 |
| 2.3 Entanglement Entropy in $2D$ CFT | 11 |
| 2.3.1 A Replica Approach | 11 |
| 2.3.2 Twist Fields | 12 |
| 2.3.3 Mapping the Riemann surface to the complex plane | 14 |
| 2.4 Discrete Time Mechanics | 15 |
| 2.4.1 Classical Mechanics in the Continuum and Discrete | 16 |
| The Hamilton-Jacobi Equation | 17 |
| 2.4.2 Quantum Mechanical Propagators in the Continuum | 17 |
| 2.4.3 Quantum Mechanical Propagators in the Discrete | 18 |
| 3 Moving Mirrors | 21 |
| 3.1 2D Minkowski Space | 21 |
| 3.2 Quantum Field Theory in 2D Minkowski Spacetime | 24 |
| 3.2.1 Bogolubov Transformation | 26 |
| 3.2.2 Vacuum Coordinates | 29 |
| 3.3 Toy-model of Cosmological Expansion | 29 |
| 3.3.1 Entanglement Entropy in Moving Mirrors | 31 |
| 3.3.2 Direct Analysis of Massless Free Scalar CFT | 34 |
| 3.3.3 Receding Mirror | 36 |
| 4 Cosmology | 43 |
| 4.1 Entanglement Entropy in Curved Spacetime | 43 |
| 4.2 Closed 1+1 Cosmology | 45 |
| 4.3 de Sitter Space | 46 |
| 4.3.1 Basics | 46 |
| 4.3.2 Global Coordinates | 47 |

| | | |
|----------|-------------------------------------------------------------|------------|
| 4.3.3 | Conformal Coordinates | 48 |
| 4.3.4 | Flat Slicing Coordinates | 49 |
| 4.3.5 | Entanglement Entropy in de Sitter | 50 |
| 5 | Lattice Discretization of Spacetime | 53 |
| 5.1 | Finite Difference Method | 53 |
| 5.2 | Finite Element Method | 56 |
| 5.2.1 | Analysis Approach to FEM | 56 |
| 5.2.2 | Geometric approach to FEM | 66 |
| 5.2.3 | Analysis vs Geometric | 68 |
| 6 | FEM in Scalar Field Theory | 69 |
| 6.1 | Classical Considerations | 69 |
| 6.1.1 | Analysis Approach to Scalar FEM on a Triangle | 69 |
| 6.1.2 | Geometric Approach to Scalar FEM on a Triangle | 70 |
| 6.2 | Quantum Considerations | 71 |
| 6.2.1 | Function Spaces Accommodating the $i\epsilon$ -prescription | 74 |
| 6.3 | Nonunitary Isometric Quantum Evolution | 76 |
| 7 | FEM in Fermionic Field Theory | 81 |
| 7.1 | Classical Considerations | 81 |
| 7.1.1 | Analysis Approach to Fermionic FEM on a Triangle | 81 |
| 7.1.2 | Geometric Approach to Fermionic FEM on a Triangle | 83 |
| 7.2 | Quantum Considerations and Isometric Evolution | 85 |
| 7.3 | Discussion | 88 |
| 8 | Closing Remarks and Future Endeavours | 93 |
| 8.1 | FEM in the Moving Mirror | 93 |
| 8.2 | The Physical Subspace and the Recovery of Unitarity | 96 |
| 8.2.1 | Comments | 96 |
| 8.3 | Apparent Degrees of Freedom (Fact or Fiction?) | 98 |
| 8.3.1 | Quantum Error Correction | 98 |
| Comments | | 100 |
| 8.4 | Closing Statement | 100 |
| A | Introduction to Conformal Field Theory | 101 |
| A.1 | Conformal Algebra in 2-dimensional Euclidean Space | 101 |
| A.2 | Constraints of Conformal Invariance in 2-dimensions | 102 |
| A.3 | The Stress-Energy Tensor | 103 |
| A.4 | Quantum Aspects | 104 |
| A.5 | Conformal Ward Identities | 105 |
| A.6 | The Central Charge | 106 |
| | Bibliography | 109 |

List of Figures

| | | |
|-----|---------------------------------------------------------------------------------------------------------------------------------------------------------------------------------------------------------------------------------------------------------------------------------------------------------------------------------------------------------------------------------------------------------------------------------------------------------------|----|
| 2.1 | Lattice quantum system divided by the boundary ∂A into subsystems A (shaded area) and B (unshaded area). | 10 |
| 2.2 | QFT on a $\mathbb{R} \times N$ manifold at fixed time $t = t_0$. The N manifold is divided by the boundary ∂A into submanifolds A and B | 10 |
| 2.3 | (a) The path integral representation of the reduced density matrix $[\rho_A]_{\phi_+, \phi_-}$. (b) The n -sheeted Riemann surface \mathcal{R}_n (for $n = 3$). | 12 |
| 2.4 | The effect of twist fields on other local fields. | 14 |
| 2.5 | $w \rightarrow \zeta = (w - u)/(w - v)$ maps the branch points $[u, v]$ to $(0, \infty)$. This is uniformized by the mapping $\zeta \rightarrow z = \zeta^{1/n}$ | 14 |
| 3.1 | A mirror following a trajectory suited for cosmological expansion. | 21 |
| 3.2 | The conformal diagram of Minkowski spacetime where the red and blue curves being the constant t -slices and x -slices. | 23 |
| 3.3 | Minkowski spacetime with a static mirror located at $x = 0$ | 30 |
| 3.4 | Caption | 30 |
| 3.5 | The green field modes reflect upon the blue mirror trajectory and arrive at the region $[\tilde{t}_1^-, \tilde{t}_2^-]$. We illustrated only the boundary green modes of the interval, there are also in-between modes that arrive at $[\tilde{t}_1^-, \tilde{t}_2^-]$. The quantum state on the interval $[\tilde{t}_1^-, \tilde{t}_2^-]$ is equivalent to a state defined upon the red spacelike interval. | 32 |
| 3.6 | Every mode that reflects upon the mirror and arrives at $(-\infty, \tilde{t}^-]$ belongs to the quantum state on the semi-infinite interval. We illustrated with green colour only the last mode that belongs in this state. Again, the quantum state is equally defined in any semi-infinite spacelike interval with one point being the intersection point with the right green moving mode and the other point being the right spacelike infinity. | 34 |
| 3.7 | Mirror trajectory depicted by the blue curve for $T_H = 1/2\pi$ and $L = 1$ | 37 |
| 4.1 | The spacelike slice Σ is chosen to be at $t = 0$. The state upon $[P_2, P_1]$ is equivalent to the state on $[\tilde{t}_1^-, \tilde{t}_2^-] \cup [\tilde{t}_2^+, \tilde{t}_1^+]$, since these two are causally connected with left and right null rays, which are depicted with green colour. | 44 |
| 4.2 | Expanding closed $1 + 1$ cosmology. Our system A is defined upon a time-slice as the upper half of the circle which is divided at $\tilde{\sigma} = 0, \pi$. The complementary is denoted by B | 46 |
| 4.3 | dS_2 viewed as a hyperbola in $R^{1,2}$. The cross sections are S^1 's. | 47 |
| 4.4 | Penrose diagram for dS_2 <u>Note</u> : Later we will use only half of the Penrose diagram of dS_2 for a better clarity of the illustrations. | 49 |
| 4.5 | Blue curves are constant t -slices and red curves are constant x -slices. We used half of the Penrose diagram of dS_2 , the other half is just a mirroring with respect to the left axis of this diagram. | 50 |
| 4.6 | The region A consists of the points upon the t -slice which belong between the two red intersections with the $x_{1,2}$ -slice. | 51 |

| | | |
|-----|---------------------------------------------------------------------------------------------------------------------------------------------------------------------------------------------------------------------------------------------------------------------------------------------------------------------------------------------------------------------------------------------------------------------------------------|-----|
| 5.1 | FDM discretization of spacetime. The figure was taken from [19]. | 54 |
| 5.2 | Saw tooth converging to the diagonal of a unit square, but not converging into its length. | 55 |
| 5.3 | Plot of a $\phi(t)$ in $CPL_a([0, T])$ | 59 |
| 5.4 | Affine transformation A from the 'standard' triangle to a random triangle. | 65 |
| 5.5 | A triangular FEM lattice regularization of a $1 + 1$ scalar field in a spacetime with a moving boundary. The moving boundary is piecewise-linear-approximated by the lattice discretization, which is continuous for any cutoff scale; this is in contrast to the FDM saw-tooth approximation of Fig 5.1. Note that the number of lattice sites on each Cauchy slice is increasing with time. The figure was taken from [19]. | 66 |
| 6.1 | The triangle $\tilde{\Delta}$ in R^2 with vertices $(t, x) = (0, 0), (\delta t, -\delta x)$ and $(\delta t, \delta x)$. We have labeled the vertices by their corresponding field values ϕ_0, ϕ_1, ϕ_2 | 69 |
| 6.2 | The triangle $\tilde{\Delta}$ parametrized by $\vec{l}_{10}, \vec{l}_{20}$ | 71 |
| 7.1 | The triangle $\tilde{\Delta}$ in R^2 with vertices $(t, x) = (0, 0), (\delta t, -\delta x)$ and $(\delta t, \delta x)$. We have labeled the vertices by their corresponding field values $\Psi_0 - \Psi_0^\dagger, \Psi_1 - \Psi_1^\dagger, \Psi_2 - \Psi_2^\dagger$ | 82 |
| 7.2 | The triangle $\tilde{\Delta}$ parametrized by $\vec{l}_{10}, \vec{l}_{20}$ with the addition of the vector \vec{l}_{21} | 84 |
| 8.1 | A triangulation of \mathbb{R}^2 for $t \geq 0$, built out of isosceles triangles. The figure was taken from [19]. | 94 |
| 8.2 | Triangulation with modified triangles. The figure was taken from [19]. | 95 |
| A.1 | Map of the cylinder to the plane | 104 |
| A.2 | Caption | 106 |

List of Tables

| | |
|-----------------------------------------------------------------------------------------------|----|
| 5.1 Comparison between the functional analysis approach of FEM and the geometric one. | 68 |
|-----------------------------------------------------------------------------------------------|----|

List of Abbreviations

| | |
|------------|--------------------------|
| QFT | Quantum Field Theory |
| CFT | Conformal Field Theory |
| QCD | Quantum Chromo Dynamics |
| FDM | Finite Difference Method |
| FEM | Finite Element Method |
| sec. | section |
| ssec. | subsection |
| sssec. | subsubsection |

Conventions

The metric that is being used throughout the thesis is the following,

$$\eta_{\mu\nu} = \begin{bmatrix} -1 & 0 \\ 0 & 1 \end{bmatrix}.$$

The Dirac gamma matrices that are being used in the thesis are the following,

$$\gamma^0 = \begin{bmatrix} 1 & 0 \\ 0 & -1 \end{bmatrix}, \quad \gamma^1 = \begin{bmatrix} 0 & 1 \\ -1 & 0 \end{bmatrix}.$$

Dedicated to my father

Chapter 1

Introduction

A jarring divide cleaves modern physics. On one side lies quantum theory, which portrays subatomic particles as probabilistic waves. On the other lies general relativity, Einstein's theory that space and time can bend, causing gravity. The quest for reconciliation of both quantum mechanics and gravity is running up against thorny paradoxes for over 90 years.

Hints are mounting that at least part of the problem lies with a principle at the center of quantum mechanics. Unitarity, the main principle of quantum mechanics, says that probabilities are conserved. When particles interact, the probability of all possible outcomes must sum to 100%. Unitarity severely limits how subatomic particles might evolve from moment to moment. It also ensures that change is a two-way street: any imaginable event at the quantum scale can be undone, at least on paper. It is a very restrictive condition, even though it might seem a little bit trivial at first glance.

Unitarity in quantum gravity and even in black holes is a very open question. In both situations problems arise when predictions of general relativity and quantum mechanics are combined. In the 1970s, Stephen Hawking applied the rules of quantum mechanics to black holes and found that an isolated black hole would emit a form of radiation called Hawking radiation [37]. This led to the famous black hole information paradox, when one considers a process in which a black hole is formed through a physical process and then evaporates away entirely through Hawking radiation. Hawking's calculation suggests that the final state of radiation would retain information only about the total mass, electric charge and angular momentum of the initial state. Since many different states can have the same mass, charge and angular momentum this suggests that many initial physical states could evolve into the same final state. Therefore, information about the details of the initial state would be permanently lost. This violates unitarity since, the evolution of the state is determined by a unitary operator, and unitarity implies that the state at any instant of time can be used to determine the state either in the past or the future. A similar paradox arises in cosmology, the main problem is that the universe is expanding. This expansion is well described by general relativity. But it means that the future of the cosmos looks totally different from its past, while unitarity demands a tidy symmetry between past and future on the quantum level.

The expansion of the cosmos and the fact that there are no degrees of freedom on length scales shorter than the Planck scale suggest that the dimension of the Hilbert space that describe the quantum states of subatomic particles grows with time. This led Andrew Strominger and Jordan Cotler to propose the radical idea that a more relaxed principle called isometry can accommodate an expanding universe while still satisfying the stringent requirements of unitarity [19].

Isometries are maps from a smaller to a larger Hilbert space which preserve the inner product between any two states. If the Hilbert spaces have the same size, the

isometry is unitary. In an expanding universe they allow new degrees of freedom to be added without affecting inner products. While the expanding universe is a perfectly valid solution to the equations of general relativity, its growth troubles quantum mechanics, by presenting particles with an expanding variety of options for where to be and how to behave. With the help of isometries, the above intuitive statement which is equivalent to "new degrees of freedom appear in their ground state" [57, 60] gets mathematical precision. Adding to that isometries also specify the quantum correlations of the new degrees of freedom with the preexisting ones.

We motivate this hypothesis from two different approaches, all in $1 + 1$ dimensions: a continuum analysis of entanglement entropy using toy and cosmological models, and a latticization of quantum field theory on an expanding geometry using the finite elements method. While in our closing remarks we mention the interplay of isometries in encodings of quantum information theory [3, 56] and their fundamental role in physical law.

The first example is a toy model that we will use is a $1 + 1$ free field theory with a moving mirror [30, 1, 2]. The mirror is initially at rest, and then uniformly accelerates from infinity. After that, the mirror stops accelerating and remains at a final receding velocity. The problem is analytically soluble and in order to examine the Hilbert space evolution we mainly use entanglement entropy. The entanglement entropy of the outgoing radiation rises thermally during acceleration and then remains at a nonzero constant. An observer at infinity with any finite UV cutoff will never see the thermal radiation purified no matter how long they wait. This is due to the fact that some super-cutoff incoming modes are redshifted below the cutoff by the receding mirror before arriving at the observer. Hence there is an increase in the amount of modes that contribute to entanglement entropy before and after acceleration. Because new effective degrees of freedom have emerged, the description of time evolution is isometric and non-unitary. This continuum example illustrates the fact that non-unitary isometries arise no matter how high we place the cutoff.

After that example, we examine entanglement entropy in continuum closed expanding cosmologies [27]. Basically, we show that the same principles hold true for de Sitter spacetime in $1 + 1$ -dimensions. That is, new effective degrees of freedom are being added with cosmological expansion indicating the need of non-unitary isometric time evolution.

The second approach is the lattice discretization of spacetime in which a finite UV cutoff manifests. Our goal is to formulate and study the finite elements method (FEM) [24, 9] in a Lorentzian setting of a $1 + 1$ -dimensional quantum field theory (QFT). We would try to incorporate two separate field theories, one with a free massless scalar field and a corresponding one with a fermion. The part with FEM and fermions corresponds to our own research that came to be problematic. A discussion about the nourishment of the problems that arose will follow. Many lattice realizations of QFT in an expanding geometry necessitate adding lattice points, and a unitary transformation between time slices is clearly impossible. We construct the Lorentzian FEM path integral and show that time evolution between subsequent slices is an isometry. This demonstrates that discrete path integral methods are not restricted to unitary systems and naturally describe the more general isometries of interest to us here. There have been related work connecting the canonical and path integral quantization setting in [28, 43, 23].

The thesis is organized as follows. In chapter 2 we included the preliminaries that are needed in order to achieve a self-contained manuscript. In chapter 3 we examine the properties of a receding mirror boundary in $1 + 1$ -dimensional conformal field theory (CFT). In chapter 4 we study the entanglement of $1 + 1$ -dimensional

conformal field theory (CFT) in closed expanding cosmological models. In chapter 5 we review the finite elements method (FEM) by using two approaches: one based on functional analysis and another based on geometry. We also explain its necessity for discretizing classical equations of motion for fields curved or time-dependent backgrounds. In chapter 6 we perform a Lorentzian path integral quantization for a massless scalar field in $1 + 1$ -dimensions and show that time evolution is isometric. In chapter 7 which contains our own independent research, we again perform a Lorentzian path integral quantization but this time for a fermionic field in $1 + 1$ -dimensions and discuss the troublesome nature of the finite element method (FEM) and fermions. Chapter 8 contains some closing comments for our work and some proposals for further research, while the connection between quantum error correction schemes and their role in physical law is being proposed. The appendix A contains a review of basic facts of conformal field theory (CFT) that were needed in the calculation of entanglement entropy of moving mirrors.

Chapter 2

Preliminaries

Before diving into the main thesis we review basic facts that will be useful in understanding the details of our work and make the thesis relatively self-contained. The organization of this chapter is as follows. In sec. 2.1 we review quantum states in the path integral formulation. In sec. 2.2 and 2.3 we provide a summary of the basics of entanglement entropy in discrete and continuum field theories. Lastly, in sec. 2.4 we review the classical and quantum formalism for the evolution operator in discrete time mechanics.

2.1 Path Integrals and Quantum states

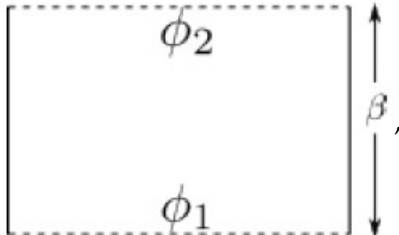
In this section we will explain the relationship between path integrals and states in quantum field theory [36]. This material is not normally covered in detail in QFT courses or the author of this thesis was not that familiar with it. It will turn out being extremely useful for moving mirrors in chapter 3, since it provides a pictorial representation of path integrals and quantum states.

2.1.1 Transition Amplitudes

Path integrals define transition amplitudes. A Euclidean path integral defines a transition amplitude under evolution by the operator $e^{-\beta H}$

$$\langle \phi_2 | e^{-\beta H} | \phi_1 \rangle = \int_{\phi(\tau=0)=\phi_1}^{\phi(\tau=\beta)=\phi_2} D\phi e^{-S_E[\phi]}. \quad (2.1)$$

This involves a split into space and time; $\phi_{1,2}$ is a boundary condition that specifies data at a fixed time. If space is a line in $2D$, then we depict this by

$$\langle \phi_2 | e^{-\beta H} | \phi_1 \rangle = \left[\begin{array}{c} \phi_2 \\ \phi_1 \end{array} \right]_{\beta}, \quad (2.2)$$


meaning it is a Euclidean path integral over an infinite line, with the boundary conditions shown and the interval has length β .

2.1.2 Wavefunctions

The transition amplitude defines the wavefunction, in the Schrödinger picture. The wavefunction for the state

$$|\Psi\rangle = |\phi_1(\tau)\rangle = e^{-\tau H}|\phi_1\rangle, \quad (2.3)$$

is the overlap

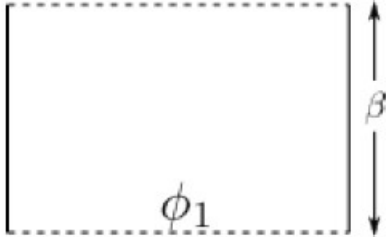
$$\Psi[\phi_2] \equiv \langle\phi_2|\Psi\rangle. \quad (2.4)$$

2.1.3 Cutting the Path Integral

To define the transition amplitude, we specified data on two cuts, at $\tau = 0$ and $\tau = \beta$. We can formally think of a path integral with one set of boundary conditions and one open cut as a quantum state. That is, the state

$$|\Psi\rangle = e^{-\beta H}|\phi_1\rangle, \quad (2.5)$$

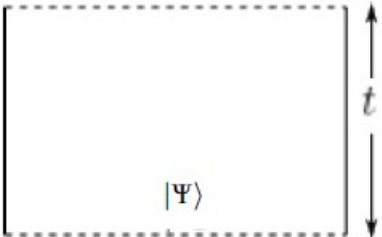
is the path integral

$$|\Psi\rangle = \int_{\phi(\tau=0)=\phi_1}^{\phi(\tau=\beta)=??} D\phi e^{\mathcal{S}[\phi]} = \boxed{\phi_1} \quad \beta. \quad (2.6)$$


It is a functional $|\Psi\rangle$ that turns field data $\langle\phi_2|$ into complex numbers $\langle\phi_2|\Psi\rangle$.

2.1.4 Euclidean vs. Lorentzian

States are defined on a spatial surface and do not care about Lorentzian vs Euclidean. The state $|\Psi\rangle$, defined above by a Euclidean path integral, is a state in the Hilbert space of the Lorentzian theory. It is defined at a particular Lorentzian time, call it $t = 0$. It can be evolved forward in Lorentzian time by acting with the operator e^{-iHt} , or equivalently by performing the Lorentzian path integral

$$|\Psi(t)\rangle = e^{-iHt}|\Psi\rangle = \boxed{|\Psi\rangle} \quad t. \quad (2.7)$$


Remark: To be more precise, states are defined upon Cauchy surfaces [64]. A Cauchy surface intuitively is a slice at a fixed time, thus points on the Cauchy surface are related spacelike i.e. there are not causally connected. Think of Cauchy surface as signifying an instant of time. Physics can be predicted to the future or (retroacted to the) past from data prescribed on the Cauchy surface. In the case of a

massless theory, which is the main theory of this thesis, null surfaces are Cauchy surfaces since particles travel only in null trajectories. A state that is defined upon a spacelike surface is equally well defined upon a null surface with the requirement that these two are causally connected.

2.1.5 The Ground State

Evolution in Euclidean time damps excitations. Suppose we start in some state $|\Psi\rangle$ and expand in energy eigenstates

$$|\Psi\rangle = \sum_n \psi_n |n\rangle, \quad H|n\rangle = E_n |n\rangle. \quad (2.8)$$

By evolving over a long Euclidean time we can project onto the lowest energy state,

$$e^{-\tau H} |\Psi\rangle \approx e^{-\tau E_0} \psi_0 |0\rangle, \quad (\tau \rightarrow \infty). \quad (2.9)$$


It follows that we can define the (unnormalized) ground state by doing a path integral that extends all the way to infinity in one direction. In 2D spacetime the ground state in the line is produced by the Euclidean path integral

$$|0\rangle = \int_{-\infty}^{\infty} \mathcal{D}\phi e^{-S_E[\phi]} \quad (2.10)$$


It is a path integral on the semi-infinite plane, with an open cut at the edge.

2.1.6 Glueing Path Integrals

Path integrals with cuts can be glued together to make transition amplitudes. On a 2D theory the vacuum-to-vacuum amplitude is

$$\langle 0|0\rangle = \int \mathcal{D}\phi e^{-S_E[\phi]} = \int_{-\infty}^{\infty} \mathcal{D}\phi e^{-S_E[\phi]} \quad (2.11)$$


The lower half-plane produces $|0\rangle$, the upper half-plane produces $\langle 0|$, and glueing them together along the cuts at $\tau = 0$ produces the transition amplitude. One way to see the glueing is to insert the identity

$$\langle 0|0\rangle = \sum_{\phi_1} \langle 0|\phi_1\rangle \langle \phi_1|0\rangle. \quad (2.12)$$

The first term is a path integral on the upper half plane; the second term is a path integral on the lower half plane; and summing over all possible boundary conditions ϕ_1 in the middle just says that fields should be continuous across $\tau = 0$ and therefore glues the half-planes together.

2.1.7 Density Matrices

A density matrix is an operator; it takes a bra and a ket, and produces a complex number. Thus any path integral with two open cuts defines a density matrix. For example, the density matrix $\rho = e^{-\beta H}$, for a $2D$ theory on a line, is formally the doubly-cut Euclidean path integral

$$\rho \equiv e^{-\beta H} = \left[\begin{array}{c} \text{---} \\ \text{---} \\ \text{---} \\ \text{---} \end{array} \right] \beta \quad (2.13)$$

The matrix elements $\langle \phi_2 | \rho | \phi_1 \rangle$ are computed by the path integral with boundary conditions $\phi_{1,2}$ on the cuts.

2.1.8 Thermal Partition Function

The density matrix $\rho = e^{-\beta H}$ is the density matrix in a thermal ensemble at temperature $T = 1/\beta$. The thermal partition function is

$$Z(\beta) = \text{tr} e^{-\beta H}. \quad (2.14)$$

This can be represented by a Euclidean path integral as follows

$$\begin{aligned} Z(\beta) &= \text{tr} e^{-\beta H} \\ &= \sum_{\phi_1} \langle \phi_1 | e^{-\beta H} | \phi_1 \rangle \\ &= \sum_{\phi_1} \left[\begin{array}{c} \phi_1 \\ \text{---} \\ \phi_1 \end{array} \right] \beta \end{aligned} \quad (2.15)$$

By summing over ϕ_1 we are really just imposing periodic boundary conditions on the plane. This glues together the two lines, producing an infinitely long cylinder of

period β

$$Z(\beta) = \text{[Diagram of a cylinder with a vertical arrow labeled } \beta \text{ on its right side]} \quad (2.16)$$

The trace 'glues together' parts of the Euclidean manifold that computes ρ .

2.2 Basics of Entanglement Entropy

In this section we will review basic elements of entanglement entropy which are based on the lectures notes of M. Rangamani and T. Takayanagi [58].

In statistical mechanics one averages over physically distinct states of a system which have common values of a macroscopic state variables. Many microscopically different states look alike macroscopically. Entropy is a precise measure of this lack of resolution.

In quantum mechanics there is an additional source of entropy. This comes from the fact that an observer has access only to a partial set of observables.

Consider a quantum mechanical system with many degrees of freedom such as arbitrary lattice model (later on we will include QFTs and CFTs). The total quantum system is described by the pure ground state $|\Psi\rangle$. Then, the density matrix is that of a pure state

$$\rho_{tot} = |\Psi\rangle\langle\Psi| \quad (2.17)$$

The von Neumann entropy of a quantum state is defined as

$$S = -\text{tr} \rho \log \rho \quad (2.18)$$

which is clearly zero for the total system $S = -\text{tr} \rho_{tot} \log \rho_{tot} = 0$.

Next, we divide the total system into two subsystems A and B , as shown in Fig. 2.1. Note that physically we do not do anything to the system and the cutting procedure is an imaginary process. We could hypothesize that A is the accessible part of the universe for an observer and B the inaccessible one. The total Hilbert space can be written as a direct product $\mathcal{H}_{tot} = \mathcal{H}_A \otimes \mathcal{H}_B$ ¹. The observer who has access only to the subsystem A will feel as if the total system is described by the reduced density matrix ρ_A

$$\rho_A = \text{tr}_B \rho_{tot} \quad (2.19)$$

where trace is taken only over the Hilbert space \mathcal{H}_B .

Now we define the entanglement entropy of the subsystem A as the von Neumann entropy of the reduced density matrix ρ_A

$$S = -\text{tr} \rho_A \log \rho_A \quad (2.20)$$

This quantity provides us with a convenient way to measure how quantum information is stored in a given state $|\Psi\rangle$. It counts the number of entangled bits between A and B . Roughly speaking, entropy is the logarithm of the number of states of the

¹Note that the splitting of the total Hilbert space is doable since we are currently working on a lattice model. Generally, in quantum gravity it is unknown if the Hilbert space splits.

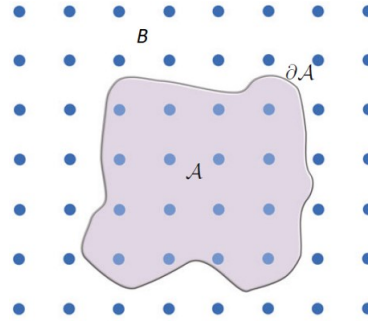


FIGURE 2.1: Lattice quantum system divided by the boundary ∂A into subsystems A (shaded area) and B (unshaded area).

inaccessible, for the observer, part of the universe B that are consistent with all measurements restricted to the accessible part A , together with *a priori* knowledge that the universe as a whole is in a pure state.

Now, consider a quantum field theory on a $d + 1$ dimensional manifold $\mathbb{R} \times N$, where \mathbb{R} and N denote the time direction and the d dimensional space-like manifold, respectively. We define the subsystem by a d dimensional submanifold $A \subset N$ at fixed time $t = t_0$. We call its complement the submanifold B , as shown in Fig. 2.2. The boundary of A , which is denoted by ∂A , divides the manifold N into two submanifolds A and B . Then we can define the entanglement entropy S_A by using (2.20). Sometimes, this kind of entropy is called geometric entropy as it depends on the geometry of the submanifold A .

Entanglement Entropy in continuum QFTs is a divergent quantity. There are ultraviolet (UV) modes at arbitrarily small scales across the dividing surface ∂A , this makes it impossible to actually split the full Hilbert space, $\mathcal{H}_{AB} \neq \mathcal{H}_A \otimes \mathcal{H}_B$. For example, no realistic measuring apparatus resolves infinitely small distances, so the sharp distinction between inside and outside might appear to be an unrealistic idealization. To deal with this, we must impose a UV cutoff by introducing the 'lattice scale' ϵ_{UV} . With a finite cutoff, the Hilbert space of a finite region is finite-dimensional. In the end we usually want to regulate and renormalize these divergences in such a way that physically meaningful quantities are assigned definite finite values in the theory.

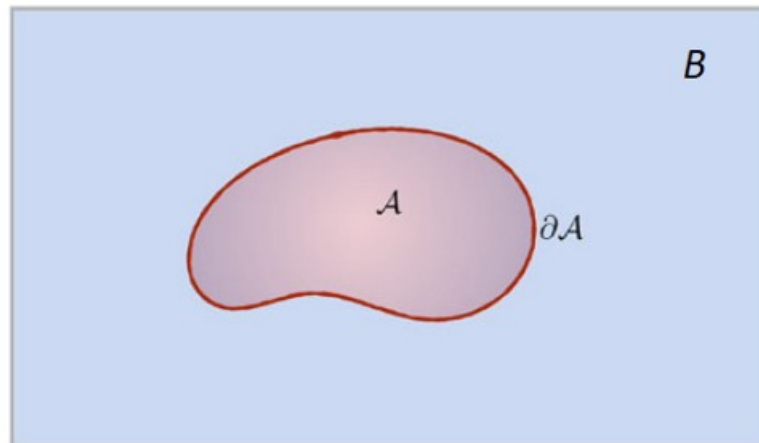


FIGURE 2.2: QFT on a $\mathbb{R} \times N$ manifold at fixed time $t = t_0$. The N manifold is divided by the boundary ∂A into submanifolds A and B .

2.3 Entanglement Entropy in 2D CFT

Here we review existing computations of entanglement entropy in $(1+1)D$ CFTs. The central charge of a given CFT is denoted by c . Such a computation was initiated by C. Holzhey, F. Larsen and F. Wilczek [40]; see also P. Calabrese and J. Cardy [15].

2.3.1 A Replica Approach

In order to find the entanglement entropy we will use the so called replica trick. Very helpful quantities for this kind of procedure are the so called Rényi entropies. These are defined as follow

$$S_A^{(n)} = \frac{1}{1-n} \log \text{tr} \rho_A^n. \quad (2.21)$$

The replica trick consists of evaluating $\text{tr} \rho_A^n$, differentiate it with respect to n and finally take the limit $n \rightarrow 1$,

$$S_A = - \lim_{n \rightarrow 1} \frac{\partial}{\partial n} \text{tr} \rho_A^n = - \lim_{n \rightarrow 1} \frac{\partial}{\partial n} \log \text{tr} \rho_A^n = \lim_{n \rightarrow 1} S_A^{(n)}, \quad (2.22)$$

since $\text{tr} \rho_A = 1$.

This can be done in the path-integral formalism as follows. We first assume that A is the single interval $x \in [u, v]$ at $t_E = 0$ in the flat Euclidean coordinates $(t_E, x) \in \mathbb{R}^2$. The ground state wave function Ψ can be found by path-integrating from $t_E = -\infty$ to $t_E = 0$ in the Euclidean formalism, cf. ssec 2.1.5 ,

$$\Psi(\phi_0(x)) = \int_{t_E=-\infty}^{\phi(t_E=0,x)=\phi_0(x)} D\phi e^{-S(\phi)}, \quad (2.23)$$

where $\phi(t_E, x)$ denotes the field which defines the 2D CFT. The values of the field at the boundary ϕ_0 depends on the spatial coordinate x . The total density matrix ρ is given by two copies of the wave function $[\rho]_{\phi_0\phi'_0} = \Psi(\phi)\bar{\Psi}(\phi'_0)$, cf. Ssec 2.1.7. The complex conjugate on $\bar{\Psi}$ can be obtained by path-integrating from $t_E = \infty$ to $t_E = 0$. To obtain the reduced density matrix ρ_A , we need to integrate ϕ_0 on B assuming $\phi_0(x) = \phi'_0(x)$ when $x \in B$

$$[\rho]_{\phi_+\phi_-} = (Z_1)^{-1} \int_{t_E=-\infty}^{t_E=\infty} D\phi e^{-S(\phi)} \prod_{x \in A} \delta(\phi(+0, x) - \phi_+(x)) \cdot \delta(\phi(-0, x) - \phi_-(x)), \quad (2.24)$$

where Z_1 is the vacuum partition function on \mathbb{R}^2 and we multiply its inverse in order to normalize ρ_A such that $\text{tr}_A \rho_A = 1$. This computation is sketched in Fig. 2.3 (a).

To find $\text{tr}_A \rho_A^n$, we can prepare n copies of (2.24)

$$[\rho_A]_{\phi_{1+}\phi_{1-}} [\rho_A]_{\phi_{2+}\phi_{2-}} \cdots [\rho_A]_{\phi_{n+}\phi_{n-}} \quad (2.25)$$

and take the trace successively. In the path-integral formalism this is realized by gluing $\{\phi_{i\pm}(x)\}$ as $\phi_{i-}(x) = \phi_{(i+1)+}(x)$ ($i = 1, 2, \dots, n$) and integrating $\phi_{i+}(x)$. Hence, the calculation of $\text{tr}_A \rho_A^n$ reduces to that of a partition function on a complicated Riemann surface \mathcal{R}_n (see Fig. 2.3 (b)) that is analytically achievable in a quantum field theory

$$\text{tr}_A \rho_A^n = (Z_1)^{-n} \int_{(t_E, x) \in \mathcal{R}_n} D\phi e^{-S(\phi)} \equiv \frac{Z_n}{(Z_1)^n}. \quad (2.26)$$

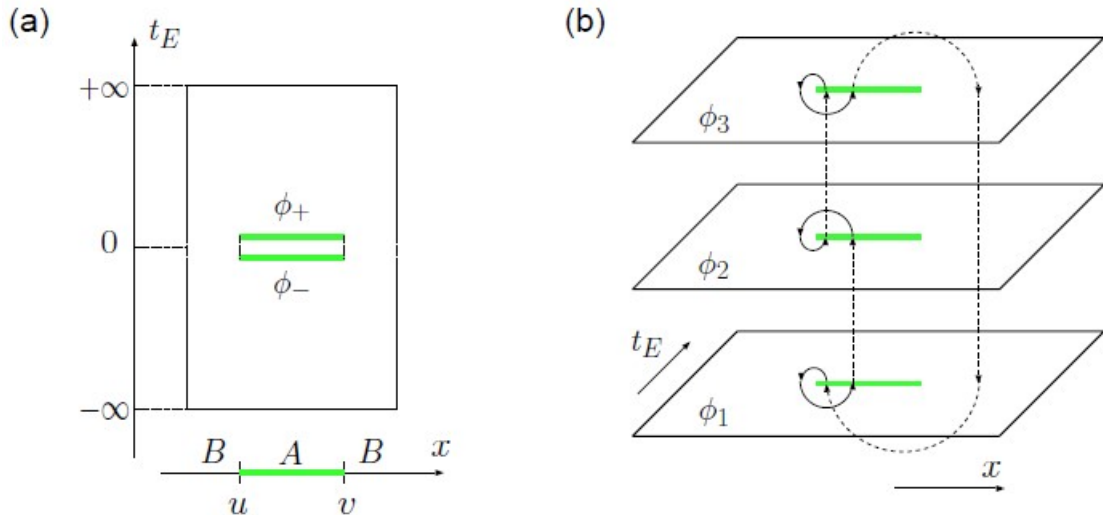


FIGURE 2.3: (a) The path integral representation of the reduced density matrix $[\rho_A]_{\phi_+\phi_-}$. (b) The n -sheeted Riemann surface \mathcal{R}_n (for $n = 3$).

When the right hand side of equation (2.26) has a unique analytic continuation to $\text{Re } n > 1$, its first derivative at $n = 1$ combined with the equation (2.22) gives the required entropy

$$S_A = -\frac{\partial}{\partial n} \log \frac{Z_n}{(Z_1)^n} \Big|_{n=1}. \quad (2.27)$$

The problem is now moved to the existence and uniqueness of a proper analytic continuation to extract the entanglement entropy. In some cases this is trivial, in others difficult, and in several others beyond our present understanding.

2.3.2 Twist Fields

The partition function of a model of 2D QFT (or CFT) with local Lagrangian $\mathcal{L}(\phi)$ on a (euclidean-signature) Riemann surface \mathcal{R} is formally obtained by the path integral

$$Z_{\mathcal{L},\mathcal{R}} = \int_{\mathcal{R}} d\phi \exp\left(-\int_{\mathcal{R}} dx dt_E \mathcal{L}(\phi)\right) \quad (2.28)$$

where $d\phi$ is an infinite measure on the set of configurations of some field ϕ living on the Riemann surface \mathcal{R} . Since the Lagrangian density does not depend on the Riemann surface \mathcal{R} , as a consequence of its locality, it is expected that the partition function can be expressed as an object calculated from a model on the complex plane \mathbb{C} , where the structure of the Riemann surface is implemented through appropriate boundary conditions around the points with non-zero curvature.

In our case, the n -sheeted Riemann surface \mathcal{R}_n has zero curvature everywhere except at a finite number of points (i.e. the boundaries between A and B which are denoted by the points u and v respectively). We expect that there is a model in which the associated partition function in a theory defined on the complex plane \mathbb{C} with coordinates $z = x + it_E$ can be written in terms of certain "fields" at $z = u$ and $z = v$. Equation (2.28) essentially defines these fields, i.e. it gives their correlation functions, up to a normalization independent of their positions. However in the model on the complex plane, this definition makes them non-local (ref). Locality is at the basis of QFT, so it is important to recover it.

The idea is again to use the Replica trick and consider a larger model formed by n independent copies of the original model, where n is the number of Riemann sheets necessary to describe the Riemann surface \mathcal{R} by coordinates on the complex plane \mathbb{C} . The partition function in equation (2.28) can be re-written as the path integral on the complex plane

$$Z_{\mathcal{L}, \mathcal{R}_n} = \int_{\mathcal{C}_{u,v}} d\phi_1 \cdots d\phi_n \exp\left(- \int_{\mathcal{C}} dx dt_E (\mathcal{L}(\phi_1) + \dots + \mathcal{L}(\phi_n))\right) \quad (2.29)$$

where with $\int_{\mathcal{C}_{u,v}}$ we indicated the restricted path integral with boundary conditions

$$\phi_{i-}(x) = \phi_{(i+1)+}(x), \quad x \in [u, v], \quad n+i \equiv i, \quad i = 1, 2, \dots, n. \quad (2.30)$$

The Lagrangian density of the multi-copy model is

$$\mathcal{L}^{(n)}(\phi_1, \dots, \phi_n) = \mathcal{L}(\phi_1) + \dots + \mathcal{L}(\phi_n) \quad (2.31)$$

since we duplicated the theory n times without adding interactions, we have a Lagrangian which is the sum of the Lagrangians of the n individual copies. The equation (2.29) takes the form of

$$Z_{\mathcal{L}, \mathcal{R}_n} = \int_{\mathcal{C}_{u,v}} d\phi_1 \cdots d\phi_n \exp\left(- \int_{\mathbb{C}} dx dt_E \mathcal{L}^{(n)}(\phi_1, \dots, \phi_n)\right) \quad (2.32)$$

and indeed defines local fields at $z = u$ and $z = v$ in the multi-copy model.

These local fields are examples of twist fields. They are made up fields and act to change the path integral boundary conditions. Twist fields exist in a quantum field theory whenever there is a global internal symmetry σ : $\int dx dt \mathcal{L}(\sigma\phi)(x, t) = \int dx dt \mathcal{L}(\phi)(x, t)$. In the model with Lagrangian $\mathcal{L}^{(n)}$, there are two opposite cyclic permutation symmetries $i \rightarrow i+1$ and $i+1 \rightarrow i$ under exchange of the copies. We can denote them by Φ and $\bar{\Phi}$, respectively

$$\begin{aligned} \Phi_n &\equiv \Phi_{\sigma}, \quad \sigma : i \rightarrow i+1 \text{ mod } n, \\ \bar{\Phi}_n &\equiv \Phi_{\sigma^{-1}}, \quad \sigma^{-1} : i \rightarrow i+1 \text{ mod } n. \end{aligned} \quad (2.33)$$

Notice that $\bar{\Phi}_n$ can be identified with Φ_{-n} .

For the n -sheeted Riemann surface along the set A we then have

$$Z_{\mathcal{L}, \mathcal{R}_n} \propto \langle \Phi_n(u, 0) \Phi_{-n}(v, 0) \rangle_{\mathcal{L}^{(n)}, \mathbb{C}}. \quad (2.34)$$

This can be seen on Fig. 2.4 by observing the effect of the twist fields on the local fields. For $x \in [u, v]$, consecutive copies are connected through $t_E = 0$ due to the presence of $\Phi_n(u, 0)$, whereas for x in B , copies are connected to themselves through $t_E = 0$ because the conditions arising from the definition of $\Phi(u, 0)$ and $\Phi_{-n}(v, 0)$ cancel each other. More generally, the identification holds for correlation functions in the model \mathcal{L} on \mathcal{R}_n

$$\langle O(x, t_E : \text{sheet } i) \cdots \rangle_{\mathcal{L}, \mathcal{R}_n} = \frac{\langle \Phi_n(u, 0) \Phi_{-n}(v, 0) O_i(x, t_E) \cdots \rangle_{\mathcal{L}^{(n)}, \mathbb{C}}}{\langle \Phi_n(u, 0) \Phi_{-n}(v, 0) \rangle_{\mathcal{L}^{(n)}, \mathbb{C}}}. \quad (2.35)$$

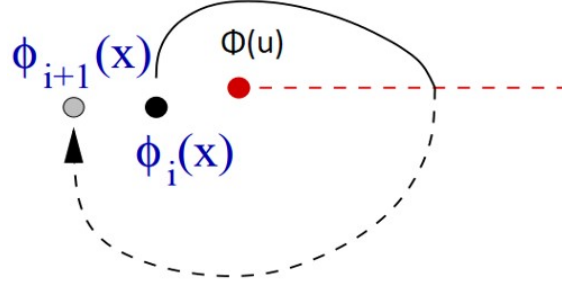


FIGURE 2.4: The effect of twist fields on other local fields.

2.3.3 Mapping the Riemann surface to the complex plane

We will use the complex coordinate $w = x + it_E$ and $\bar{w} = x - it_E$, note that this is a coordinate on a single sheet. The conformal mapping $w \rightarrow \zeta = (w - u)/(w - v)$ maps the points $[u, v]$ to $(0, \infty)$. This is uniformized by the mapping $\zeta \rightarrow z = \zeta^{1/n} = ((w - u)/(w - v))^{1/n}$. This maps the whole n -sheeted Riemann surface \mathcal{R}_n to the z -plane \mathbb{C} , see Fig. 2.5 for an illustration of this.

Now consider the holomorphic component of the stress tensor $T(w)$. This is related to the transformed stress tensor $T(z)$ by

$$T(w) = \left(\frac{dz}{dw}\right)^2 T(z) + \frac{c}{12}\{z, w\} \quad (2.36)$$

where $\{z, w\} = (z'''z' - \frac{3}{2}z''^2)/z'^2$ is the Schwarzian derivative. Taking the expectation value of equation (2.36), and using $\langle T(z) \rangle_{\mathbb{C}} = 0$ by translational and rotational invariance, we find

$$\langle T(w) \rangle_{\mathcal{R}_n} = \frac{c}{12}\{z, w\} = \frac{c(1 - n^{-2})}{24} \frac{(v - u)^2}{(w - u)^2(w - v)^2} \quad (2.37)$$

From equation (2.35), we have

$$\langle T(w) \rangle_{\mathcal{R}_n} = \frac{\langle \Phi_n(u, 0) \bar{\Phi}_n(v, 0) T_j(w) \rangle_{\mathcal{L}^{(n), \mathbb{C}}}}{\langle \Phi(u, 0) \bar{\Phi}(v, 0) \rangle_{\mathcal{L}^{(n), \mathbb{C}}}} \quad (2.38)$$

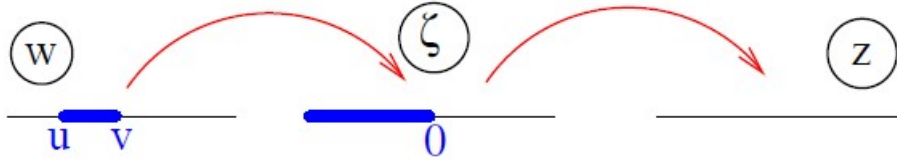


FIGURE 2.5: $w \rightarrow \zeta = (w - u)/(w - v)$ maps the branch points $[u, v]$ to $(0, \infty)$. This is uniformized by the mapping $\zeta \rightarrow z = \zeta^{1/n}$.

for all j , where j is the number of the sheet. We can then obtain the correlation function involving the stress-energy tensor of $\mathcal{L}^{(n)}$ by multiplying by n :

$$\begin{aligned} \langle T^{(n)}(w) \rangle_{\mathcal{L}, \mathcal{R}_n} &= \frac{\langle \Phi_n(u, 0) \Phi_n(v, 0) T^{(n)}(w) \rangle_{\mathcal{L}^{(n)}, \mathcal{C}}}{\langle \Phi_n(u, 0) \Phi_n(v, 0) \rangle_{\mathcal{L}^{(n)}, \mathcal{C}}} \\ &= \frac{c(n^2 - 1)}{24n} \frac{(u - v)^2}{(w - u)^2 (w - v)^2}. \end{aligned} \quad (2.39)$$

The comparison with the conformal Ward identity, see Appendix A equation (A.26),

$$\begin{aligned} \langle \Phi_n(u, 0) \bar{\Phi}_n(v, 0) T^{(n)}(W) \rangle_{\mathcal{L}^{(n)}, \mathcal{C}} &= \left(\frac{1}{w - u} \frac{\partial}{\partial u} + \frac{h_{\Phi_n}}{(w - u)^2} + \frac{1}{w - v} \frac{\partial}{\partial v} \right. \\ &\quad \left. + \frac{h_{\bar{\Phi}_n}}{(w - v)^2} \right) \langle \Phi_n(u, 0) \bar{\Phi}_n(v, 0) \rangle_{\mathcal{L}^{(n)}, \mathcal{C}}, \end{aligned} \quad (2.40)$$

allow us to identify the scaling dimension of the primary fields Φ_n and $\bar{\Phi}_n$ (same dimension $d_n = \bar{d}_n$), using $\langle \Phi_n(u, 0) \bar{\Phi}_n(v, 0) \rangle_{\mathcal{L}^{(n)}, \mathcal{C}} = |u - v|^{-2d_n}$, to be

$$d_n = \frac{c}{12} \left(n - \frac{1}{n} \right). \quad (2.41)$$

The above equation determines all the properties under conformal transformations and we therefore conclude that $Z_n/Z^n \propto \text{tr} \rho_A^n$ behaves under scale and conformal transformations identically to the two-point function of a primary operator with dimension d_n . In particular, this means that

$$\text{tr} \rho_A^n = \left(\frac{v - u}{\epsilon} \right)^{-c(n-1/n)/6}. \quad (2.42)$$

The power of ϵ corresponds to the renormalization constant (plus the constant that arises due to the ambiguity of this method). Using equation (2.22) we get the entanglement entropy of A to be

$$S_A = \frac{c}{3} \log \frac{l}{\epsilon}, \quad (2.43)$$

where $l = v - u$ is the length of system A . For a general conformal field theory, where we are interested in both holomorphic and antiholomorphic modes, equation (2.43) takes the following form

$$S_A = \frac{c + \bar{c}}{6} \log \frac{l}{\epsilon}. \quad (2.44)$$

This equation will turn out particularly useful in conformal field theories, such as the moving mirror model in chapter 3, where we only use one set of modes.

2.4 Discrete Time Mechanics

In this section we will describe the operator for time evolution in discrete time mechanics. This operator will be useful later on when we will examine the time evolution of a free massless scalar field on a lattice. The section is based on the papers of P. A. Höhn [43, 44] on evolving Hilbert spaces. For related work on classical discrete time mechanics, see [45, 46].

2.4.1 Classical Mechanics in the Continuum and Discrete

In continuous time mechanics Lagrangian dynamics is conventionally formulated via an action principle based on the action integral

$$S_{if}[\gamma] = \int_{t_i}^{t_f} dt L(q, \dot{q}, t), \quad (2.45)$$

where t_i and t_f are the initial and final times respectively along some given path γ . In our version of discrete time mechanics we postulate that the dynamical variables $q(t)$ are observed at a finite number of times $t_n, n = 0, 1, \dots, N$, where $t_0 = t_i$ and $t_N = t_f$, such that the intervals are all equal to some fundamental interval a . For convenience we will write $q_n \equiv q(t_n)$.

In our formulation of discrete time mechanics we replace the action integral by an action sum of the form

$$S^N[\gamma] = \sum_{n=0}^{N-1} F^n, \quad (2.46)$$

where $F^n \equiv F(q_n, q_{n+1}, n)$ will be referred to as the *system function*. The system function has the same central role in discrete time mechanics as the Lagrangian has in continuous time mechanics.

A necessary condition to extremise the action (2.46) is that

$$\frac{\partial F[\{q_n\}]}{\partial q_m} = 0, \quad m = 0, 1, \dots, N. \quad (2.47)$$

It is assumed that $F(x, y, z)$ is a continuously differentiable function with respect to the arguments x and y . Performing this differentiation gives

$$\frac{\partial}{\partial q_n} \{F^{n-1} + F^n\} = 0, \quad 0 < n < N, \quad (2.48)$$

where the equality holds over a true or dynamical trajectory. For a more detailed discussion which includes the boundary equations of motion at $m = 0, N$ see [14]. We now discuss the interpretation of this equation.

Suppose we have a continuous time action integral of the form (2.45). First, partition the time interval $[t_0, t_N]$ into N equal subintervals. Then the action integral may be written as a sum of sub-integrals, *i.e.*,

$$S_{if}[\gamma] = \sum_{n=0}^{N-1} \int_{t_n}^{t_{n+1}} dt L(q(t), \dot{q}(t), t). \quad (2.49)$$

Now suppose that we fixed the co-ordinates q_n at the various times t_0, t_1, \dots, t_N and then chose the path connecting each pair of points (q_n, q_{n+1}) to be the true or dynamical path, that is, a solution to the Euler-Lagrange equations of motion for those boundary conditions. If this partially extremised path is denoted by γ_c then we may write

$$S_{if}[\gamma_c] = \sum_{n=0}^{N-1} S^n, \quad (2.50)$$

where $S^n \equiv S(q_{n+1}, t_{n+1}; q_n, t_n)$ is known as Hamilton's principal function, being just the integral of the Lagrangian along the true path from q_n at time t_n to q_{n+1} at time t_{n+1} . The Hamilton's principal function will play the role of the system function for the discrete system.

The Hamilton-Jacobi Equation

Here we will build intuition about the *Hamilton's principal function* which is a generating function for canonical time. Consider the action (2.45) evaluated only along the *true* path γ_c and define

$$W(q_i^{initial}, q_i^{final}, T) = S[q_i^{classical}(t)] \equiv S[\gamma_c], \quad (2.51)$$

where $T = t_f - t_i$. While S is a functional on any path, W is to be considered as a function of the initial and final configurations $q_i^{initial}$ and q_i^{final} as well as the time T it takes to get between them. Now if we keep $q_i^{initial}$ fixed but vary the end point q_i^{final} we get

$$\delta S = \int_0^T dt \left[\frac{\partial L}{\partial q_i} - \frac{d}{dt} \left(\frac{\partial L}{\partial \dot{q}_i} \right) \right] \delta q_i(t) + \left[\frac{\partial L}{\partial \dot{q}_i(t)} \delta q_i(t) \right]_0^T, \quad (2.52)$$

which on the classical path takes the form,

$$\frac{\partial W}{\partial q_i^{final}} = \left. \frac{\partial L}{\partial \dot{q}_i} \right|_T = p_i^{final}. \quad (2.53)$$

Consider a classical path with fixed initial configuration $q_i^{initial}$ and the fact that $dS/dT = L$. Then we get

$$L(q_i^{final}, \dot{q}_i^{final}, T) = \frac{dW}{dT} = \frac{\partial W}{\partial T} + \frac{\partial W}{\partial q_i^{final}} \dot{q}_i^{final}. \quad (2.54)$$

By relabelling $T \mapsto t$ and dropping the word "final" we have found ourselves a time dependent function on configuration space $W = W(q_i, t)$ which satisfies

$$\frac{\partial W}{\partial t} = -H(q_i, \partial W / \partial q_i, t). \quad (2.55)$$

This is the *Hamilton-Jacobi Equation*. Combine this with the first of Hamilton's equations we get

$$\dot{q}_i = \left. \frac{\partial H}{\partial p_i} \right|_{p_i = \partial W / \partial q_i}. \quad (2.56)$$

In this manner the function W determines the path of the classical system: start it off at a point in configuration space and W can be considered as a real valued classical wavefunction which tells it how to evolve. The function $W \equiv S[\gamma_c]$ is called *Hamilton's principal function*. Notice that in the discretized case (2.50) the action is a sum of Hamilton's principal functions S^n that evolve the system in each time step $t_n \mapsto t_{n+1}$.

2.4.2 Quantum Mechanical Propagators in the Continuum

In continuum quantum mechanics, the propagator is defined, in the position representation, as the transition amplitude between states at different times

$$K(q_1, t_1; q_0, t_0) = \langle q_1 | e^{-i(t_1 - t_0)\hat{H}/\hbar} | q_0 \rangle = \int DQ e^{iS}, \quad (2.57)$$

where \hat{H} is the Hamiltonian of the system and $q_{0,1}$ coordinatize the configuration manifold \mathcal{Q} . Remember that in the construction of the path integral we partition the time interval $t_1 - t_0$ into n segments and we take the limit of $n \rightarrow \infty$. The path integral measure is of the form $DQ \propto \int \lim_{n \rightarrow \infty} (\prod_{k=1}^{n-1} \int dQ_k)$ where $|Q_k\rangle$ are states inserted in-between the boundary states $|q_0\rangle, |q_1\rangle$.

The propagator satisfies the Schrödinger equation in both sets of variables

$$i\hbar\partial_{t_1}K(q_1, t_1; q_0, t_0) = \hat{H}K(q_1, t_1; q_0, t_0), \quad i\hbar\partial_{t_0}K^*(q_1, t_1; q_0, t_0) = \hat{H}K^*(q_1, t_1; q_0, t_0), \quad (2.58)$$

and, importantly, maps wave functions at t_0 one-to-one to wave functions at t_1

$$\psi(q_1, t_1) = \int_{\mathcal{Q}} dq_0 K(q_1, t_1; q_0, t_0) \psi(q_0, t_0). \quad (2.59)$$

An illuminating illustration of the fact the K operator in position space generates time evolution can be seen by using the Dirac notation,

$$\langle q_1 | \psi \rangle = \int_{\mathcal{Q}} dq_0 \langle q_1 | \hat{K} | q_0 \rangle \langle q_0 | \psi_0 \rangle, \quad (2.60)$$

and the fact that $\int_{\mathcal{Q}} dq_0 |q_0\rangle \langle q_0| = \hat{I}$,

$$|\psi\rangle = \hat{K}|\psi_0\rangle, \quad \text{where } \hat{K} = e^{-i(t_1-t_0)\hat{H}/\hbar}. \quad (2.61)$$

Four of the continuum propagator's basic properties are

- (i) *Composition*: $K(q_2, t_2; q_0, t_0) = \int_{\mathcal{Q}} dq_1 K(q_2, t_2; q_1, t_1) K(q_1, t_1; q_0, t_0)$, where $t_1 < t_0$ and $t_2 < t_1$,
- (ii) *Time reversal*: $K(q_0, t_0; q_1, t_1) = (K(q_1, t_1; q_0, t_0))^*$,
- (iii) *Invertibility*: $\int_{\mathcal{Q}} dq_1 (K(q_1, t_1; q_0, t_0))^* K(q_1, t_1; q'_0, t_0) = \delta(q_0 - q'_0)$, and,
- (iv) *Infinitesimal transition*: $\lim_{t_1 \rightarrow t_0} K(q_1, t_1; q_0, t_0) = \delta(q_1 - q_0)$.

Next, we shall examine how these well-known continuum properties of the propagator do or do not translate into a consistent quantum formalism for discrete systems.

2.4.3 Quantum Mechanical Propagators in the Discrete

Consider an evolution from $(t_0, x_0) \rightarrow (t_1, x_1)$ or just $0 \rightarrow 1$. The discrete propagator associated to the move cannot be given as a transition amplitude between states on one and the same Hilbert space in the form of the right hand side of (2.57): the eigenstates of the 'position operators' \hat{x}^i at time steps $n = 0, 1$ $|x_0\rangle \in \mathcal{H}_0$ and $|x_1\rangle \in \mathcal{H}_1$, respectively, are elements of two distinct Hilbert spaces $\mathcal{H}_0 := L^2(\mathcal{Q}_0, dx_0)$, $\mathcal{H}_1 := L^2(\mathcal{Q}_1, dx_1)$ and refer to different variables where $\mathcal{Q}_0, \mathcal{Q}_1$ are the configuration manifolds with Lebesgue measure $dx_n, n = 0, 1$. Correspondingly, an expression such as $\langle x_1 | x_0 \rangle$ is not defined. Instead, we shall construct the propagator directly as the quantum time evolution map between \mathcal{H}_0 and \mathcal{H}_1 - in analogy to (2.59). In addition, given that time evolution is generated by the move $0 \rightarrow 1$, a Hamiltonian (which would generate infinitesimal time evolution, *i.e.* continuous time evolution) is absent in the discrete systems. Consequently, in the quantum theory a unitary map of the type $\hat{U}(t_1, t_0) = e^{-i(t_1-t_0)\hat{H}/\hbar}$ cannot arise and be used to define the map between Hilbert spaces associated to time steps 1, 0.

We must therefore proceed differently, we shall employ the action (or rather Hamilton's principal function) which also generates time evolution, instead of a Hamiltonian, to construct the propagator (and thereby the transition amplitude) and to define the dynamics.

More precisely, in the spirit of the configuration space path integral expression for the continuum propagator, we shall make the following ansatz for the propagator of an evolution move $0 \rightarrow 1$. We associate a (possibly complex) path integration measure C_{01} to this move and absorb it in the definition of the propagator

$$K_{0 \rightarrow 1}(x_1, x_0) := C_{01} e^{iS^1(x_1, x_0)/\hbar}, \quad (2.62)$$

where $S^1(x_1, x_0)$ is the classical action, or Hamilton's principal function, associated to $0 \rightarrow 1$.

Let us now begin with the construction: Classically, to every evolution move $0 \rightarrow 1$ there is associated a pair of phase spaces $\mathcal{P}_0 := T^*R^N$ and $\mathcal{P}_1 := T^*R^N$ at steps $n = 0, 1$, respectively. In analogy, in the quantum theory we associate a pair of Hilbert spaces $\mathcal{H}_0 := L^2(\mathcal{Q}_0, dx_0)$ and $\mathcal{H}_1 := L^2(\mathcal{Q}_1, dx_1)$ with every evolution $0 \rightarrow 1$. We refer to the elements $\psi_0(x_0) \in \mathcal{H}_0$ and $\psi_1(x_1) \in \mathcal{H}_1$ associated with the move $0 \rightarrow 1$. We use the discrete propagator (2.62)-in analogy to (2.59)- to define the time evolution map $U_{0 \rightarrow 1} : \mathcal{H}_0 \rightarrow \mathcal{H}_1$ from states at $n = 0$ to states at $n = 1$ vis $U_{0 \rightarrow 1} := \int dx_0 K_{0 \rightarrow 1}$ such that

$$\psi_1(x_1) = \int dx_0 K_{0 \rightarrow 1}(x_0, x_1) \psi_0(x_0). \quad (2.63)$$

Just as in the continuum (property (ii) of ssec. 2.4.2), we require the reverse propagator to be the complex conjugate

$$K_{1 \rightarrow 0}(x_0, x_1) = C_{01}^* e^{-iS^1(x_0, x_1)/\hbar} = (K_{0 \rightarrow 1}(x_1, x_0))^*. \quad (2.64)$$

Hence,

$$\psi_1(x_1) = \int dx_0 K_{0 \rightarrow 1}(x_1, x_0) \psi_0(x_0) = \int dx_0 K_{0 \rightarrow 1}(x_1, x_0) \int dx'_1 (K_{0 \rightarrow 1}(x'_1, x_0))^* \psi_1(x'_1). \quad (2.65)$$

This entails

$$\int dx_0 K_{0 \rightarrow 1}(x_1, x_0) (K_{0 \rightarrow 1}(x'_1, x_0))^* = \delta^{(N)}(x'_1 - x_1) \quad (2.66)$$

which, by (2.62), is a condition on the measure C . In complete analogy, by considering ψ_0 in terms of ψ_1 ,

$$\int dx_1 (K_{0 \rightarrow 1}(x_1, x_0))^* K_{0 \rightarrow 1}(x_1, x'_0) = \delta^{(N)}(x'_0 - x_0). \quad (2.67)$$

Both equations (2.66) and (2.67) are the discrete incarnation of the continuum property (iii) in ssec 2.4.2 above.

Provided the two conditions (2.66, 2.67) are fulfilled, the propagator defines a bijective quantum time evolution map between \mathcal{H}_0 and \mathcal{H}_1 . Using (2.67),

$$\begin{aligned} \int dx_1 (\psi_1(x_1))^* \psi_1(x_1) &= \int dx_1 dx_0 dx'_0 (K_{0 \rightarrow 1}(x_1, x_0))^* K_{0 \rightarrow 1}(x_1, x'_0) (\psi_0(x_0))^* \psi_0(x'_0) \\ &= \int dx_0 (\psi_0(x_0))^* \psi_0(x_0) \end{aligned} \quad (2.68)$$

and thus

$$\langle \phi_1 | \psi_1 \rangle_{\mathcal{H}_1} = \langle \phi_0 | \psi_0 \rangle_{\mathcal{H}_0}. \quad (2.69)$$

By using (2.66), one can prove the reverse direction.

The transition amplitudes for the evolution $0 \rightarrow 1$ can now be written as

$$\langle \phi_1 | U_{0 \rightarrow 1} \psi_0 \rangle = \int dx_1 dx_0 (\phi_1)^* K_{0 \rightarrow 1} \psi_0. \quad (2.70)$$

Notice that in the regular case where the configuration manifolds at different time steps are isomorphic, *aka* they have the same dimension, to one another $\mathcal{Q}_0 \simeq \mathcal{Q}_1 \simeq \mathbb{R}^N$ the discrete time evolution move $0 \rightarrow 1$ is unitary. Later, we will see that, when this is not the case, the time evolution map could be an isometry.

In analogy to the continuum (property (i) in ssec. 2.4.2), the propagator of the composition of the moves is to be the convolution

$$K_{0 \rightarrow 2}(x_2, x_0) = \int dx_1 K_{1 \rightarrow 2}(x_2, x_1) K_{0 \rightarrow 1}(x_1, x_0). \quad (2.71)$$

This allows us to consistently write

$$\begin{aligned} \psi_2(x_2) &= \int dx_1 K_{1 \rightarrow 2} \psi_1(x_1) \\ &= \int dx_1 K_{1 \rightarrow 2} \int dx_0 K_{0 \rightarrow 1}(x_1, x_0) \psi_0(x_0) \\ &= \int dx_0 K_{0 \rightarrow 2}(x_2, x_0) \psi_0(x_0). \end{aligned} \quad (2.72)$$

The composition of the sequence of moves $0 \rightarrow 1 \rightarrow 2 \rightarrow \dots \rightarrow n$ to the effective move $0 \rightarrow n$ yields the path integral (PI)

$$\begin{aligned} K_{0 \rightarrow n}(x_n, x_0) &= \int \prod_{l=1}^{n-1} dx_l \prod_{j=0}^{n-1} K_{j \rightarrow j+1}(x_{j+1}, x_j) \\ &= \int \prod_{l=1}^{n-1} dx_l \prod_{j=0}^{n-1} C_{jj+1} e^{i/\hbar \sum_{k=1}^n S^k(x_k, x_{k-1})}. \end{aligned} \quad (2.73)$$

In the case of only one move, *i.e.* $0 \rightarrow 1$, the path integral of our discrete system is just the propagator $K_{0 \rightarrow 1}$.

Remark: The continuum property (iv) is meaningless in the systems under consideration because of the absence of a time variable which could be made arbitrarily small.

Chapter 3

Moving Mirrors

Moving mirrors have led to interesting and tractable classes of time-dependent backgrounds in quantum field theories [30]. A moving mirror model is described by a QFT defined on a spacetime with a time-dependent boundary, which is identified with the mirror trajectory. Note that in two dimensions the mirror actually consists of a point which follows a given trajectory.

Moving mirrors could also be used as toy-models for cosmological expansion which is the main subject of this thesis. In particular, we examine an $1+1$ free field theory with a moving mirror. The mirror is initially at rest, then accelerates uniformly away from infinity. Subsequently the mirror stops accelerating and remains at final receding velocity. As depicted in Fig. 3.1, the mirror models an expanding universe since the volume of space, in the right hand side of the boundary, is increasing with time.

This chapter is organized as follows. In sec. 3.1 we set up the spacetime of our toy-model. In sec. 3.2 we equip the spacetime with a scalar field. Both sections 3.1 and 3.2 are based on the book of S. Carroll [17]. Finally, in sec. 3.3 we examine our toy-model of cosmological expansion.

3.1 2D Minkowski Space

In this section we set up the spacetime background for our toy-model.

The two dimensional Minkowski space metric, in inertial coordinates $t^\pm = t \pm x$, is the following

$$ds^2 = -dt^2 + dx^2 = -dt^+ dt^-. \quad (3.1)$$

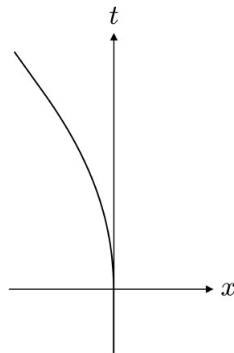


FIGURE 3.1: A mirror following a trajectory suited for cosmological expansion.

We refer to these coordinates as inertial due to the fact that inertial trajectories are of the form $t^+ = \alpha t^- + b$. This can be seen from the geodesic equation

$$\frac{d^2 x^\mu}{d\lambda^2} + \Gamma_{\alpha\beta}^\mu \frac{dx^\alpha}{d\lambda} \frac{dx^\beta}{d\lambda} = 0 \rightarrow \frac{d^2 x^\mu}{d\lambda^2} = 0 \rightarrow \frac{d^2 t^\pm}{d\lambda^2} = 0 \rightarrow t^+ = \alpha t^- + b, \quad (3.2)$$

when applied to a two dimensional flat spacetime with the given coordinates.

Another useful aspect of 2D Minkowski is the Poincaré transformation which is the combination of Lorentz coordinate transformations, *aka* boosts, and translations

$$\begin{cases} \tilde{t} = \gamma(t - ux) + t_0 \\ \tilde{x} = \gamma(x - ut) + x_0 \end{cases} \quad c = 1, \gamma = \frac{1}{\sqrt{1-u^2}}, \quad (3.3)$$

where u is the velocity of the coordinate system (\tilde{t}, \tilde{x}) with respect to the coordinate system (t, x) and (t_0, x_0) is the amount of translation between the two coordinate systems. In inertial coordinates, equation (3.3) takes the form

$$\begin{cases} \tilde{t}^+ = \tilde{t} + \tilde{x} = \frac{1-u}{\sqrt{1-u^2}} t^+ + t_0^+ \\ \tilde{t}^- = \tilde{t} - \tilde{x} = \frac{1+u}{\sqrt{1-u^2}} t^- + t_0^- \end{cases} \quad (3.4)$$

Moreover, an important tool that allow us to better visualize the spacetime is conformal diagrams (or just Penrose diagrams). It captures the global properties and causal structure of sufficiently symmetric spacetimes such as Minkowski. Our goal is to portray the causal structure of spacetime, which is defined by its light cones, and aim for coordinates in which infinity is only a finite coordinate value away, so that the structure of the entire spacetime is immediately apparent.

A conformal transformation is essentially a local change of scale, *cf.* Appendix A. Since distances are measured by the metric, such transformations are implemented by multiplying the metric by a spacetime-dependent function:

$$\tilde{g}_{\mu\nu} = \Omega(x) g_{\mu\nu}, \quad (3.5)$$

or equivalently

$$\tilde{d}s^2 = \Omega^2(x) ds^2 \quad (3.6)$$

for some nonvanishing function $\Omega(x)$. (Here x is used to denote the collection of spacetime coordinates x^μ which in our case are inertial coordinates).

We define new inertial coordinates

$$\begin{cases} T^+ = \arctan(t^+), & -\pi/2 < T^+ < \pi/2 \\ T^- = \arctan(t^-), & -\pi/2 < T^- < \pi/2, T^- \leq T^+ \end{cases} \quad (3.7)$$

The Minkowski metric takes the form

$$ds^2 = -\frac{1}{\cos^2 T^+ \cos^2 T^-} dT^+ dT^-. \quad (3.8)$$

Equation (3.8) defines a conformal transformation of the form (3.6) with $\Omega^2(x) = \cos^2(T^+) \cos^2(T^-)$. Since conformal diagrams care about the causal structure of the spacetime, which is given by the light cones, we can forget about the conformal factor Ω . Our new Minkowski metric has the form

$$\tilde{d}s^2 = -dT^+ dT^-. \quad (3.9)$$

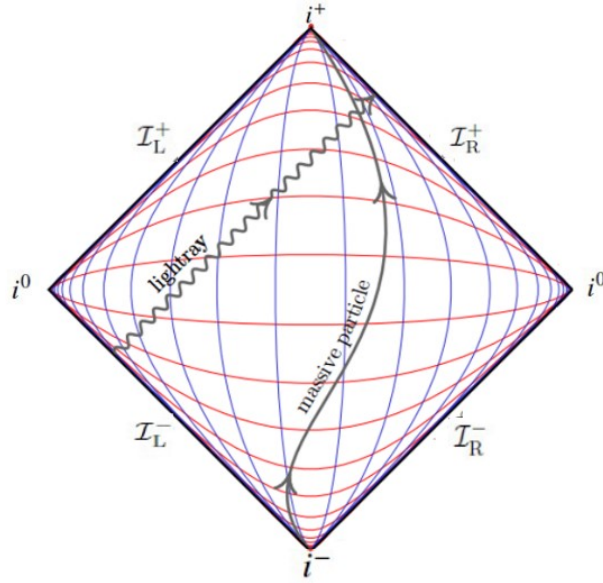


FIGURE 3.2: The conformal diagram of Minkowski spacetime where the red and blue curves being the constant t -slices and x -slices.

We can unfold the metric by using the following coordinates

$$\begin{cases} T = T^+ + T^-, & -\pi \leq T \leq \pi \\ X = T^+ - T^-, & -\pi \leq X \leq \pi. \end{cases} \quad (3.10)$$

The metric (3.10) takes the form

$$\tilde{d}s^2 = -dT^2 + dX^2, \quad (3.11)$$

again we threw away a factor of 4 since it does not affect the causal structure of the Minkowski spacetime.

Another important feature of the conformal diagram is the lines of constant time and constant space. These can be found by setting either t or x constant in equation (3.10) where $t^\pm = t \pm x$, see also Fig. 3.2

In Fig. 3.2, you can see the structure of the conformal diagram. In fact, Minkowski spacetime is only the interior of the diagram; the boundaries are not part of the original spacetime. The boundaries are referred to as conformal infinity, and the union of the original spacetime with conformal infinity is the conformal compactification, which is a manifold with a boundary. The structure of the conformal diagram allows us to subdivide conformal infinity into a few different regions:

$$\begin{aligned} i^+ &= \text{future timelike infinity } (T = \pi, X = 0) \\ i^0 &= \text{spatial infinity } (T = 0, X = \pi) \\ i^- &= \text{past timelike infinity } (T = -\pi, X = 0) \\ \mathcal{I}_{R/L}^+ &= \text{future null infinity } (T = \pi - X, 0 < X < \pi) \\ \mathcal{I}_{R/L}^- &= \text{past null infinity } (T = -\pi + X, 0 < X < \pi), \end{aligned}$$

where R/L means right and left, respectively.

3.2 Quantum Field Theory in 2D Minkowski Spacetime

In this section we are going to add a free massless scalar field ϕ upon the Minkowski spacetime. We will consider the Klein-Gordon Lagrangian

$$\mathcal{L} = -\frac{1}{2}\eta^{\mu\nu}\partial_\mu\phi\partial_\nu\phi, \quad (3.12)$$

for a free massless field ϕ .

The equation of motion is the Klein-Gordon equation,

$$\partial_\mu\partial^\mu\phi = 0. \quad (3.13)$$

Its solution is of the form

$$\phi(x^0, x^1) = H(\omega x^0) + G(\omega x^1), \quad (3.14)$$

where H and G are arbitrary function and $\omega \in \mathbb{R}$, later on ω will be more constricted.

We can observe that this quantum field theory is also a conformal field theory. In particular, a conformal transformation, *cf.* Appendix A, on equations (3.12) and (3.13) gives the following

$$\mathcal{L} = -\frac{1}{2}\Omega(x)\eta^{\mu\nu}\partial_\mu\phi\partial_\nu\phi \quad (3.15)$$

$$\Omega(x)\partial_\mu\partial^\mu\phi = 0. \quad (3.16)$$

Obviously, the solution of the equation of motion is unaffected by the conformal transformation. This is true due to the fact that there are no interactions and the field is massless. For that reason, our QFT is also an CFT.

For our Lagrange density (3.12), the conjugate momentum is

$$\pi = \dot{\phi}. \quad (3.17)$$

It is not hard to write down solutions to equation (3.13). One good example is a plane wave,

$$\phi(x^\mu) = \phi_0 e^{ik_\mu x^\mu} = \phi_0 e^{-i\omega t + ikx}, \quad (3.18)$$

where the wave vector has components $k^\mu = (\omega, k)$ and the frequency must satisfy $\omega = k$.

The most general solution is constructed by a complete, orthonormal set of modes in terms of which any solution may be expressed. To make sense of "orthonormal", we need to define an inner product on the space of solutions to the equation (3.13). Although the modes themselves are functions of spacetime, the appropriate inner product can be expressed as an integral over a constant-time plane Σ_t ,

$$(\phi_1, \phi_2) = -i \int_{\Sigma_t} (\phi_1 \partial_t \phi_2^* - \phi_2^* \partial_t \phi_1) dx. \quad (3.19)$$

Applying this inner product (3.19) to two plane waves of different wave vectors gives

$$(e^{ik_1^\mu x_\mu}, e^{ik_2^\nu x_\nu}) = (\omega_2 + \omega_1)(2\pi)\delta(k_1 - k_2), \quad (3.20)$$

where we have used $\int e^{ikx} dx = 2\pi\delta(k)$. Thus, the inner product vanishes unless the frequencies $\omega = k$ are equal for both modes. An orthonormal set of mode solutions

is thus given by

$$f_k(x^\mu) = \frac{e^{ik_\mu x^\mu}}{(4\pi\omega)^{1/2}}, \quad (3.21)$$

so that

$$(f_{k_1}, f_{k_2}) = \delta(k_1 - k_2). \quad (3.22)$$

Our strategy will be to insist that ω always be a positive number (since it is associated with the energy of the field), and complete the set of modes by including the complex conjugates $f_k^*(x^\mu)$. The f_k modes are said to be positive-frequency meaning they satisfy

$$\partial_t f_k = -i\omega f_k, \quad \omega > 0, \quad (3.23)$$

while the f_k^* modes are negative-frequency¹, satisfying

$$\partial_t f_k^* = i\omega f_k^*, \quad \omega > 0. \quad (3.24)$$

The complex conjugate modes are orthogonal to the original modes, $(f_{k_1}, f_{k_2}^*) = 0$, and orthonormal with each other but with a negative norm, $(f_{k_1}^*, f_{k_2}^*) = -\delta(k_1 - k_2)$. Together, the modes f_k and f_k^* form a complete set, in terms of which we can expand any solution to the equation (3.13).

To canonically quantize this theory, we promote our classical variables (the fields and their conjugate momenta) to operators acting on a Hilbert space, and impose the canonical commutation relations on equal-time surfaces:

$$[\phi(t, x), \phi(t, x')] = 0, \quad (3.25)$$

$$[\pi(t, x), \pi(t, x')] = 0, \quad (3.26)$$

$$[\phi(t, x), \pi(t, x')] = i\delta(x - x'). \quad (3.27)$$

We can expand the field operator $\phi(t, x)$ in terms of the modes (3.21). Denoting the coefficients of the mode expansion of the field operator by \hat{a}_k^\dagger and \hat{a}^\dagger , we have

$$\phi(t, x) = \int dk [\hat{a}_k f_k(t, x) + \hat{a}_k^\dagger f_k^*(t, x)]. \quad (3.28)$$

We observe that distinguishing between positive and negative frequencies, allows for an interpretation of their coefficients in the mode expansion of ϕ as annihilation and creation operators. Plugging this expansion into (3.25), (3.26) and (5.16) we find that the operators \hat{a}_k^\dagger and \hat{a}^\dagger obey commutation relations

$$[\hat{a}_k^\dagger, \hat{a}_{k'}] = 0,$$

$$[\hat{a}_k^\dagger, \hat{a}_{k'}^\dagger] = 0,$$

$$[\hat{a}_k^\dagger, \hat{a}_{k'}^\dagger] = \delta(k - k').$$

We can use the operators \hat{a}_k^\dagger and \hat{a}^\dagger to define a basis for the Hilbert space. There will be a single vacuum state $|0\rangle$, characterized by the fact that it is annihilated by each \hat{a}_k ,

$$\hat{a}_k |0\rangle = 0, \quad \text{for all } k. \quad (3.29)$$

¹Be careful; these modes are called negative-frequency even though $\omega > 0$, because the time derivative pulls down a factor $+i\omega$ rather than $-i\omega$.

A state with n_i excitations of various momenta k_i would be

$$|n_1, n_2, \dots, n_j\rangle = \frac{1}{\sqrt{n_1! n_2! \dots n_j!}} (\hat{a}_{k_1}^\dagger)^{n_1} (\hat{a}_{k_2}^\dagger)^{n_2} \dots (\hat{a}_{k_j}^\dagger)^{n_j} |0\rangle. \quad (3.30)$$

We can define a number operator for each k ,

$$\hat{n}_k = \hat{a}_k^\dagger \hat{a}_k, \quad (3.31)$$

which obeys

$$\hat{n}_{k_i} |n_1, n_2, \dots, n_i, \dots, n_j\rangle = n_i |n_1, n_2, \dots, n_i, \dots, n_j\rangle. \quad (3.32)$$

The states that are eigenstates of the number operators form a basis for the entire Hilbert space, known as the **Fock basis**; the space constructed from this basis is often called "Fock space", but of course it is just the original Hilbert space.

3.2.1 Bogolubov² Transformation

We will always be able to find a set of solutions $f_i(x)$ to equation (3.13) that are orthonormal,

$$(f_i, f_j) = \delta_{ij}, \quad (3.33)$$

and corresponding conjugate modes with negative norm,

$$(f_i^*, f_j^*) = -\delta_{ij}. \quad (3.34)$$

The index i may be continuous or discrete; we will adopt the discrete case for the sake of clarity. We may expand our field as

$$\phi = \sum_i (\hat{a}_i f_i + \hat{a}_i^\dagger f_i^*), \quad (3.35)$$

since the modes can be chosen to be a complete set. The coefficients \hat{a}_i and \hat{a}_i^\dagger have the familiar commutation relations

$$\begin{aligned} [\hat{a}_i, \hat{a}_j] &= 0, \\ [\hat{a}_i^\dagger, \hat{a}_j^\dagger] &= 0, \\ [\hat{a}_i, \hat{a}_j^\dagger] &= \delta_{ij}. \end{aligned}$$

There is also a vacuum state $|0_f\rangle$ that is annihilated by all the annihilation operators,

$$\hat{a}_i |0_f\rangle = 0, \quad \text{for all } i. \quad (3.36)$$

As in the previous section, for this vacuum state we can define an entire Fock basis for the Hilbert space. A state with n_i excitations is created by repeated action by \hat{a}_i^\dagger ,

$$|n_i\rangle = \frac{1}{\sqrt{n_i!}} (\hat{a}_i^\dagger)^{n_i} |0_f\rangle, \quad (3.37)$$

and likewise for states with different kind of excitations.

²Nikolay Nikolayevich Bogolyubov, also transliterated as Bogoliubov and Bogolubov, was a Soviet, Ukrainian and Russian mathematician and theoretical physicist known for a significant contribution to quantum field theory, classical and quantum statistical mechanics, and the theory of dynamical systems; he was the recipient of the 1992 Dirac Medal [66].

The basis modes $f_i(x^\mu)$ are highly nonunique. There are other choices we could have made. Consider an alternative set of modes $g_i(x^\mu)$ with all of the properties that our original modes possessed. They, also, form a complete basis that we expand our field operator,

$$\phi = \sum_i (\hat{b}_i g_i + \hat{b}_i^\dagger g_i^*). \quad (3.38)$$

The annihilation and creation operators \hat{b}_i and \hat{b}_i^\dagger have commutation relations

$$[\hat{b}_i, \hat{b}_j] = 0, \quad (3.39)$$

$$[\hat{b}_i^\dagger, \hat{b}_j^\dagger] = 0, \quad (3.40)$$

$$[\hat{b}_i, \hat{b}_j^\dagger] = \delta_{ij}. \quad (3.41)$$

There will be again a vacuum state $|0_g\rangle$ that is annihilated by all the annihilation operators,

$$\hat{b}_i |0_g\rangle = 0, \quad \text{for all } i. \quad (3.42)$$

The transformation from one set of bases modes into another is known as a **Bogolubov transformation**,

$$g_i = \sum_j (\alpha_{ij} f_j + \beta_{ij} f_j^*), \quad (3.43)$$

$$f_i = \sum_j (\alpha_{ji}^* g_j - \beta_{ji} g_j^*), \quad (3.44)$$

where the matrices α_{ij} and β_{ij} that are implementing the transformation are known as Bogolubov coefficients. Using the orthonormality of the mode functions, they can be expressed as

$$\alpha_{ij} = (g_i, f_j), \quad (3.45)$$

$$\beta_{ij} = -(g_i, f_j^*), \quad (3.46)$$

and they satisfy their own normalization conditions,

$$\sum_j (\alpha_{ik} \alpha_{jk}^* - \beta_{ik} \beta_{jk}^*) = \delta_{ij}, \quad (3.47)$$

$$\sum_j (\alpha_{ik} \beta_{jk} - \beta_{ik} \alpha_{jk}) = 0. \quad (3.48)$$

The Bogolubov coefficients can be also used to transform between the operators

$$\hat{a}_i = \sum_j (\alpha_{ij} \hat{b}_j + \beta_{ji}^* \hat{b}_j^\dagger), \quad (3.49)$$

$$\hat{b}_i = \sum_j (\alpha_{ij}^* \hat{a}_j - \beta_{ij} \hat{a}_j^\dagger). \quad (3.50)$$

Now imagine that the system is in the f -vacuum $|0_f\rangle$, in which no f -particles would be observed; we would like to know how many particles are observed by an observer using the g -modes. We therefore calculate the expectation value of the g

number operator, equation (3.31) in the f -vacuum

$$\begin{aligned}
\langle 0_f | \hat{n}_{gi} | 0_f \rangle &= \langle 0_f | b_i^\dagger b_i | 0_f \rangle \\
&= \langle 0_f | \sum_{jk} (\alpha_{ij} \hat{a}^\dagger - \beta_{ij} \hat{a}_j) (\alpha_{ik}^* \hat{a}_k - \beta_{ik}^* \hat{a}_k^\dagger) | 0_f \rangle \\
&= \sum_{jk} (-\beta_{ij}) (-\beta_{ik}^*) \langle 0_f | \hat{a}_j \hat{a}_k^\dagger | 0_f \rangle \\
&= \sum_{jk} \beta_{ij} \beta_{ik}^* \langle 0_f | (\hat{a}_k^\dagger \hat{a}_j + \delta_{jk}) | 0_f \rangle \\
&= \sum_{jk} \beta_{ij} \beta_{ik}^* \delta_{jk} \langle 0_f | 0_f \rangle \\
&= \sum_j \beta_{ij} \beta_{ij}^*.
\end{aligned}$$

Thus the number of g -particles in the f -vacuum can be expressed in terms of the Bogolubov coefficients as

$$\langle 0_f | \hat{n}_{gi} | 0_f \rangle = \sum_j |\beta_{ij}|^2. \quad (3.51)$$

The index j may be continuous or discrete; we adopt notation appropriate to the discrete case but the same results hold true for the continuous one, i.e. $\sum_j \rightarrow \int dj$.

The fact that the g -Fock space has a different choice of 'time' coordinate means it has a different choice of 'energy' and therefore a different notion of 'particle' and 'vacuum':

$$\text{time coordinate} \leftrightarrow \text{energy} \leftrightarrow \text{particle} \leftrightarrow \text{vacuum}. \quad (3.52)$$

The ambiguity comes from the fact that energy is observer dependent. The energy is the expectation value of the Hamiltonian; and the Hamiltonian is the operator that generates time evolution

$$\frac{i}{\hbar} [H, O] = \partial_t O. \quad (3.53)$$

Therefore the Hamiltonian depends on a choice of time t . Different choices of this coordinate correspond to different choices of Hamiltonian, and therefore different notions of positive energy, and therefore different notions of vacuum state.

One last thing that we need for the upcoming sections is how our Fock space basis behaves under Poincaré coordinate transformations (3.3). The time derivative of our mode functions (3.21) in the tilde-frame is

$$\begin{aligned}
\partial_{\tilde{t}} f_k &= \frac{\partial x^\mu}{\partial \tilde{t}} \partial_\mu f_k \\
&= \gamma(-i\omega) f_k + \gamma u(ik) f_k \\
&= -i\tilde{\omega} f_k,
\end{aligned}$$

where $\tilde{\omega} = \gamma\omega - \gamma uk$ is simply the frequency in the tilde-frame. Clearly, then, a state describing a collection of particles with certain momenta is transformed into a state describing the same particles, but with boosted momenta. Thus, the total number operator in the two frames will coincide, and in particular the vacuum state will coincide.

3.2.2 Vacuum Coordinates

It is now obvious that we have the freedom to choose between different sets of solutions in the Klein-Gordon equation (3.13). These solutions provides as with a set of modes, with which we can expand solutions to the Klein-Gordon equation in a flat two-dimensional space-time. The coefficients of the modes in the expansion of the Klein-Gordon solution are used to define the vacuum state. Although the Hilbert space for the theory is the same in either set of solutions, its interpretation as a Fock space will be different; in particular, the vacuum states will be different.

The usual set of solutions arises in inertial coordinates $t^\pm = t \pm x$ and it defines the Minkowski vacuum $|0_M\rangle$, satisfying

$$\hat{a}_k|0_M\rangle = 0, \quad \text{for all } k. \quad (3.54)$$

Let's examine a set of coordinates that will be useful later on for the mirror toy model. Apply a conformal transformation in the inertial coordinates of the form

$$t^- \rightarrow \tilde{t}^-(t^-), \quad (3.55)$$

$$t^+ \rightarrow \tilde{t}^+(t^+). \quad (3.56)$$

In these new coordinates the two dimensional Minkowski space-time metric (3.1) takes the form

$$ds^2 = -e^{2\rho} d\tilde{t}^+ d\tilde{t}^-, \quad \rho = -\frac{1}{2} \log \partial_+ \tilde{t}^+ \partial_- \tilde{t}^-. \quad (3.57)$$

The conformal factor of the transformation is $\Omega = e^\rho$.

So far, so good. These new coordinates will lead to a different set of solutions of the Klein-Gordon equation and as a result a new set of modes. As previously stated, we can expand the field operator ϕ in terms of these modes, and interpret the operator coefficients as creation and annihilation operators. By doing this, we get a different representation of the same Hilbert space and a different Fock space; in particular, the vacuum states will be different. The new Minkowski vacuum $|\tilde{0}_M\rangle$, satisfies

$$\hat{a}_k|\tilde{0}_M\rangle = 0. \quad (3.58)$$

3.3 Toy-model of Cosmological Expansion

Our toy model for cosmological expansion consists of a massless scalar field upon the 2D Minkowski spacetime with a boundary. In particular, we are interesting in studying 2D conformal field theory with a moving mirror. This section is based on reference [1]; see [2] for a complete overview of moving mirrors.

In a typical moving mirror setup, considering the 2D Minkowski spacetime defined by equation (3.1)

$$ds^2 = -dt^2 + dx^2 = -dt^+ dt^-, \quad \text{with} \quad t^\pm = t \pm x, \quad (3.59)$$

one initially places a mirror, which is the boundary $\partial\Sigma$, at $x = 0$, so that the physical space Σ is given by $x > 0$, see Fig (3.3).

Next, the location of the mirror moves according to $x = Z(t)$, as sketched in the left picture in Fig. (3.4). The physical picture of our spacetime consists of moving modes that begin from the past null infinity \mathcal{I}_R^- , reflect upon the mirror and end up propagating to the future null infinity \mathcal{I}_R^+ .

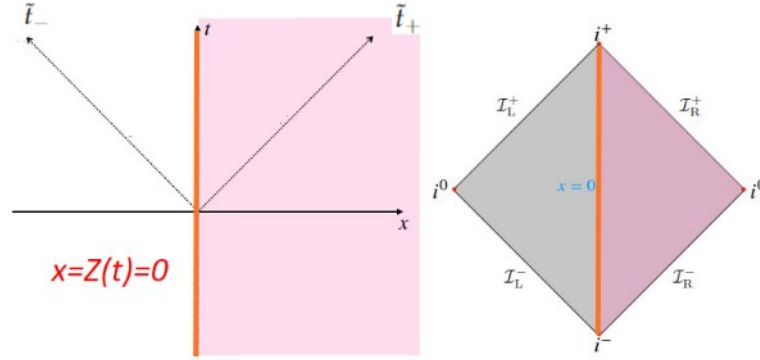


FIGURE 3.3: Minkowski spacetime with a static mirror located at $x = 0$.

Although we are going to choose a specific trajectory for the moving mirror later on, simplifications occur with mapping the original configuration to the simple setup of a boundary 2D conformal field theory with a static mirror by employing conformal transformations, see right picture in Fig. (3.4).

We start from a vacuum state in the static mirror tilde-coordinates, in 2D Minkowski with

$$ds^2 = -d\tilde{t}^2 + d\tilde{x}^2 = -d\tilde{t}^+ d\tilde{t}^-, \quad \tilde{t}_\pm = \tilde{t} \pm \tilde{x}, \quad (3.60)$$

where \tilde{t}_+, \tilde{t}_- denote advanced and retarded (null) vacuum coordinates on $\mathcal{I}_R^-, \mathcal{I}_R^+$, respectively. The static mirror as the boundary $\partial\Sigma$ is a timelike straight line located at $\tilde{x} = 0$, i.e., $\tilde{t}_- = \tilde{t}_+$. In sec. 3.2.2 we saw that the vacuum coordinates (t^+, t^-) and $(\tilde{t}^+, \tilde{t}^-)$ could be related by a conformal transformation. Assuming that in this particular case the coordinates are related by a chiral conformal transformation as follows

$$\tilde{t}^- = p(t^-), \quad \tilde{t}^+ = q(t^+) = t^+, \quad (3.61)$$

one can also map the static mirror with $\tilde{t}_- = \tilde{t}_+$ to a moving mirror at $x = Z(t)$ by using the reflection boundary condition

$$t^+ = p(t^-), \quad (3.62)$$

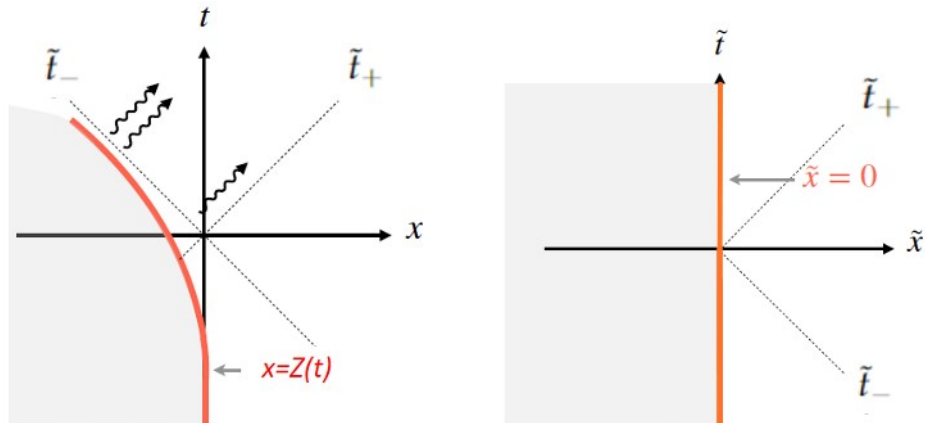


FIGURE 3.4: Caption

or

$$t(t^-) = \frac{p(t^-) + t^-}{2}, \quad (3.63)$$

$$x(t^-) = Z(t^-) = \frac{p(t^-) - t^-}{2}. \quad (3.64)$$

Using equation (3.57) and (3.62) it is straight forward to find that the metric, in vacuum coordinates, takes the form

$$ds^2 = -e^{2\rho} d\tilde{t}^- dt^+, \quad \rho = -\frac{1}{2} \log \partial_- \tilde{t}^- = -\frac{1}{2} \log \partial_- p(t^-). \quad (3.65)$$

Since the state in $(\tilde{t}^+, \tilde{t}^-)$ corresponds to the vacuum state, we would have a vanishing stress-energy tensor $T_{\tilde{t}^+ \tilde{t}^+} = T_{\tilde{t}^- \tilde{t}^-} = 0$. Therefore after performing the conformal transformation of equation (3.61), we can evaluate the energy flux in terms of the Schwarzian derivative. Namely, using equations (A.30)³ and (A.31) from Appendix A we find

$$T_{--} = \left(\frac{d\tilde{t}^-}{dt^-} \right) T_{\tilde{t}^- \tilde{t}^-} + \frac{1}{2\pi} \frac{c}{12} \{ \tilde{t}^-, t^- \} \quad (3.66)$$

$$= \frac{c}{24\pi} \left(\frac{3}{2} \left(\frac{p''(t^-)}{p'(t^-)} \right)^2 - \frac{p'''(t^-)}{p'(t^-)} \right), \quad (3.67)$$

where c denotes the central charge of the CFT we are interested in and the prime corresponds to the (partial) derivative with respect to t^- . It is clear that the non-vanishing energy flux is completely determined by the mapping function $p(t^-)$, *i.e.*, by the trajectory of the mirror.

A better suited form of equation (3.67) for the moving mirror model is obtained by using equation (3.65) and the identity $e^{-\rho} \partial_-^2 e^\rho = \partial_-^2 \rho + (\partial_- \rho)^2$ to get

$$T_{--} = \frac{c}{24\pi} e^{-\rho} \partial_-^2 e^\rho. \quad (3.68)$$

3.3.1 Entanglement Entropy in Moving Mirrors

An important quantity for measuring the spacetime expansion of our toy-model is entanglement entropy; see [68, 7]. In sec. 2.2 we have discussed the concept of entanglement entropy, and evaluated it for finite intervals relative to the vacuum state of conformal field theories in 1 + 1 dimensions. Since the high-energy modes responsible for the divergence are not easily excited, however, we might expect that the divergent piece of the entanglement entropy will not change if we evaluate it relative to some other low-energy state. This suggests that the difference between the entanglement entropy of a given state and that of the vacuum is a finite quantity characterizing an interesting physical property of the state.

To an observer far to the right of the mirror, the moving mirror manifests itself as a change in the radiation field compared to the case of a stationary mirror. Thus each mirror trajectory corresponds to a state. It is natural to identify the stationary mirror with the vacuum.

Let us use this procedure to calculate the entanglement entropy as seen by a distant observer. Our observer will have access to a finite interval $[\tilde{t}_1^-, \tilde{t}_2^-]$ upon the null

³There is an extra rescaling factor $1/2\pi$ which helps the calculations that concern moving mirrors.

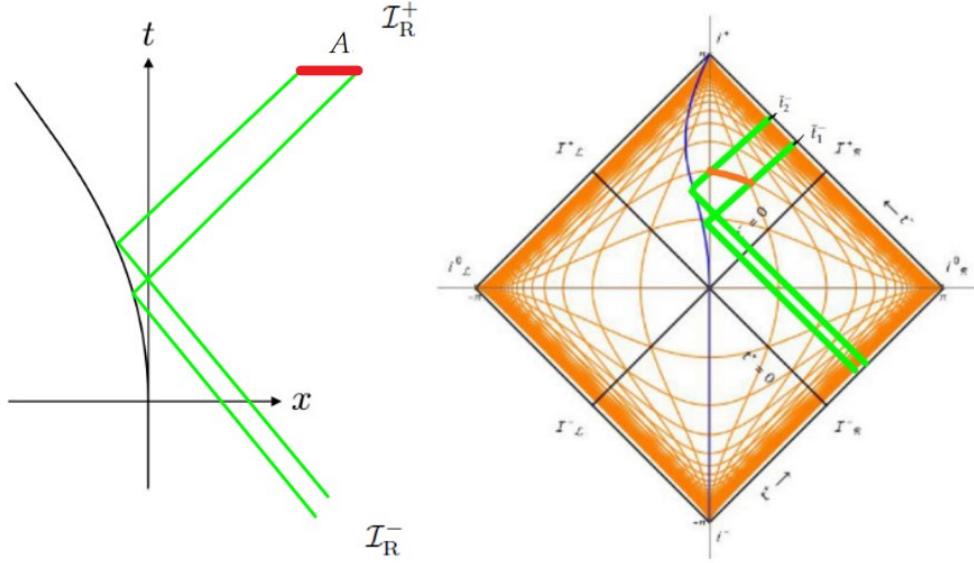


FIGURE 3.5: The green field modes reflect upon the blue mirror trajectory and arrive at the region $[\tilde{t}_1^-, \tilde{t}_2^-]$. We illustrated only the boundary green modes of the interval, there are also in-between modes that arrive at $[\tilde{t}_1^-, \tilde{t}_2^-]$. The quantum state on the interval $[\tilde{t}_1^-, \tilde{t}_2^-]$ is equivalent to a state defined upon the red spacelike interval.

future infinity \mathcal{I}_R^+ , which we will call it A . This interval is light-like so the material observer can not choose it as her or his world line; nevertheless it is possible to monitor a null interval $[\tilde{t}_1^-, \tilde{t}_2^-]$ by appropriate organization of the measuring apparatus, see ssec. 2.1.4. For right-moving modes, as we consider, it is only necessary to monitor a surface that intersected by the same light-rays; this surface can be chosen spacelike or even at a fixed time, see Fig. (3.5).

Applying equation (2.44) we should take $\bar{c} = 0$ since we only consider one set of modes. In this case, the entanglement entropy takes the form

$$S_{ent}(t^-) = \frac{c}{6} \log \frac{\tilde{t}_2^- - \tilde{t}_1^-}{\tilde{\epsilon}}. \quad (3.69)$$

It is natural for the observer to choose the cutoff at the ends of the interval symmetrically as seen in her or his coordinate system. In our case that is

$$\tilde{\epsilon} = \partial_- \tilde{t}^-(t^-) \epsilon. \quad (3.70)$$

This choice corresponds to an asymmetric choice of cutoff in the tilde-coordinate system, where the mirror is stationary. The expression of equation (3.69) for the entropy in the vacuum state is valid in the coordinate system where the mirror is stationary. For an asymmetric choice of smearing we can use the fact that $\tilde{\epsilon} = \sqrt{\tilde{\epsilon}_1 \tilde{\epsilon}_2}$. Plugging into equation (3.69) and using equation (3.62), we find

$$S_{ent}(t^-) = \frac{c}{12} \log \frac{(\tilde{t}_2^- - \tilde{t}_1^-)^2}{\tilde{\epsilon}_1 \tilde{\epsilon}_2} = \frac{c}{12} \log \frac{(p(t_2^-) - p(t_1^-))^2}{\partial_- p(t_1^-) \partial_- p(t_2^-) \epsilon^2}. \quad (3.71)$$

When expressed in terms of the new $(\tilde{t}^-, \tilde{t}^+)$ vacuum coordinates, the Minkowski spacetime metric takes the form of equation (3.65) where

$$\rho = -\frac{1}{2} \log \partial_- \tilde{t}^- = -\frac{1}{2} \log \partial_- p(t^-). \quad (3.72)$$

In terms of this metric, the expression for the entropy becomes

$$S_{ent} = \frac{c}{6}(\rho_1 + \rho_2) + \frac{c}{12} \log \frac{(p(t_2^-) - p(t_1^-))^2}{\epsilon^2}. \quad (3.73)$$

Clearly the entropy of the system is infinite in the limit $\epsilon \rightarrow 0$.

However, the observer would find this infinity even if the mirror were not moving at all, *i.e.* if observation were made in vacuum. It is therefore natural to define the renormalized version of entanglement entropy to be

$$S_{ren} = S_{ent} - S_{ent}|_{vac}, \quad (3.74)$$

where $S_{ent}|_{vac}$ is the entropy expected for a stationary mirror, that is, for $\tilde{t}^- = p(t^-) = t^-$. The renormalized entropy S_{ren} is

$$S_{ren} = \frac{c}{6}(\rho_1 + \rho_2) + \frac{c}{12} \log \frac{(p(t_2^-) - p(t_1^-))^2}{(t_2^- - t_1^-)^2}, \quad (3.75)$$

and it is independent of the cutoff ϵ , and in particular it is finite as $\epsilon \rightarrow 0$. This is the physical entropy. It is a property of the state of the system, which expresses the information content of the state.

Remark: A useful case is when an observer is measuring the entanglement entropy in a semi-infinite line $(-\infty, \tilde{t}^-(t^-)]$, see Fig (3.6) and [7].

This is characterized by the entanglement entropy of the portions of the quantum state on \mathcal{I}_R^+ before and after \tilde{t}^- , and as an extrapolation of the fact that $\tilde{t}^-(t^-)$ we will often say before and after t^- . This set up corresponds to taking the limit $t_1^- \rightarrow -\infty$ and relabelling $t_2^- \mapsto t^-$ in the equation (3.75) of the renormalized entropy. By imposing an extra assumption of the form $\partial_- p(t^-) \rightarrow 1$ as $t^- \rightarrow -\infty$, it is easy to see that,

$$\begin{aligned} \lim_{t_1^- \rightarrow -\infty} \frac{c}{12} \log \frac{(p(t^-) - p(t_1^-))^2}{(t^- - t_1^-)^2} &= \lim_{t_1^- \rightarrow -\infty} \frac{c}{6} \log \frac{p(t_1^-)}{t_1^-} = \lim_{t_1^- \rightarrow -\infty} \frac{c}{6} \log \partial_- p(t_1^-) = 0, \\ \lim_{t_1^- \rightarrow -\infty} \rho(t_1^-) &= \lim_{t_1^- \rightarrow -\infty} \left(-\frac{1}{2} \log \partial_- p(t_1^-) \right) = 0, \\ \lim_{t_1^- \rightarrow -\infty} S_{ren} &= \frac{c}{6} \rho(t^-), \end{aligned} \quad (3.76)$$

where in the last equality of the first equation we used the l'Hospital's limit rule(ref).

The physical meaning of our assumption $\partial_- p(t^-) \rightarrow 1$ as $t^- \rightarrow -\infty$ is that the moving mirror is initially located at the past timelike infinity i^- . This can be seen in the line element on the moving mirror. Using equations (3.60),(3.62) and (3.63) we find

$$ds^2|_{Mirror} = -\partial_- p(t^-) dt^{-2} = -\partial_- p(t^-) \left(\frac{2}{\partial_- p(t^-) + 1} \right)^2 dt^2, \quad (3.77)$$

which simply implies that, in general, the moving mirror is timelike when $\partial_- p(t^-) >$

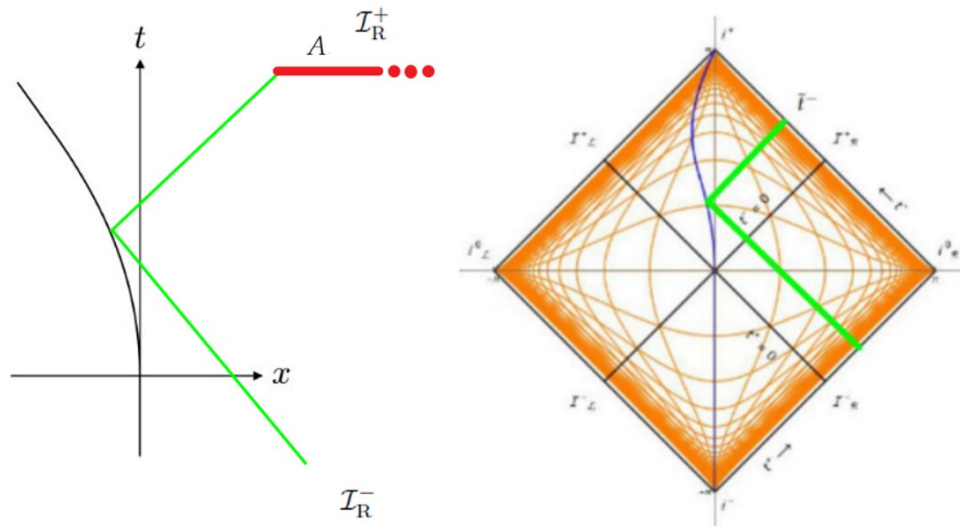


FIGURE 3.6: Every mode that reflects upon the mirror and arrives at $(-\infty, \tilde{t}^-]$ belongs to the quantum state on the semi-infinite interval. We illustrated with green colour only the last mode that belongs in this state. Again, the quantum state is equally defined in any semi-infinite spacelike interval with one point being the intersection point with the right green moving mode and the other point being the right spacelike infinity.

0 and by taking the limit of $t^- \rightarrow -\infty$ the mirror is placed at the past timelike infinity i^- . This is the setup that we are going to use later on a specific application of moving mirrors.

3.3.2 Direct Analysis of Massless Free Scalar CFT

In the present subsection, we discuss the explicit quantization of a free massless scalar field ϕ in 2D Minkowski spacetime with a moving mirror; see [1]. We urge the reader to revise ssec. 3.2 where we have set the basics of scalar field quantization. The field equation (3.13) reads

$$\frac{\partial^2 \phi}{\partial t^- \partial t^+} = 0. \quad (3.78)$$

The scalar field ϕ shall satisfy the reflection boundary condition (3.62), *i.e.*

$$\phi(t, Z(t)) = 0, \quad (3.79)$$

where $Z(t)$ denotes the moving boundary of the spatial direction.

A complete set of positive frequency modes, *i.e.* solutions to (3.78) and (3.79), is given by

$$\phi_\omega = H(\omega t^+) + G(\omega t^-) \quad (3.80)$$

where $\omega = k$, with H and G being arbitrary functions, *cf.* equation (3.14). More specifically, we may write the incoming mode as

$$\phi_{\omega'}^{in} = i(4\pi\omega')^{-1/2} (e^{-i\omega' t^+} - e^{-i\omega' p(t^-)}). \quad (3.81)$$

You can check that the equation for the boundary condition of the field (3.79) is satisfied with the use of the reflection boundary condition (3.62). Intuitively, the

incoming mode is a combination of a standard incoming Minkowski mode $e^{-i\omega't^+}$ from \mathcal{I}_R^- and a complicated one $e^{-i\omega'p(t^-)}$ due to the reflection upon the moving mirror. An incoming mode function describing Minkowski spacetime with a static boundary would correspond to $p(t^-) = t^-$, hence

$$\phi_{\omega'}^{in}(t, x) = (\pi\omega')^{-1/2} \sin(\omega'x)e^{-i\omega't}. \quad (3.82)$$

The field ϕ can be expanded in terms of the incoming mode,

$$\phi = \int_0^\infty d\omega' [a_{\omega'}\phi_{\omega'}^{in} + a_{\omega'}^\dagger\phi_{\omega'}^{in*}], \quad (3.83)$$

where $a_{\omega'}$ and $a_{\omega'}^\dagger$ are the standard annihilation and creation operators, such that $a|0\rangle_{in} = 0$ and $|0\rangle_{in}$ is the incoming vacuum state at \mathcal{I}_R^- .

Alternatively, the outgoing mode can be expressed as

$$\phi_\omega^{out} = i(4\pi\omega)^{-1/2} (e^{-i\omega f(t^+)} - e^{-i\omega t^-}), \quad (3.84)$$

where $f \equiv p^{-1}$. Again intuitively the outside mode is a combination of a regular Minkowski mode $e^{-i\omega t^-}$ on \mathcal{I}_R^+ and a complicated one $e^{-i\omega f(t^+)}$ due to reflection upon a moving mirror with an inverse trajectory.

Similarly, the field ϕ can also be expanded in terms of the outgoing mode

$$\phi = \int_0^\infty d\omega [b_\omega\phi_\omega^{out} + b_\omega^\dagger\phi_\omega^{out*}], \quad (3.85)$$

where b_ω and b_ω^\dagger correspond to the annihilation and creation operators defined with respect to the outgoing vacuum state $|0\rangle_{out}$ at \mathcal{I}_R^+ , such that $b|0\rangle_{out} = 0$.

One can expand the positive frequency modes ϕ_ω^{out} at \mathcal{I}_R^+ in terms of the positive frequency modes $\phi_{\omega'}^{in}$ at \mathcal{I}_R^- and vice versa, means

$$\phi_\omega^{out} = \int d\omega' [\alpha_{\omega\omega'}^*\phi_{\omega'}^{in} - \beta_{\omega\omega'}\phi_{\omega'}^{in*}], \quad (3.86)$$

$$\phi_{\omega'}^{in} = \int d\omega [\alpha_{\omega\omega'}^*\phi_\omega^{out} + \beta_{\omega\omega'}\phi_\omega^{out*}], \quad (3.87)$$

where

$$\alpha_{\omega\omega'} = (\phi_\omega^{out}, \phi_{\omega'}^{in}), \quad \beta_{\omega\omega'} = -(\phi_\omega^{out}, \phi_{\omega'}^{in*}), \quad (3.88)$$

are the corresponding Bogoliubov coefficients, cf. equations (3.45), (3.46). The scalar product in equation (3.88) is defined as

$$(\phi_1, \phi_2) = -i \int_\Sigma (\phi_1 \partial_\mu \phi_2^* - \phi_2^* \partial_\mu \phi_1) d\Sigma^\mu, \quad (3.89)$$

where Σ is a Cauchy surface. The mode functions are orthonormal with respect to this scalar product,

$$(\phi_\omega, \phi_{\omega'}) = \delta(\omega - \omega'), \quad (\phi_\omega, \phi_{\omega'}^*) = 0. \quad (3.90)$$

The number of particles that are detected by an observer due to the motion of the moving mirror can be found by using equation (3.31) for the continuum case

$$\langle 0_{in} | \hat{n}_{out} | 0_{in} \rangle = \int_{\omega'} d\omega' |\beta_{\omega\omega'}|^2. \quad (3.91)$$

Remark: In this section we used the Heisenberg picture of quantum field theory. We took the state to be a solution to the equation of motion/ the field equation for all times. There was clearly a set of states that looked like energy eigenstates at early times, although they don't look that way in the future; we called such states the "in states". There was also a separate set of states that looked like energy eigenstates at late times, correspondingly called "out states". Both sets of states exist at all times, but they looked like energy eigenstates only in the appropriate asymptotic regime.

The Heisenberg picture will be used only in the calculation of the average number of particles due to the moving mirrors. Elsewhere, we will use the Schrödinger picture where there is a time dependence and evolution of each state.

3.3.3 Receding Mirror

It is already obvious that our toy model consists of a free scalar, upon the Minkowski spacetime, in the presence of a mirror. For our chosen trajectory of the moving mirror there will be no \mathcal{I}_L^\pm . We take the incoming state to be the vacuum on \mathcal{I}_R^- , cf. ssec. 2.1.4 and 2.1.5, and the mirror to be initially stationary; then the mirror accelerates away from infinity for a retarded time L on \mathcal{I}_R^+ , and then moves inertially. This models an expanding universe because the volume of spacetime is increasing. The mirror trajectory is described by the reflection boundary condition, equation (3.62), with

$$p(t^-) = t^-, \quad t^- < 0, \quad (3.92)$$

$$= \frac{1}{2\pi T_H} (1 - e^{-2\pi T_H t^-}), \quad 0 < t^- < L, \quad (3.93)$$

$$= e^{-2\pi T_H L} (t^- - L) + \frac{1}{2\pi T_H} (1 - e^{-2\pi T_H L}), \quad t^- > L. \quad (3.94)$$

Note that the final trajectory emerges from the initial one under a Poincaré transformation, *i.e.* equation (3.4), with

$$u = \frac{1 - e^{4\pi T_H L}}{1 + e^{4\pi T_H L}},$$

$$t_0^- = \frac{1}{2\pi T_H} (1 - e^{-2\pi T_H L}) - L e^{-2\pi T_H L}.$$

The outgoing state is the vacuum state on \mathcal{I}_R^+ with respect to the vacuum coordinates (t^+, \tilde{t}^-) . In Fig. (3.7), you can see an example of the mirror trajectory on the Penrose diagram.

We denote the initial state of the full system at null past infinity \mathcal{I}_R^- to be

$$\rho = |0_{in}\rangle\langle 0_{in}|, \quad (3.95)$$

which is the vacuum in Minkowski spacetime with a boundary. In the case of a static mirror in (t^+, t^-) -coordinates, the modes of the vacuum state at \mathcal{I}_R^- propagate, reflect upon the mirror and arrive at \mathcal{I}_R^+ unchanged. Let us divide the null infinity \mathcal{I}_R^+ into a region A prior to a fixed retarded time t^- and a region B later than t^- . The reduced density matrix in region A is

$$\rho_A \equiv tr_B \rho \quad (3.96)$$

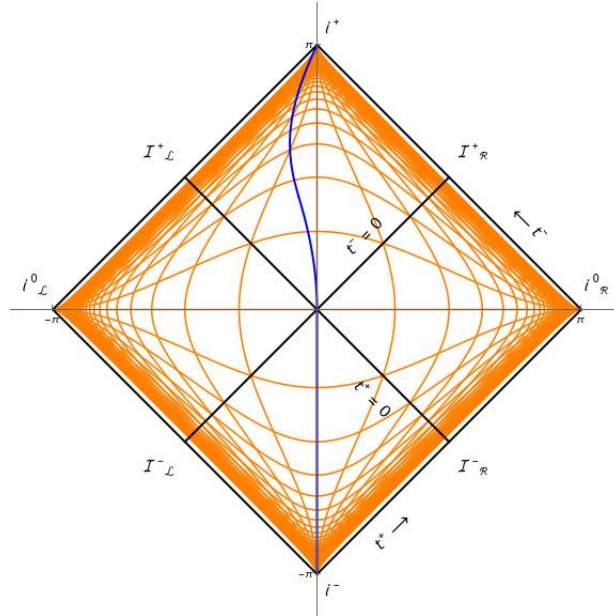


FIGURE 3.7: Mirror trajectory depicted by the blue curve for $T_H = 1/2\pi$ and $L = 1$.

As argued before ssec. 2.1.4, a state that is defined upon a null surface is equivalent to a state defined upon a spacelike surface in which their points are causally connected. As a result, the state in the region A on null infinity \mathcal{I}_R^+ is equivalent to a state on a constant-time surface. The time-slice that we choose could be arbitrary, see Fig. 3.6 for an example.

The path integral representation of ρ_A^4 , equation (3.96), is

$$\langle \phi_2 | \rho_A | \phi_1 \rangle = \sum_{\tilde{\phi}} \langle \tilde{\phi}, \phi_2 | 0 \rangle \langle 0 | \phi_1, \tilde{\phi} \rangle$$

$$= \frac{\text{Diagram 1}}{\text{Diagram 2}} \quad (3.97)$$

The upper half of this diagram corresponds to the transition amplitude $\sum_{\tilde{\phi}} \langle \tilde{\phi}, \phi_2 | 0 \rangle$ and the lower half to the transition amplitude $\langle 0 | \phi_1, \tilde{\phi} \rangle$. The trace sums over fields in region B, which glues together slits in the path integral, so in fact

$$\langle \phi_2 | \rho_A | \phi_1 \rangle = \text{Diagram 3} \quad (3.98)$$

⁴In Euclidean spacetime signature but one could easily Wick rotate back to Minkowskian.

Now comes the key observation: we can re-slice this path integral by going to the new vacuum coordinates (t^+, \tilde{t}^-) , and calling \tilde{t}^- 'time'. Let \tilde{H} be the operator that generates \tilde{t}^- -evolution. That is,

$$\frac{1}{\hbar}[\tilde{H}, O] = \frac{\partial O}{\partial \tilde{t}^-} \quad (3.99)$$

for any operator O . In the intermediate accelerating phase, \tilde{t}^- is invariant under $t^- \rightarrow t^- + \frac{i}{T_H}$. Then we can translate this *same* path integral back into operator language in a different way. That is, the path integral (3.98) is equal to $\langle \phi_2 | e^{-\frac{1}{T_H} \tilde{H}} | \phi_1 \rangle$, cf. ssec. 2.1.8. Therefore

$$\rho_A = e^{-\frac{1}{T_H} \tilde{H}} \quad (3.100)$$

This look just like a thermal state at temperature T_H ⁵. Inertial detectors do not move along lines of constant $\tilde{t}^- - t^+$ and so will detect particles. Outside the time period $0 < t^- < L$ the mirror is inertial and there is no detection of particles at infinity.

A way to see particle creation due to the acceleration of the mirror is by examining the entanglement entropy $S_{ent}(t^-)$ of the state ρ_A . In vacuum coordinates (t^+, \tilde{t}^-) the Minkowskian metric takes the form, see equation (3.65),

$$ds^2 = -e^{2\rho} d\tilde{t}^- dt^+ \quad \rho = -\frac{1}{2} \log \partial_- \tilde{t}^-. \quad (3.101)$$

The entanglement entropy of region A is given by equation (3.76)

$$S_{ent}[\rho_A](t^-) = \frac{c}{6} \rho(t^-), \quad (3.102)$$

where $\rho(t^-)$ is given in equation (3.101). For a free scalar field $c = 1$. We find

$$S_{ent}[\rho_A] = 0, \quad t^- < 0 \quad (3.103)$$

$$= \frac{\pi c T_H t^-}{6}, \quad 0 < t^- < L, \quad (3.104)$$

$$= \frac{\pi c T_H L}{6}, \quad t^- > L. \quad (3.105)$$

This can be compared to the formula for the stress-energy tensor and the expectation value of the particle number operator.

For the stress-energy tensor (3.68) we find

$$T_{--} = \frac{c}{12\pi} e^{-\rho} \partial_-^2 e^\rho = 0, \quad t^- < 0, \quad (3.106)$$

$$= \frac{c\pi T_H^2}{12}, \quad 0 < t^- < L, \quad (3.107)$$

$$= 0, \quad t^- > L, \quad (3.108)$$

which is thermal during the acceleration phase.

To compute the expectation value of the number operator (3.51) we need to calculate the Bogoliubov coefficient $\beta_{\omega\omega'}$ (3.88). The calculation of $\beta_{\omega'\omega}$ is done on \mathcal{I}_R^+ .

⁵In fact, \tilde{H} is a Hamiltonian like operator since we are in the massless case. One can easily check that the acceleration is invariant under $t \rightarrow t + \frac{i}{T_H}$. So, if one is pedantic the same reasoning applies for the Hamiltonian operator H that generates t -evolution.

Using the equations (3.88,3.89) we get

$$\beta_{\omega'\omega} = i \int_{-\infty}^{\infty} dt^- (\phi_{\omega'}^{out} \partial_- \phi_{\omega'}^{in} - \phi_{\omega'}^{in} \partial_- \phi_{\omega'}^{out}) = -2i \int_{-\infty}^{\infty} dt^- \phi_{\omega'}^{in} \partial_- \phi_{\omega'}^{out}, \quad (3.109)$$

where we integrated by parts and used the fact that modes vanish at infinite distances. The modes take the form, see equations (3.81,3.84),

$$\phi_{\omega'}^{in} = i(4\pi\omega')^{-\frac{1}{2}} (e^{-i\omega't^+} - e^{-i\omega'p(t^-)}), \quad \phi_{\omega'}^{out} = i(4\pi\omega)^{-\frac{1}{2}} (e^{-i\omega f(t^+)} - e^{-i\omega t^-}). \quad (3.110)$$

Plugging into (3.109) yields,

$$\beta_{\omega'\omega} = -\frac{1}{2\pi} \left(\frac{\omega}{\omega'}\right)^{\frac{1}{2}} \int_{-\infty}^{\infty} dt^- e^{-i\omega t^- - i\omega' p(t^-)}, \quad (3.111)$$

where we used the identity $\delta(\omega) = \int_{-\infty}^{\infty} dx e^{-i\omega x}$; see [25] for an overview of beta coefficients for moving mirror trajectories.

For our inertial trajectories (3.92,3.94) the Bogoliubov coefficient is vanishing since

$$\beta_{\omega'\omega}|_{3.92} = -\frac{1}{2\pi} \left(\frac{\omega}{\omega'}\right)^{\frac{1}{2}} \int_{-\infty}^{\infty} dt^- e^{-i\omega t^- - i\omega' t^-} = -\frac{1}{2\pi} \left(\frac{\omega}{\omega'}\right)^{\frac{1}{2}} \delta(\omega' + \omega) = 0, \quad (3.112)$$

$$\begin{aligned} \beta_{\omega'\omega}|_{3.94} &= -\frac{1}{2\pi} \left(\frac{\omega}{\omega'}\right)^{\frac{1}{2}} \int_{-\infty}^{\infty} dt^- e^{-i\omega t^- - i\omega' e^{-2\pi T_H L} t^-} e^{+i\omega' L e^{-2\pi T_H L} - \frac{i\omega'}{2\pi T_H} (1 - e^{-2\pi T_H L})} \\ &= -\frac{1}{2\pi} \left(\frac{\omega}{\omega'}\right)^{\frac{1}{2}} e^{+i\omega' L e^{-2\pi T_H L} - \frac{i\omega'}{2\pi T_H} (1 - e^{-2\pi T_H L})} \delta(\omega' e^{-2\pi T_H L} + \omega) = 0, \end{aligned} \quad (3.113)$$

where again we used the identity $\delta(\omega + \omega') = \int_{-\infty}^{\infty} dx e^{-i(\omega + \omega')x}$. It is to be expected that there is no particle creation in the non-accelerating phases of our trajectory since the Minkowski vacuum is invariant under Poincaré transformations, *cf.* end of ssec. 3.2.1 and the stress-energy tensor (3.106,3.108) was zero. For the intermediate accelerating phase (3.93), we anticipate the Bogoliubov coefficient to correspond with the black-body radiation spectrum. We already have hints towards this direction from the value of the stress-energy tensor (3.107) that is proportional to T_H^2 . In addition, the path integral derivation of the state (3.96) utilized only the symmetries of our spacetime and we ended up with a thermal state (3.100) with temperature T_H . The calculation of the Bogoliubov coefficient is as follows⁶,

$$\begin{aligned} \beta_{\omega'\omega}|_{3.93} &= -\frac{1}{2\pi} \left(\frac{\omega}{\omega'}\right)^{\frac{1}{2}} \int_{-\infty}^{\infty} dt^- e^{-i\omega t^- - \frac{i\omega'}{2\pi T_H} (1 - e^{-2\pi T_H t^-})} \\ &= -\frac{1}{2\pi} \left(\frac{\omega}{\omega'}\right)^{\frac{1}{2}} e^{\frac{-i\omega'}{2\pi T_H}} \int_{-\infty}^{\infty} dt^- e^{-i\omega t^- + \frac{i\omega'}{2\pi T_H} e^{-2\pi T_H t^-}}, \end{aligned} \quad (3.114)$$

using the substitution $e^t = -\frac{i\omega'}{2\pi T_H} e^{-2\pi T_H t^-} \rightarrow t = \log\left(-\frac{i\omega'}{2\pi T_H}\right) - 2\pi T_H t^-$, where $dt = -2\pi T_H dt^-$, gives

$$\beta_{\omega'\omega}|_{3.93} = -\frac{1}{4\pi^2 T_H} \left(\frac{\omega}{\omega'}\right)^{\frac{1}{2}} e^{\frac{-i\omega'}{2\pi T_H}} e^{-\frac{i\omega}{2\pi T_H} \log\left(\frac{-i\omega'}{2\pi T_H}\right)} \int_{-\infty}^{\infty} dt^- e^{\frac{i\omega}{2\pi T_H} t^- - e^t}, \quad (3.115)$$

⁶Actually, the beta coefficient $\beta_{\omega'\omega}|_{3.93}$ is the 'Right' bogolubov coefficient, in the Carlitz-Willey construction [16].

where we now use $\Gamma(z) = \int_{-\infty}^{\infty} dt e^{zt-e^t}$ and $-\frac{i\omega}{2\pi T_H} \log\left(\frac{-i\omega}{2\pi T_H}\right) = -i\left(\frac{\omega}{2\pi T_H}\right)^2 - \frac{\omega}{4T_H}$ to obtain

$$\beta_{\omega'\omega}|_{3.93} = -\frac{1}{4\pi^2 T_H} \left(\frac{\omega}{\omega'}\right)^{\frac{1}{2}} e^{-i\left(\frac{\omega}{2\pi T_H}\right)^2} e^{-\frac{\omega}{4T_H}} \Gamma\left(i\frac{\omega}{2\pi T_H}\right). \quad (3.116)$$

With the use of Bogoliubov coefficient we can calculate the expectation value of the number of particles (3.91) that are created. This is

$$\begin{aligned} \langle 0_{in} | \hat{n}_{out} | 0_{in} \rangle &= 0, & t^- < 0, \\ &= \int_{\omega'} d\omega' \frac{1}{4\pi^2 T_H \omega'} \frac{1}{e^{\frac{\omega}{T_H}} - 1}, & 0 < t^- < L, \\ &= 0, & t^- > L. \end{aligned}$$

As you can see, in the intermediate accelerating phase there is particle creation. It precisely matches with the well known black-body radiation spectrum as obtained by Hawking [38].

Therefore the entanglement entropy is zero prior to acceleration, increases as expected for thermal radiation/particle production at temperature T_H during acceleration, and then remains constant afterward. The same pattern is followed by the stress-energy tensor and the expectation value of the number operator until $t^- = L$. After $t^- = L$ both of them vanish. As we will see in a moment, this is due to the fact that there is no involvement of a UV-cutoff in the calculation of these physical quantities and the fact that the entropy formula gather information from the initial moment $t^- \rightarrow \infty$ until t^- while the other two quantities are calculated in a given t^- regardless of the past.

Perhaps one should have anticipated entropy to be trivial/zero in the limit of the entanglement point t^- going to future timelike infinity i^+ . At the end of the day, our toy-model consists of the Minkowski spacetime with a boundary and the quantum field theories' rules, where a pure quantum vacuum state at past null infinity \mathcal{I}_R^- propagates in time, reflects upon the mirror and arrives at the future null infinity \mathcal{I}_R^+ . There is no reason for information loss. The state on \mathcal{I}_R^+ should be pure and indeed it is manifestly pure.

Recall from ssec. 3.3.1 that in the calculation for entanglement entropy we regulated for the UV divergences. In particular, we threw away the entanglement across t^- of modes with proper wavelength shorter than the UV cutoff. However during acceleration, the wavelengths above the cutoff from \mathcal{I}_R^- reflect upon the mirror and get red-shifted into the IR below the cutoff before they reach \mathcal{I}_R^+ . After the end of the acceleration phase, there is a total residual Doppler red-shift for wavelengths above the cutoff in \mathcal{I}_R^- to wavelengths below the cutoff in \mathcal{I}_R^+ . Hence some wavelengths on \mathcal{I}_R^- which do not contribute to the entanglement on \mathcal{I}_R^+ in the early period do contribute in the late period because the cutoff is shifted. This can be seen from equation (3.70) in the region of the trajectory of the mirror (3.94) where t^- approaches future timelike infinity

$$\tilde{\epsilon} = \frac{1}{e^{2\pi T_H L}} \epsilon. \quad (3.117)$$

Besides cosmological expansion, these phenomenon is potentially relevant to the black hole information paradox [47]. This ambiguity arises due to the ill-defined nature of entropy and its pathological divergences which need to be nourished. Surprisingly, an experimentalist stationed at \mathcal{I}_R^+ , uniformed of these subtleties will never see the purity of the quantum state restored for any finite t^- and will conclude that information is destroyed.

In our toy-model, the effective Hilbert space - composed of modes below the cutoff- is larger on \mathcal{I}_R^+ than on \mathcal{I}_R^- as a consequence of the expansion of the bulk space and associated new degrees of freedom due to red-shifting. Hence there is no effective unitary description no matter the choice of the UV cutoff. In the following sections we will see that the map from the in to the out Hilbert space can be effectively described by an isometry.

Chapter 4

Cosmology

In this chapter we examine particular expanding cosmologies by utilizing entanglement entropy. Again, our calculation of entropy includes a cutoff pointing us to an effective field theory approach to the upcoming cosmological models. Our goal is to explore the time evolution of the effective Hilbert space of certain spacetime regions in these models.

The organization of the chapter goes as follows. In sec. 4.1 we calculate the entanglement entropy in curved spacetimes. Next, in sec. 4.2 and sec. 4.3 we apply the result of sec. 4.1 in a closed 1 + 1 and de Sitter cosmology, respectively.

4.1 Entanglement Entropy in Curved Spacetime

In ssec. 3.2.2 we saw that the vacuum state in Minkowski spacetime is defined with respect to a given coordinate system. In moving mirrors we introduced a new null coordinate $\tilde{t}^-(t^-)$, and defined a vacuum relative to this new coordinate. In that case the entanglement entropy of an interval $[\tilde{t}_1^-, \tilde{t}_2^-]$ is given by the equation (3.69). This formula is true for a spacetime with a boundary where we only care about one set of moving modes.

At this stage let us combine together the contributions to the entropy due to the right-moving and left-moving modes and work with a spacetime without a boundary. Our result will be based on the reference [27]. Suppose that the left moving "vacuum" state is defined relative to the coordinate $\tilde{t}^+(t^+)$. We consider a space-like slice Σ , and a region $[P_2, P_1]$ on this slice bounded on the left by the point $(\tilde{t}_2^+, \tilde{t}_2^-)$ and on the right by the point $(\tilde{t}_1^+, \tilde{t}_1^-)$. The quantum state upon $[P_2, P_1]$ is equivalent to the quantum state upon the union of the two null-intervals $[\tilde{t}_1^-, \tilde{t}_2^-]$ and $[\tilde{t}_2^+, \tilde{t}_1^+]$, as shown in Fig. 4.1. The entanglement entropy on $[P_2, P_1]$ is given by

$$S_{ent} = \frac{c}{6} \log \frac{\tilde{t}_2^- - \tilde{t}_1^-}{\tilde{\epsilon}^-} + \frac{c}{6} \log \frac{\tilde{t}_1^+ - \tilde{t}_2^+}{\tilde{\epsilon}^+}, \quad (4.1)$$

where $\tilde{\epsilon}^+, \tilde{\epsilon}^-$ are the cutoffs with respect to the new coordinates $(\tilde{t}^+, \tilde{t}^-)$. As discussed in ssec. 3.3.1 equation (3.70), the cutoffs can be expressed in terms of the original vacuum coordinates (t^+, t^-) . Using an asymmetric choice of the cutoff $\tilde{\epsilon} = \sqrt{\tilde{\epsilon}_1 \tilde{\epsilon}_2}$ we get

$$\tilde{\epsilon}_1^- = \partial_- \tilde{t}^-(t_1^-) \epsilon^-, \quad \tilde{\epsilon}_2^- = \partial_- \tilde{t}^2(t_2^-), \epsilon^- \quad (4.2)$$

$$\tilde{\epsilon}_1^+ = \partial_+ \tilde{t}^+(t_1^+) \epsilon^+, \quad \tilde{\epsilon}_2^+ = \partial_+ \tilde{t}^2(t_2^+) \epsilon^+. \quad (4.3)$$

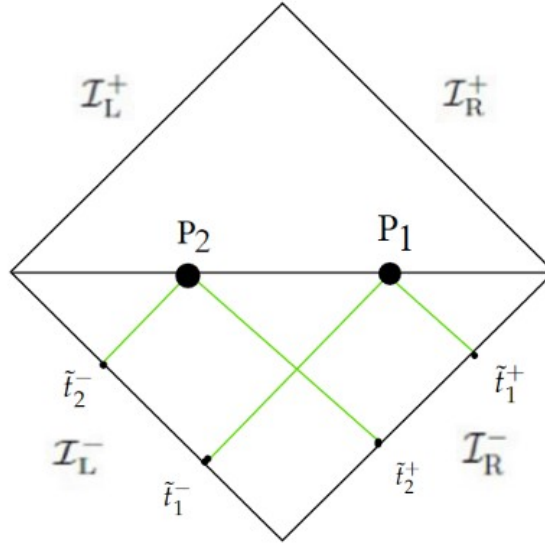


FIGURE 4.1: The spacelike slice Σ is chosen to be at $t = 0$. The state upon $[P_2, P_1]$ is equivalent to the state on $[\tilde{t}_1^-, \tilde{t}_2^-] \cup [\tilde{t}_2^+, \tilde{t}_1^+]$, since these two are causally connected with left and right null rays, which are depicted with green colour.

When the cutoff is expressed in (t^+, t^-) vacuum coordinates, the entanglement entropy (4.1) becomes

$$S_{ent} = \frac{c}{12} \log \frac{(\tilde{t}_2^- - \tilde{t}_1^-)^2}{\partial_- \tilde{t}_1^- \partial_- \tilde{t}_2^- \epsilon^{-2}} + \frac{c}{12} \log \frac{(\tilde{t}_2^+ - \tilde{t}_1^+)^2}{\partial_+ \tilde{t}_1^+ \partial_+ \tilde{t}_2^+ \epsilon^{+2}}, \quad (4.4)$$

where, *e.g.*, ϵ^- denotes the short-distance cutoff, in (t^+, t^-) , on the wavelength of the right-moving modes. By combining together the contributions of the right-movers and the left-movers, we thus obtain an expression that is invariant under Lorentz boosts, for the product $\epsilon^- \epsilon^+$ of the cutoffs on the right-moving and left-moving modes is boost-invariant. This quantity is just (the square of) a proper length measured on the spacelike slice Σ .

When expressed in terms of the new $(\tilde{t}^-, \tilde{t}^+)$ coordinates, the Minkowski spacetime metric is given by equation (3.57). In terms of this metric, the expression (4.4) for the entropy becomes

$$S_{ent} = \frac{c}{6} (\rho_1 + \rho_2) + \frac{c}{12} \log \frac{(\tilde{t}_2^- - \tilde{t}_1^-)^2}{\epsilon^{-2}} + \frac{c}{12} \log \frac{(\tilde{t}_2^+ - \tilde{t}_1^+)^2}{\epsilon^{+2}}, \quad (4.5)$$

where $\rho = -\frac{1}{2} \log \partial_+ \tilde{t}^+ \partial_- \tilde{t}^-$.

This formula has the advantage that it can be applied to curved spacetime as well. In curved spacetime, there is no global inertial frame. But we are free to introduce coordinates $(\tilde{t}^+, \tilde{t}^-)$, and to consider the vacuum state defined by these coordinates. The metric (3.57) is called a conformal metric since it is a product of a scaling factor and a flat metric, while the coordinates that describe this metric are called conformal coordinates. If the spacetime metric has the form of equation (3.57) in terms of the $(\tilde{t}^+, \tilde{t}^-)$ -coordinates, then equation (4.5) gives the entanglement entropy of a system defined by a finite interval upon a spacelike slice. The cutoffs in equation (4.5) are expressed in terms of the locally flat coordinates (t^+, t^-) at the endpoints of the interval, for which the metric takes the form $ds^2 = -dt^+ dt^-$.

We should also remark that, for a given vacuum state, the coordinates $(\tilde{t}^+, \tilde{t}^-)$ are not uniquely defined. We have the freedom to perform a Poincaré $SL(2, \mathbf{C})$ transformation on the coordinates without changing the vacuum, *c.f.* ssec. 3.2.1. It is easy to check that equation (4.4) is Poincaré-invariant. A Poincaré transformation (3.4) from a coordinate system $(\tilde{t}^+, \tilde{t}^-)$ to a coordinate system $(\tilde{t}^{+'}, \tilde{t}^{-'})$ takes the form

$$\begin{cases} \tilde{t}^+ = \frac{1-u}{\sqrt{1-u^2}} \tilde{t}^{+'} + \tilde{t}_0^{+'}, \\ \tilde{t}^- = \frac{1+u}{\sqrt{1-u^2}} \tilde{t}^{-'} + \tilde{t}_0^{-'}. \end{cases} \quad (4.6)$$

Applying equation (4.6) to the equation (4.4) of entanglement entropy we get

$$\begin{aligned} S_{ent} &= \frac{c}{12} \log \frac{\frac{(1+u)^2}{1-u^2} (\tilde{t}_2^{-'} - \tilde{t}_1^{-'} + \tilde{t}_0^{-'} - \tilde{t}_0^{-'})^2}{\frac{(1+u)^2}{1-u^2} \partial_- \tilde{t}_1^{-'} \partial_- \tilde{t}_2^{-'} \epsilon^{-2}} + \frac{c}{12} \log \frac{\frac{(1-u)^2}{1-u^2} (\tilde{t}_2^{+'} - \tilde{t}_1^{+'} + \tilde{t}_0^{+'} - \tilde{t}_0^{+'})^2}{\frac{(1-u)^2}{1-u^2} \partial_+ \tilde{t}_1^{+'} \partial_+ \tilde{t}_2^{+'} \epsilon^{+2}} \\ &= \frac{c}{12} \log \frac{(\tilde{t}_2^{-'} - \tilde{t}_1^{-'} + \tilde{t}_0^{-'})^2}{\partial_- \tilde{t}_1^{-'} \partial_- \tilde{t}_2^{-'} \epsilon^{-2}} + \frac{c}{12} \log \frac{(\tilde{t}_2^{+'} - \tilde{t}_1^{+'})^2}{\partial_+ \tilde{t}_1^{+'} \partial_+ \tilde{t}_2^{+'} \epsilon^{+2}} \\ &= S'_{ent}, \end{aligned}$$

which mean that entanglement entropy is $SL(2, \mathbf{C})$ -invariant. As expected, then, the conformal transformations that preserve the quantum state of the fields also preserve our expression for the entanglement entropy for a finite interval.

4.2 Closed 1+1 Cosmology

Consider a free massless scalar field in a closed 1 + 1 cosmology in conformal coordinates

$$ds^2 = -R^2(\tilde{t}) d\tilde{t}^+ d\tilde{t}^-, \quad \tilde{t}^\pm = \tilde{t} \pm \tilde{\sigma}, \quad \tilde{\sigma} \sim \tilde{\sigma} + 2\pi. \quad (4.7)$$

The radius R is an increasing function and goes to a constant in the far past, $R(-\infty) \equiv R_{-\infty} = \text{constant}$. Hence our cosmology is an expanding one, starting from a minimum radius which grows into the future, see Fig 4.2. The conformal coordinates $\tilde{t}^\pm = \tilde{t} \pm \tilde{\sigma}$ define a vacuum in which inertial detectors in the far past see no particles. A time-slice in our cosmology is a spacelike circle. We divide this circle in half at points $\tilde{t}^+ - \tilde{t}^- = 0, 2\pi$ which is $\tilde{\sigma} = 0, \pi$. We define the upper half of the circle to be region A and the lower half to be region B . We are interested in the entanglement entropy between the states of these regions.

The metric (4.7) is of the conformal form (3.57) with

$$\rho = \log R(\tilde{t}). \quad (4.8)$$

The entanglement entropy is given by equation (4.5). For our region A in any given time-slice it takes the form

$$S_{ent} = \frac{c}{3} \log R(\tilde{t}) + \frac{c}{12} \log \frac{\pi^2}{\epsilon^{-2}} + \frac{c}{12} \log \frac{\pi^2}{\epsilon^{+2}} \quad (4.9)$$

As in the moving mirror case, *c.f.* ssec 3.3.1, in the limit of $\epsilon^\pm \rightarrow 0$ the entropy is infinite due to UV-divergences. To get rid of the divergences we define the renormalized entanglement entropy to be

$$S_{ren} = S_{ent} - S_{ent}|_{vac}, \quad (4.10)$$

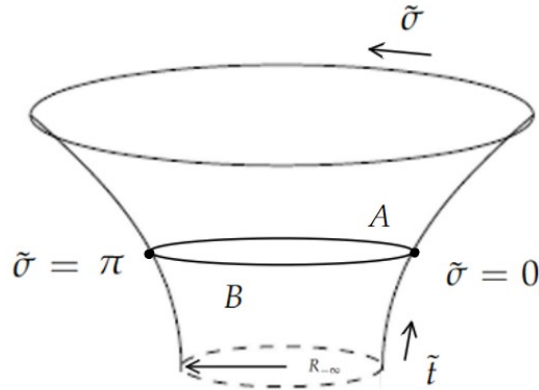


FIGURE 4.2: Expanding closed 1 + 1 cosmology. Our system A is defined upon a time-slice as the upper half of the circle which is divided at $\tilde{\sigma} = 0, \pi$. The complementary is denoted by B .

where in the case the $S_{ent}|_{vac}$ is the entropy in the far past, that is, for $R(t) = R_{-\infty}$. That is

$$S_{ren} = \frac{c}{3} \log \frac{R(\tilde{t})}{R_{-\infty}}. \quad (4.11)$$

Hence, as the universe expands, the entanglement entropy grows. The interpretation of this phenomenon originates from the addition of new entangled degrees of freedom which are redshifted below the cutoff due to the cosmological expansion.

4.3 de Sitter Space

de Sitter spacetime is the maximally symmetric spacetime of constant curvature. It is a solution of the vacuum Einstein equations with a positive cosmological constant. It is relevant for cosmological observations and not just a toy-model like our previous examples. There is evidence that the very early universe had a period of rapid expansion, 'inflation', well approximated by the de Sitter spacetime. Moreover, currently the tiny cosmological constant accounts for about 68% of the energy density of the universe, and this fraction is growing as the universe continues to expand. This means we are entering a second de Sitter phase. Below we will describe the basics of de Sitter spacetime according to the lecture notes of M. Spradlin, A. Strominger and A. Volovich [59].

4.3.1 Basics

Usually in GR we define manifolds intrinsically, not by embedding them in a higher dimensional spacetime. But for de Sitter, the embedding is actually intuitive: 2-dimensional de Sitter spacetime can be viewed as a timelike hyperbola, embedded in 3-dimensional Minkowski spacetime $\mathcal{R}^{1,2}$. The metric in the embedding space $\mathcal{R}^{1,D}$ is

$$ds_{embed}^2 = -dX_0^2 + dX_1^2 + dX_2^2. \quad (4.12)$$

de Sitter, with radius l , is the hypersurface defined by the equation

$$X_\mu X^\mu = l^2. \quad (4.13)$$

This is just a hyperbola. See Fig. 4.3 for an embedding of dS_2 in $\mathcal{R}^{1,2}$

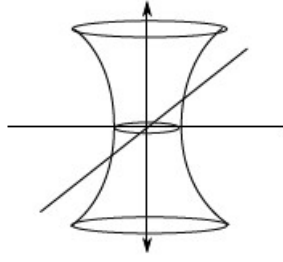


FIGURE 4.3: dS_2 viewed as a hyperbola in $R^{1,2}$. The cross sections are S^1 's.

4.3.2 Global Coordinates

The cross-sections of the dS_2 hyperbola (constant X^0 -slices) are S^1 spheres. We can put down *global coordinates* on the hyperbola by defining

$$X^0 = \ell \sinh \frac{\tau}{\ell}, \quad X^1 = \ell \omega^1 \cosh \frac{\tau}{\ell}, \quad X^2 = \ell \omega^2 \cosh \frac{\tau}{\ell}, \quad (4.14)$$

with $-\infty < \tau < \infty$, where

$$\omega^1 = \cos \theta_1, \quad \omega^2 = \sin \theta_1, \quad \theta_1 \in [-\pi, \pi). \quad (4.15)$$

This parametrization is designed so that plugging into the hyperbola equation (4.13) automatically solves it. By computing the details we get

$$\begin{aligned} dX^0 &= \cosh(\tau/\ell) dt, \\ dX^1 &= \ell d\omega^1 \cosh(\tau/\ell) + \omega^1 \sinh(\tau/\ell) dt, \\ dX^2 &= \ell d\omega^2 \cosh(\tau/\ell) + \omega^2 \sinh(\tau/\ell) dt. \end{aligned}$$

It is clear that by plugging into the flat metric (4.12) we obtain the induced metric on dS_2

$$ds^2 = -d\tau^2 + \ell^2 \cosh^2\left(\frac{\tau}{\ell}\right) d\theta_1^2. \quad (4.16)$$

In these coordinates dS_2 looks like a 1-sphere which starts out infinitely large at $\tau \rightarrow -\infty$, then shrinks to a minimal finite size at $t = 0$, then grows again to infinite size as $\tau \rightarrow \infty$.

Relation to FRW

Recall that the FRW metric for any homogeneous, isotropic universe is

$$ds_{FRW}^2 = -d\tau^2 + \alpha(\tau)^2 d\Sigma^2, \quad (4.17)$$

where the spatial slices Σ are either open (hyperbolas), flat (R^2), or closed (spheres). Clearly de Sitter is an example of a closed FRW universe. The scale factor $\alpha(\tau) = \ell \cosh(\tau/\ell)$ is exponentially decreasing, reaches a minimum at $\tau = 0$, $\alpha(0) = \ell$, then expands exponentially into the future.

Analytic Continuation to the Sphere

dS_2 is a Minkowski-signature version of the Euclidean sphere, S^2 . It is easy to see that under

$$\tau \rightarrow i\tau, \quad \Theta = \frac{\tau}{\ell} + \frac{\pi}{2}, \quad (4.18)$$

the metric (4.16) becomes

$$ds_{2\text{-sphere}}^2 = \ell^2(d\Theta^2 + \sin^2\Theta d\theta_1), \quad (4.19)$$

with the help of the identities $\cosh ix = (e^{ix} + e^{-ix})/2 = \cos x$ and $\cos(x - \frac{\pi}{2}) = \sin x$. The shift by $\pi/2$ is there so that the metric on the sphere is written in the usual way.

4.3.3 Conformal Coordinates

Now we want to draw an intrinsic picture of de Sitter, *i.e.*, without an embedding into a higher-dimensional spacetime. To capture the global properties of the spacetime we are going to use the Penrose diagram. Previously we saw that global de Sitter in 2-dimensions can be viewed as a contracting-then-expanding 2-sphere on either the Euclidean or Minkowskian signature. We foliate this 2-sphere by 1-spheres. The form of the metric (4.16) is already favorable for that foliation due to the fact that we are working in 2-dimensions. We will relabel θ_1 to θ for the convenience of the writer, so

$$ds^2 = -d\tau^2 + \ell^2 \cosh(\tau/\ell)^2 d\theta. \quad (4.20)$$

In the (τ, θ) -coordinates, null geodesics do not travel at 45° . To draw the Penrose diagram, *aka* the conformal diagram, we need a coordinate system that:

- (i) covers the whole spacetime
- (ii) makes massless particles travel at 45°
- (iii) fits on the page.

Condition (i) is accomplished by the choice of global coordinates. To impose the condition (ii), we change coordinates $t \rightarrow \sigma(\tau)$, and require

$$-d\tau^2 + \ell^2 \cosh(\tau/\ell) d\theta^2 = \Omega(\sigma)[-d\sigma^2 + d\theta^2]. \quad (4.21)$$

The conformal factor Ω does not affect null geodesics, so null geodesics will satisfy condition (ii). From equation (4.21) we read off $\Omega = \ell \cosh(\tau/\ell)$ and $dt = \Omega d\sigma$, so

$$\int \frac{d\tau}{\ell \cosh \tau/\ell} = \int d\sigma. \quad (4.22)$$

Integrating,

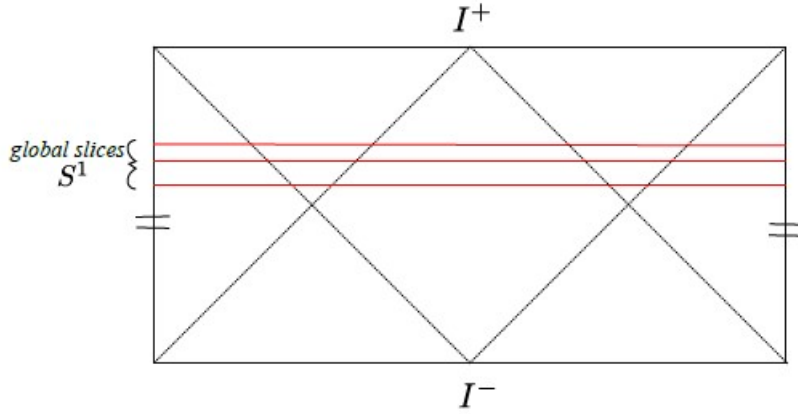
$$\begin{aligned} \tan\left(\sinh \frac{\tau}{\ell}\right)^{-1} &= \sigma, \\ \tan \sigma &= \sinh \frac{\tau}{\ell}. \end{aligned} \quad (4.23)$$

Note that $\tau \in (-\infty, \infty)$ corresponds to $\sigma \in (-\pi/2, \pi/2)$, so automatically condition (iii) is satisfied. Using the identity $\cosh(\tau/\ell)^2 = 1 + \sinh(\tau/\ell)^2$ and equation (4.23) we get $\Omega^2 = \ell^2 / \cos^2 \sigma$. The metric (4.20) is now

$$ds^2 = \frac{\ell^2}{\cos^2 \sigma} (-d\sigma^2 + d\theta^2), \quad (4.24)$$

where the (σ, θ) -coordinates are used to draw the Penrose diagram in Fig. 4.4.

Comments:

FIGURE 4.4: Penrose diagram for dS_2

Note: Later we will use only half of the penrose diagram of dS_2 for a better clarity of the illustrations.

- The σ -spatial slices are simple the 2-spheres on X_0 -slices of the embedding picture in Fig 4.4 .
- There are past and future conformal boundaries \mathcal{I}^- and \mathcal{I}^+ . Everyone approaches them in the infinite past and infinite future.
- The left and right edges are identified, $\theta \sim \theta + 2\pi$, since $\theta \in (-\pi, \pi)$. This is a special case only for 2-dimensions.
- There is an observer-dependent horizon, called the *cosmological horizon*. This is the null surface beyond which the observer can never receive a signal.

4.3.4 Flat Slicing Coordinates

In terms of the embedding space $R^{1,2}$, the flat slicing of dS_2 is

$$X_0 = \ell \sinh(t/\ell) + \frac{x^2}{2\ell} e^{t/\ell}, \quad X_1 = \ell \cosh(t/\ell) - \frac{x^2}{2\ell} e^{t/\ell}, \quad X_2 = x e^{t/\ell}. \quad (4.25)$$

Plugging into equation (4.12) gives de Sitter in the flat slicing coordinates

$$ds^2 = -dt^2 + e^{2t/\ell} dx^2, \quad (4.26)$$

where dx is the flat metric on R . Note that here the time coordinate t is different than the time coordinate τ of the global coordinates.

From equation (4.25) we see that these coordinates only cover

$$X_0 + X_1 > 0. \quad (4.27)$$

This corresponds to the future expanding triangle of the Penrose diagram. Comparing equations (4.14) and (4.25) for the global and flat slicing coordinates we find the simple coordinate change

$$e^{t/\ell} = \cos \theta \cosh(\tau/\ell) + \sinh(\tau/\ell), \quad \frac{\ell}{x} e^{t/\ell} = \sin \theta \cosh(\tau/\ell), \quad (4.28)$$

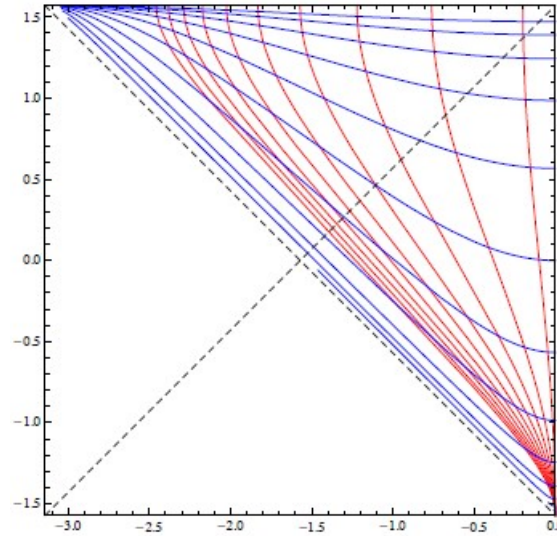


FIGURE 4.5: Blue curves are constant t -slices and red curves are constant x -slices. We used half of the Penrose diagram of dS_2 , the other half is just a mirroring with respect to the left axis of this diagram.

which allow us to draw the constant time and space surfaces of the flat slicing (t, x) -coordinates on the half of the Penrose diagram, see Fig. 4.5.

4.3.5 Entanglement Entropy in de Sitter

Consider a free massless scalar field upon de Sitter. We will use the flat slicing (t, x) -coordinates (4.25), define $u = \ell e^{-t/\ell}$ and plug it into the metric (4.26) to get

$$ds^2 = \frac{\ell^2}{u^2}(-du^2 + dx^2). \quad (4.29)$$

Introducing the null coordinates $u^\pm = u \pm x$,

$$ds^2 = -\frac{\ell^2}{\left(\frac{u^+ + u^-}{2}\right)^2} du^+ du^-. \quad (4.30)$$

These coordinates cover a future expanding half of de Sitter with flat u -slices.

Consider region A to be one with fixed unit coordinate length in x and on a u -slice, *i.e.* a slice of constant u which is a slice of constant t . For an example see Fig. 4.6. We are interested in the entanglement entropy between A and its complement upon the u -slice. The metric (4.30) is of the conformal form (3.57) with

$$\rho = \log \frac{\ell}{u}. \quad (4.31)$$

The entanglement entropy is given by equation (4.5). For our region A in any given u -slice it takes the form

$$S_{ent} = \frac{c}{3} \log \frac{\ell}{u} + \frac{c}{12} \log \frac{1}{(\epsilon^-)^2} + \frac{c}{12} \log \frac{1}{(\epsilon^+)^2}, \quad (4.32)$$

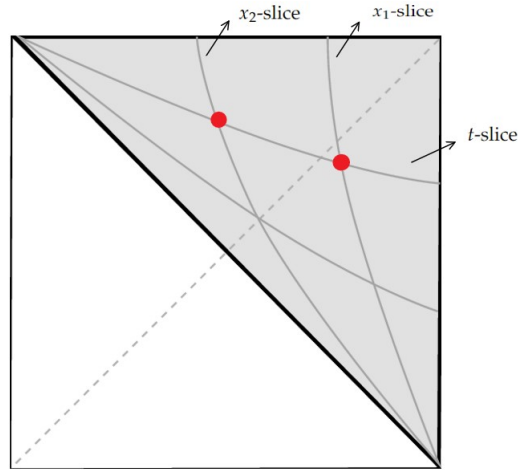


FIGURE 4.6: The region A consists of the points upon the t -slice which belong between the two red intersections with the $x_{1,2}$ -slice.

where in that case the tilde-coordinates of equation (4.5) is the (u^+, u^-) -coordinates of de Sitter. Renormalizing $S_{ren} = S_{ent} - S_{ent}|_{t=0}$, we get

$$S_{ren} = \frac{c}{3} \log \frac{\ell}{u}. \quad (4.33)$$

The $S_{ent}|_{t=0}$ corresponds to the entropy of the state defined upon $t = 0$. In these particular coordinates this state is the Hartle-Hawking vacuum [35]. Knowing that $u = \ell e^{-t/\ell}$, we see that entropy grows linearly with time t as

$$S_{ren} = \frac{ct}{3\ell}. \quad (4.34)$$

We understand this as arising from the growth of the effective Hilbert space from the redshifting cutoff.

Chapter 5

Lattice Discretization of Spacetime

Most early universe cosmological models are based on an effective field theory (EFT) analysis. An effective field theory includes the appropriate degrees of freedom to describe physical phenomena occurring at a chosen length scale or energy scale, while ignoring substructure and degrees of freedom at shorter distances (or, equivalently, at higher energies) by introducing a UV-cutoff. We followed the same approach in chapters 3 and 4 where we utilized entanglement entropy to explore the time evolution of effective Hilbert spaces. Note that the UV-cutoff has to correspond to a fixed physical scale since it is determined by local physics; a time-dependent cutoff would have led to paradoxes in an expanding universe [63]. Usually from an EFT point of view, the minimum value of the cutoff, say a , is an $O(1)$ multiple of the Planck length ℓ_P , *i.e.* $a = 100\ell_P$. When we speak of taking the limit $a \rightarrow 0$, we really mean that a is going to $\sim 100\ell_P$. The introduction of a cutoff and the fact that there are no degrees of freedom on length scales shorter than the Planck scale leads to the lattice discretization of spacetime.

Constructing a lattice discretization of a scalar field theory seems intuitive, but in time-dependent backgrounds, this procedure has interesting subtleties. An essential classical consideration is that we must choose a lattice discretization of the action such that in the appropriate continuum limit the action principle recovers the continuum classical equations of motion. Accordingly, we should understand how to appropriately discretize a PDE on a lattice.

Usually the discretization of a PDE is via the finite difference method (FDM). Historically, it was the first discretization method to be discovered since it is intuitively trivial. However, as we will shortly observe in sec. 5.1 FDM has fatal deficiencies for PDE's on certain kinds of time-dependent backgrounds, such as our mirror toy-model. These issues can be resolved using the finite elements method (FEM) which leverages comparatively more sophisticated tools from functional analysis [24, 9]. FEM and its variants are the workhorses of modern numerical PDE solvers and it is widely used in engineering [49]. In order to build intuition, we provided two reviews of this method in ssec. 5.2.1 and 5.2.2 where one is more analysis oriented and the other more geometry oriented. Both sections are aimed towards our application to lattice field theory in expanding geometries.

5.1 Finite Difference Method

The FDM is the standard approach of lattice quantum field theory (see [22] for an accessible overview in lattice QCD), usually implemented in Euclidean signature. However, there are large number of circumstances for which the FDM is unsuitable, even for reproducing the correct classical equations of motion in the continuum limit. One of these cases will be examined in this section.

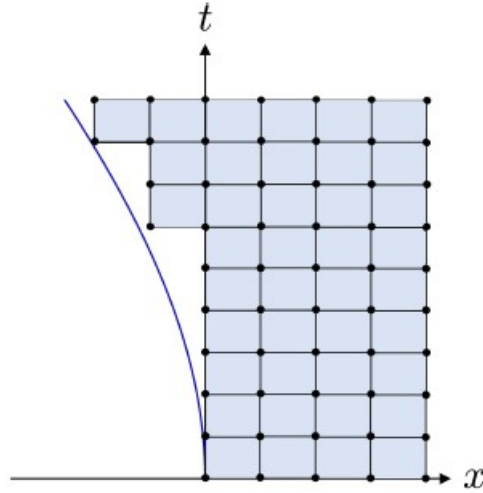


FIGURE 5.1: FDM discretization of spacetime. The figure was taken from [19].

We will consider a free massless scalar field in 1 + 1 Minkowski spacetime in the presence of the moving mirror boundary. The action of the field ϕ is given by

$$S[\phi] = -\frac{1}{2} \int d^2x \partial_\mu \phi \partial^\mu \phi. \quad (5.1)$$

The discretization with the FDM approach is of the form of lattice plaquettes that have spatial and temporal links with length δx and δt respectively. So, we have a rectangular lattice where the lattice spacing varies depending on the location in spacetime due to the presence of the moving mirror, see Fig 5.1. The recipe to go from a continuum to a discrete field ϕ that lives in a rectangular lattice is

$$\phi \longrightarrow \phi_{i,j}, \quad (5.2)$$

$$\partial_\mu \longrightarrow \Delta_\mu, \quad (5.3)$$

$$\int d^2x \longrightarrow \sum_{i,j} \delta t \delta x, \quad (5.4)$$

where Δ_μ is a finite difference of the form

$$\Delta_0 \phi_{i,j} = \frac{\phi_{i+1,j} - \phi_{i,j}}{\delta t}, \quad \Delta_1 \phi_{i,j} = \frac{\phi_{i,j+1} - \phi_{i,j}}{\delta x}. \quad (5.5)$$

Plugging everything into the action (5.1) we obtain

$$S_{FDM}[\phi_{i,j}] = -\frac{1}{2} \sum_{i,j} \delta t \delta x \eta^{\mu\nu} \Delta_\mu \phi_{i,j} \Delta_\nu \phi_{i,j}. \quad (5.6)$$

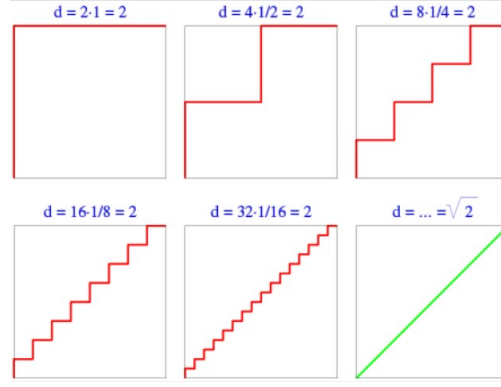


FIGURE 5.2: Saw tooth converging to the diagonal of a unit square, but not converging into its length.

Varying the discrete action (5.6) with respect to $\phi_{i,j}$ we get

$$\begin{aligned}
 \delta S_{FDM} &= -\frac{1}{2} \sum_{i,j} \delta t \delta x \eta^{\mu\nu} \Delta_\mu \delta \phi_{i,j} \Delta_\nu \phi_{i,j} - \frac{1}{2} \sum_{i,j} \delta t \delta x \eta^{\mu\nu} \Delta_\mu \phi_{i,j} \Delta_\nu \delta \phi_{i,j} \\
 \Rightarrow \delta S_{FDM} &= -\sum_{i,j} \delta t \delta x \eta^{\mu\nu} \Delta_\mu \delta \phi_{i,j} \Delta_\nu \phi_{i,j} \\
 \Rightarrow \delta S_{FDM} &= \sum_{i,j} \delta t \delta x \eta^{\mu\nu} (\Delta_\mu \Delta_\nu \phi_{i,j}) \delta \phi_{i,j}, \tag{5.7}
 \end{aligned}$$

where in the last equation we used Dirichlet boundary conditions $\delta \phi_{i,j}|_{\text{boundary}} = 0$. The lattice equation of motion are an extremum of the action S_{FDM} with respect to $\phi_{i,j}$. Using equation (5.7) we get

$$-\frac{2\phi_{i,j} - \phi_{i+1,j} - \phi_{i-1,j}}{\delta t^2} + \frac{2\phi_{i,j} - \phi_{i+1,j} - \phi_{i-1,j}}{\delta x^2} = 0, \tag{5.8}$$

where the first and second term is a discrete Laplacian with respect to time and space directions. In the case that $\delta t, \delta x \propto \alpha$, as $\alpha \rightarrow 0$, equation (5.8) becomes the usual Klein-Gordon equation.

So far so good, however this approach fails in our moving mirror toy-model which is a time-dependent boundary. In Fig. 5.1, you can observe that the saw-tooth approximation of the moving mirror boundary is inadequate for an appropriate continuum limit. At the limit $\alpha \rightarrow 0$, the limiting curve of the left boundary will be continuous but not be differentiable. Using equation (A.15) from Appendix A we find the formula for a component of the energy flux of a scalar field with the action (5.1)

$$T_{tt} = T_{xx} = \frac{1}{2} ((\partial_t \phi)^2 + (\partial_x \phi)^2). \tag{5.9}$$

As you can see, in the case of a non-differentiable boundary curve the energy flux blows up. FDM is not the main subject of this thesis, details for the failure of this method can be found on [42, 61].

Remark: Here we will try to give a short intuitive example for the failure of the saw tooth approximation in the continuum limit. Imagine trying to approximate the diagonal of a unit square with a saw tooth approximation, see Fig. 5.2. Divide the diagonal into n segments. Each triangle is $(\frac{1}{n}, \frac{1}{n}, \frac{\sqrt{2}}{n})$. So, the area between the

diagonal and the saw tooth is $n \frac{1}{2n^2}$ which converges to 0 in the continuum limit $n \rightarrow \infty$. The path length is $n \frac{2}{n}$, which gives a wrong continuum limit since $2 \neq \sqrt{2}$.

This example illustrates the fact that two functions can be very close: $|f(x) - g(x)| < \epsilon$ for x in the domain of the functions, but their derivatives can still be far apart, $|f'(x) - g'(x)| > c$ for some constant $c > 0$.

In our case, let $(t, Z(t))$ be the parametrization for the moving mirror boundary and $(c(t), d(t))$ the parametrizations of the saw tooth curve. In the continuum limit $n \rightarrow \infty$, we may assume that the two curves converge to each other $\| (t, Z(t)) \| \approx \| (c(t), d(t)) \|$ but this does not imply $\| (1, Z'(t)) \| \approx \| (c'(t), d'(t)) \|$. This means that we do not get the correct continuous limit for the derivative of the saw tooth approximation. The implication on the stress energy tensor (5.9) for the moving mirror is that

$$\lim_{n \rightarrow 0} T_{tt,xx}|_{x=Z(t),saw-tooth} \neq T_{tt,xx}|_{x=Z(t),movingmirror}. \quad (5.10)$$

In certain cases of moving mirror trajectories the derivative is not just unequal but blows up.

Similar problems occur when coupling fields to a time-dependent cosmology, such as de Sitter. Note that both the receding mirror example and the de Sitter example are expanding cosmologies. In each case the volume of spatial slices grows as a function of time, and so to maintain comparable spatial resolution we are required to increase the number of lattice sites as time advances. Persistent lattice artifacts obstructing a smooth continuum limit of both Lorentzian and Euclidean theories, especially for interacting fields, are discussed in [13, 24, 9, 28].

5.2 Finite Element Method

We now turn to the finite elements method, which provides a more sophisticated lattice discretization and can handle the above circumstances in which finite difference method fails.

5.2.1 Analysis Approach to FEM

Most problems in physics and mechanics are described as a set of partial differential equations and initial/boundary conditions. This set is called the strong form of the problem. Finite elements, however, are based on an alternative form, the weak form, which is equivalent to the former as we will shortly see.

Consider the strong form of the 0 + 1 equation of a harmonic oscillator

$$-\ddot{\phi}(t) = \phi(t), \quad \phi(0) = \phi_i, \quad \phi(T) = \phi_f. \quad (5.11)$$

First, let us observe that we can always assume that $\phi_i = \phi_f = 0$, by looking for a solution of the form $\phi(t) - (\phi_f(1-t) + \phi_i t)$; see [26] for a complete discussion on the boundaries of differential equations. If $\phi \in L^2[0, T]$ is the solution of the strong form (5.11) and ψ is any (sufficiently regular) function such that $\psi(0) = \psi(T) = 0$,

which we will call it as a test function, then integration by parts yields

$$\begin{aligned} (\psi, \phi) &:= \int_0^T \psi(t)\phi(t)dt = - \int_0^T \psi(-\ddot{\phi}(t))(t)dt \\ &= \int_0^T \dot{\psi}(t)\dot{\phi}dt := \alpha(\psi, \phi). \end{aligned} \quad (5.12)$$

Let us define the space

$$V = \{\psi \in L^2([0, T]) : \alpha(\psi, \psi) < \infty \text{ and } \psi(0) = \psi(T) = 0\}. \quad (5.13)$$

Then we can say that the solution ϕ to (5.11) is characterized by

$$\phi \in V \text{ such that } \alpha(\psi, \phi) = (\psi, \phi) \quad \forall \psi \in V, \quad (5.14)$$

that is equivalent to

$$\int_0^T dt(-\dot{\psi}(t)\dot{\phi}(t) + \psi(t)\phi(t)) = 0 \quad \forall \psi \in V, \quad (5.15)$$

which is called the weak form of (5.11). From this set up it is obvious that the strong form implies the weak form. Now we will prove the opposite direction. Suppose that $\phi \in C^2([0, T])$ satisfy the weak form (5.15) then integration by parts gives

$$\begin{aligned} (\phi, \psi) &= \alpha(\phi, \psi) = \int_0^T \psi(-\ddot{\phi})dt + \psi(T)\dot{\phi}(T) + \psi(0)\dot{\phi}(0) \\ &\iff \int_0^T \psi(t)\phi(t)dt = \int_0^T \psi(-\ddot{\phi})dt \\ &\iff \int_0^T dt\psi(t)(\ddot{\phi}(t) + \phi(t)) = 0 \quad \forall \psi \in V, \end{aligned} \quad (5.16)$$

where in the second equation we used the fact that $\psi \in V$ means that $\psi(0) = \psi(T) = 0$. Equation (5.16) is true for all ψ in V and that give us the strong form (5.11). Now the proof of equivalence between the two is completed.

The advantage of the weak form is that it allows us to weaken our criteria for what it means to solve equation (5.11). In particular, we can approximate $\phi(t)$ by a continuous (C^0), piecewise-linear function on $[0, T]$. For that case we will need a finite dimensional space for ϕ to live in and a basis for a representation of ϕ in that space.

Let $S \subset V$ be any finite dimensional subspace. We will consider the weak form (5.15) with V replaced by S , namely

$$\phi_S \in S \text{ such that } \alpha(\psi, \phi_S) = (\psi, \phi_S) \quad \forall \psi \in S. \quad (5.17)$$

Unraveling,

$$\int_0^T dt(-\dot{\psi}(t)\dot{\phi}_S(t) + \psi(t)\phi_S(t)) = 0 \quad \forall \psi \in S. \quad (5.18)$$

Now let $0 = t_0 < t_1 < \dots < t_N = 1$ be a partition of $[0, T]$, and let S be the linear space of function ψ such that

- (i) $\psi \in C^0([0, T])$,
- (ii) $\psi(t_i) = \psi_i$ for $i = 1, \dots, N$,

- (iii) $\psi|_{[t_{i-1}, t_i]}$ is a linear polynomial, $i = 1, \dots, N$, and
 (iv) $\psi(0) = \psi(T) = 0$.

For each $i = 1, \dots, N$ define b_i by the requirement that $b_i(t_j) = \delta_{ij}$. The set $\{b_i : 1 \leq i \leq N\}$ is a basis for S since $\sum_{i=1}^N c_i b_i(t_j) = 0$ implies $c_j = 0$. Moreover, the set $\{b_i\}$ spans S since $\psi - \sum_{i=1}^N \psi_i b_i(t_j) = 0$. That is true because $\psi - \sum_{i=1}^N \psi_i b_i(t_j) = 0$ is linear on each $[t_{i-1}, t_i]$ and zero at the endpoints, hence must be identically zero.

In the case where the partition of $[0, T]$ is done by linear segments with width $a = T/N$ we will call the space S to be $CPL_a([0, T])$, which is an abbreviation of continuous, piecewise-linear. The a is playing the role of our lattice cutoff. The basis b_i of our space will be called triangular basis. It is defined by three functions $b(t)$, $b_L(t)$, and $b_R(t)$ where

$$b(t) = \begin{cases} 0 & \text{if } t < -a \\ \frac{t}{a} + 1 & \text{if } -a \leq t \leq 0 \\ -\frac{t}{a} + 1 & \text{if } 0 \leq t \leq a \\ 0 & \text{if } a < t \end{cases}, \quad (5.19)$$

$$b_L(t) = \begin{cases} 0 & \text{if } t < -a \\ \frac{t}{a} + 1 & \text{if } -a \leq t \leq 0 \\ 0 & \text{if } 0 < t \end{cases}, \quad (5.20)$$

$$b_R(t) = \begin{cases} 0 & \text{if } t < 0 \\ \frac{t}{a} + 1 & \text{if } 0 \leq t \leq a \\ 0 & \text{if } a < t \end{cases}. \quad (5.21)$$

These functions are piecewise linear polynomials, see **Fig.** For our purposes,

$$b_0(t) := b_R(t), \quad b_j(t) := b(t - ja) \text{ for } j = 1, \dots, N-1, \quad b_N(t) := b_L(t - T). \quad (5.22)$$

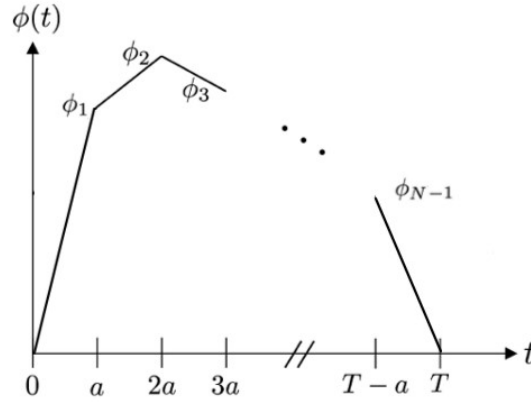
You can easily check that $b_i(t_j) = \delta_{ij}$. Then we can expand our function $\phi_S \equiv \phi_a \in CPL_a([0, T])$ in this basis,

$$\phi_a(t) = \sum_{i=0}^N \phi_i b_i(t). \quad (5.23)$$

One can appreciate the economy of this framework by unravelling equation (5.23), see also **Fig. 5.3**,

$$\phi_a(t) = \begin{cases} \frac{\phi_1}{a} t & \text{if } 0 \leq t \leq a \\ \frac{\phi_2 - \phi_1}{a} (t - a) + \phi_1 & \text{if } a \leq t \leq 2a \\ \vdots & \vdots \\ \frac{\phi_{j+1} - \phi_j}{a} (t - ja) + \phi_j & \text{if } ja \leq t \leq (j+1)a \\ \vdots & \vdots \\ -\frac{\phi_{N-1}}{a} (t - (T - a)) & \text{if } T - a \leq t \leq T \end{cases}. \quad (5.24)$$

Note that without the weak form (5.18) we could not possibly find a continuous and piecewise linear solution of the strong form (5.11) since $\dot{\phi}(t)$ is piecewise constant and discontinuous and thus $\ddot{\phi}(t)$ is a sum of delta distributions. So the left and right hand sides of (5.11) are not even in the same function space.

FIGURE 5.3: Plot of a $\phi(t)$ in $CPL_a([0, T])$.

So far so good, but in what sense does a continuous piecewise linear function achieves the correct continuum limit? Suppose that a solution to the weak form (5.18) with S being CPL_a is $\tilde{\phi}_a(t)$. Moreover, suppose $\tilde{\phi}(t)$ is an $L^2([0, T])$ solution of the strong form (5.11) with Dirichlet boundary conditions $\phi(0) = 0$ and $\phi(T) = 0$, that is $\phi \in V$. We will show that

$$\lim_{a \rightarrow 0} \int_0^T dt \psi(t) (\tilde{\phi}(t) - \tilde{\phi}_a(t)) = 0 \quad \forall \psi \in V. \quad (5.25)$$

Proof. Let us begin by

$$(\psi, \tilde{\phi} - \tilde{\phi}_a) = \int_0^T dt \psi(t) (\tilde{\phi}(t) - \tilde{\phi}_a(t)) = \int_0^T dt \dot{\psi}(t) (\dot{\tilde{\phi}}(t) - \dot{\tilde{\phi}}_a(t)), \quad (5.26)$$

where in the second equality we used manipulations of the equations of the weak (5.18) with $S = CPL_a$ and strong form (5.11) with $\phi \in V$,

$$\int_0^T dt \dot{\psi}(t) \dot{\phi}_a(t) = \int_0^T \psi(t) \phi_a(t), \quad (5.27)$$

$$\int_0^T dt \dot{\psi}(t) \dot{\phi}(t) = \int_0^T \psi(t) \phi(t) \quad \forall \psi \in V. \quad (5.28)$$

Using the Cauchy-Schwarz inequality for inner products $|(\psi, \phi)| \leq (\phi, \phi)^{1/2} (\psi, \psi)^{1/2}$ and equation (5.26) we get

$$\left| \int_0^T dt \dot{\psi}(t) (\dot{\tilde{\phi}}(t) - \dot{\tilde{\phi}}_a(t)) \right| \leq \left(\int_0^T dt (\dot{\psi}(t))^2 \right)^{1/2} \left(\int_0^T dt (\dot{\tilde{\phi}}(t) - \dot{\tilde{\phi}}_a(t))^2 \right)^{1/2}. \quad (5.29)$$

We will define as error between the discrete and continuous solution of ϕ the difference

$$e \equiv \tilde{\phi}(t) - \tilde{\phi}_a(t). \quad (5.30)$$

Since $\psi \in V$, the integral $\left(\int_0^T dt (\dot{\psi}(t))^2 \right)^{1/2}$ is a finite constant, that we will name it \mathcal{C} . Using the definition (5.30) in equation (5.29) we get

$$\left| \int_0^T dt \dot{\psi}(t) (\dot{\tilde{\phi}}(t) - \dot{\tilde{\phi}}_a(t)) \right| \leq \mathcal{C} \left(\int_0^T dt (\dot{e}(t))^2 \right)^{1/2}, \quad (5.31)$$

which is, see equation (5.26)

$$|(\psi, \tilde{\phi} - \tilde{\phi}_a)| \leq \mathcal{C} \left(\int_0^T dt (\dot{e}(t))^2 \right)^{1/2}. \quad (5.32)$$

Now we will use a property of the error variable $e(t)$ in the time interval $t \in [t_{j-1}, t_j]$. First of all we will do an affine transformation to map $t \in [t_{j-1}, t_j]$ into $\tilde{t} \in [0, 1]$. That affine transformation is of the form,

$$t = t_{j-1} + \tilde{t}(t_j - t_{j-1}) \quad \text{and} \quad \tilde{e}(\tilde{t}) = e(t_{j-1} + \tilde{t}(t_j - t_{j-1})). \quad (5.33)$$

Observe that $e(0) = e(1) = 0$ and we can use Rolle's (ref) theorem which state that there exists a $\tilde{\zeta} \in (0, 1)$ such that $e'(\tilde{\zeta}) = 0$, where the prime is a derivative with respect to \tilde{t} . So, we can write

$$\tilde{e}'(y) = \int_{\tilde{\zeta}}^y d\tilde{t} \tilde{e}''(\tilde{t}). \quad (5.34)$$

Again, by Cauchy-Schwarz's inequality.

$$\begin{aligned} |\tilde{e}'(y)| &= \left| \int_{\tilde{\zeta}}^y d\tilde{t} \tilde{e}''(\tilde{t}) \right| = \left| \int_{\tilde{\zeta}}^y d\tilde{t} 1 \cdot \tilde{e}''(\tilde{t}) \right| \\ &\leq \left| \int_{\tilde{\zeta}}^y d\tilde{t} 1 \right|^{1/2} \left| \int_{\tilde{\zeta}}^y d\tilde{t} \tilde{e}''(\tilde{t})^2 \right|^{1/2} \\ &= |y - \tilde{\zeta}|^{1/2} \left| \int_{\tilde{\zeta}}^y d\tilde{t} \tilde{e}''(\tilde{t})^2 \right|^{1/2} \\ &\leq |y - \tilde{\zeta}|^{1/2} \left(\int_0^1 d\tilde{t} \tilde{e}''(\tilde{t})^2 \right)^{1/2}. \end{aligned}$$

Squaring,

$$(\tilde{e}'(y))^2 \leq |y - \tilde{\zeta}| \left(\int_0^1 d\tilde{t} \tilde{e}''(\tilde{t})^2 \right). \quad (5.35)$$

Integrating with respect to y ,

$$\begin{aligned} \int_0^1 dy (\tilde{e}'(y))^2 &\leq \int_0^1 dy |y - \tilde{\zeta}| \left(\int_0^1 d\tilde{t} \tilde{e}''(\tilde{t})^2 \right) \\ &\leq \sup_{0 < \tilde{\zeta} < 1} \int_0^1 dy |y - \tilde{\zeta}| \left(\int_0^1 d\tilde{t} \tilde{e}''(\tilde{t})^2 \right) \\ &= \frac{1}{2} \left(\int_0^1 d\tilde{t} \tilde{e}''(\tilde{t})^2 \right). \end{aligned}$$

By reversing the affine transformation we get

$$\int_{t_{j-1}}^{t_j} dy (e'(y))^2 \leq \frac{a^2}{2} \left(\int_{t_{j-1}}^{t_j} dt e''(t)^2 \right), \quad (5.36)$$

where a is our lattice cutoff since $t_j - t_{j-1} = a$. In the interval $[t_{j-1}, t_j]$ the discretized solution $\tilde{\phi}_a$ is a linear polynomial, which mean $\ddot{\tilde{\phi}}_a = 0$. So,

$$\int_{t_{j-1}}^{t_j} dy (e'(y))^2 \leq \frac{a^2}{2} \left(\int_{t_{j-1}}^{t_j} dt \ddot{\tilde{\phi}}(t)^2 \right). \quad (5.37)$$

Summing over all the values of j ,

$$\int_0^1 dy (e'(y))^2 \leq \frac{a^2}{2} \left(\int_0^1 dt \tilde{\phi}''(t)^2 \right). \quad (5.38)$$

Plugging this into equation (5.32),

$$|(\psi, \tilde{\phi} - \tilde{\phi}_a)| \leq C \frac{a^2}{2} \left(\int_0^1 dt \tilde{\phi}''(t)^2 \right). \quad (5.39)$$

By taking the limit $a \rightarrow 0$ and remembering that the integral is finite, we get

$$\lim_{a \rightarrow 0} |(\psi, \tilde{\phi} - \tilde{\phi}_a)| \leq \lim_{a \rightarrow 0} C \frac{a^2}{2} \left(\int_0^1 dt \tilde{\phi}''(t)^2 \right) = 0. \quad (5.40)$$

This concludes our proof since

$$\lim_{a \rightarrow 0} (\psi, \tilde{\phi} - \tilde{\phi}_a) = 0, \quad (5.41)$$

which mean that

$$\lim_{a \rightarrow 0} \int_0^T dt \psi(t) (\tilde{\phi}(t) - \tilde{\phi}_a(t)) = 0 \quad \forall \psi \in V. \quad (5.42)$$

Remark: From equation (5.26) we have

$$(\psi, \tilde{\phi} - \tilde{\phi}_a) = \int_0^T dt \psi(t) (\dot{\tilde{\phi}}(t) - \dot{\tilde{\phi}}_a(t)), \quad (5.43)$$

using (5.40),

$$\lim_{a \rightarrow 0} \left| \int_0^T dt \psi(t) (\dot{\tilde{\phi}}(t) - \dot{\tilde{\phi}}_a(t)) \right| \leq 0, \quad (5.44)$$

which is equivalent to

$$\lim_{a \rightarrow 0} \int_0^T dt \psi(t) (\dot{\tilde{\phi}}(t) - \dot{\tilde{\phi}}_a(t)) = 0. \quad (5.45)$$

We see that even the derivative converges to the right continuum limit. So, FEM resolves the divergence of the energy flux where FDM fails. \square

This means that our piecewise continuous solution $\tilde{\phi}_a(t)$ better and better approximate the $L([0, T])$ solution $\tilde{\phi}(t)$ as we take the limit $a \rightarrow 0$. In fact, there are more rigorous statements about convergence that can be proved but we will not need these results in our analysis. From now on we will drop the rigorousness that came with the definitions of finite and infinite dimensional spaces of solutions and we will use $\phi(t)$ for any solution since we have a theorem of convergence.

Let us expand our function $\phi(t) \in CPA_a([0, T])$ and test function $\psi(t) \in CPA_a([0, T])$ in the $\{b_i\}$ basis as,

$$\phi(t) = \sum_{j=0}^N \phi_j b_j(t), \quad (5.46)$$

$$\psi(t) = \sum_{i=0}^N \psi_i b_i(t). \quad (5.47)$$

Plugging these into the weak form (5.18) we get

$$\sum_{i,j=1}^N \psi_i \left[\left(- \int_0^T dt \dot{b}_i(t) \dot{b}_j(t) \right) + \left(\int_0^T dt b_i(t) b_j(t) \right) \right] \phi_j = 0 \quad \forall \psi_0, \psi_1, \dots, \psi_N \in R. \quad (5.48)$$

We define the stiffness matrix S_{ij} and the mass matrix M_{ij} to be

$$S_{ij} := - \int_0^T dt \dot{b}_i(t) \dot{b}_j(t), \quad M_{ij} := \int_0^T dt b_i(t) b_j(t). \quad (5.49)$$

Then, equation (5.48) becomes

$$\sum_{i,j=0}^N \psi_i (S_{ij} + M_{ij}) \phi_j = 0 \quad \forall \psi_0, \psi_1, \dots, \psi_N \in R. \quad (5.50)$$

In matrix form,

$$\Psi \cdot (S + M) \cdot \Phi = 0 \quad \forall \Psi \in CPL_a([0, T]) \quad (5.51)$$

where $\Psi^T = [\psi_0 \ \psi_1 \ \dots \ \psi_N]$, $\Phi^T = [\phi_0 \ \phi_1 \ \dots \ \phi_N]$, $S = [S_{ij}]$, $M = [M_{ij}]$. This is equivalent to

$$(S + M) \cdot \Phi = 0 \iff \sum_{j=0}^N (S_{ij} + M_{ij}) \phi_j = 0 \quad \text{for } j = 0, 1, \dots, N. \quad (5.52)$$

This is the finite elements discretization of the continuum equation $\ddot{\phi} + \phi = 0$, with respect to the $\{b_i\}$ basis. Now, let's unravel the finite element equation. First of all notice that for a given i the only j 's that survive are $j = i - 1, i, i + 1$. That is true because the stiffness matrix S_{ij} and the mass matrix M_{ij} are product of basis functions $\{b_i\}$ and our basis' functions have no overlap for $|j - i| > 1$. From this, equation (5.52) becomes

$$S_{ii-1} \phi_{i-1} + S_{ii} \phi_i + S_{ii+1} \phi_{i+1} + M_{ii-1} \phi_{i-1} + M_{ii} \phi_i + M_{ii+1} \phi_{i+1} = 0. \quad (5.53)$$

For $i \neq 0, N$ the basis functions (5.19) that we need is

$$b_{i-1}(t - (i - 1)a) = \begin{cases} 0 & \text{if } t < (i - 2)a \\ \frac{t - (i-1)a}{a} + 1 & \text{if } (i - 2)a \leq t \leq (i - 1)a \\ -\frac{t - (i-1)a}{a} + 1 & \text{if } (i - 1)a \leq t \leq ia \\ 0 & \text{if } ia < t \end{cases}, \quad (5.54)$$

$$b_i(t - ia) = \begin{cases} 0 & \text{if } t < (i - 1)a \\ \frac{t - ia}{a} + 1 & \text{if } (i - 1)a \leq t \leq ia \\ -\frac{t - ia}{a} + 1 & \text{if } ia \leq t \leq (i + 1)a \\ 0 & \text{if } (i + 1)a < t \end{cases} \quad (5.55)$$

$$b_{i+1}(t - (i + 1)a) = \begin{cases} 0 & \text{if } t < ia \\ \frac{t - (i+1)a}{a} + 1 & \text{if } ia \leq t \leq (i + 1)a \\ -\frac{t - (i+1)a}{a} + 1 & \text{if } (i + 1)a \leq t \leq (i + 2)a \\ 0 & \text{if } (i + 2)a < t. \end{cases} \quad (5.56)$$

Let us compute some useful integrals

$$\begin{aligned}
\int_0^T \dot{b}_i(t) \dot{b}_{i-1}(t) &= \int_{(i-1)a}^{ia} dt \dot{b}_i(t) \dot{b}_{i-1}(t) = -\frac{1}{a}, \\
\int_0^T \dot{b}_i(t) \dot{b}_i(t) &= \int_{(i-1)a}^{(i+1)a} dt \dot{b}_i(t) \dot{b}_i(t) = \frac{2}{a}, \\
\int_0^T \dot{b}_i(t) \dot{b}_{i+1}(t) &= \int_{ia}^{(i+1)a} dt \dot{b}_{i+1}(t) \dot{b}_i(t) = -\frac{1}{a}, \\
\int_0^T dt b_i(t) b_{i-1}(t) &= \int_{(i-1)a}^{ia} dt \left(\frac{t-ia}{a} + 1 \right) \left(-\frac{t-(i-1)a}{a} + 1 \right) = -\frac{a}{6}, \\
\int_0^T dt b_i(t) b_i(t) &= \int_{(i-1)a}^{ia} dt \left(\frac{t-ia}{a} + 1 \right)^2 + \int_{ia}^{(i+1)a} dt \left(-\frac{t-ia}{a} + 1 \right)^2 = \frac{2a}{3}, \\
\int_0^T dt b_i(t) b_{i+1}(t) &= \int_{ia}^{(i+1)a} dt \left(-\frac{t-ia}{a} + 1 \right) \left(\frac{t-(i+1)a}{a} + 1 \right) = \frac{a}{6}.
\end{aligned}$$

From these integrals we can compute (5.52) and get the unravelled form of FEM on the 0 + 1 harmonic oscillator,

$$\frac{2\phi_i - \phi_{i-1} - \phi_{i+1}}{a^2} + \frac{1}{3} \left(\phi_i + \frac{1}{2} (\phi_i + \phi_{i+1}) + \frac{1}{2} (\phi_i - \phi_{i-1}) \right), \quad (5.57)$$

where we have divided the equation with a . Observe that the first term is the lattice second derivative. The second term approximates the value of $\phi(t)$ in the vicinity of $t = ia$ and has a "triangular" looking form. For the values of $i = 0, N$ the equation is trivial.

Note that we could have obtain equation (5.57) from the continuous action $\int_0^T dt \left(\frac{1}{2} \dot{\phi}^2 - \frac{1}{2} \phi^2 \right)$ of the 0 + 1 harmonic oscillator upon setting $\phi(t) = \sum_{i=0}^N \phi_i b_i(t)$,

$$\begin{aligned}
S_{lattice}[\{\phi_i\}] &= \int_0^T dt \left(\frac{1}{2} \sum_{i,j=0}^N \phi_i \dot{b}_i(t) \dot{b}_j(t) \phi_j - \frac{1}{2} \sum_{i,j=0}^N \phi_i b_i(t) b_j(t) \phi_j \right) \\
&= -\frac{1}{2} \sum_{i,j=0}^N \phi_i (S_{ij} + M_{ij}) \phi_j, \quad (5.58)
\end{aligned}$$

using Euler-Lagrange,

$$\frac{d}{d\phi_i} \left(\sum_{j=0}^N \phi_j (S_{ij} + M_{ij}) \phi_j \right) = 0 \Rightarrow \sum_j (S_{ij} + M_{ij}) \phi_j = 0, \quad (5.59)$$

which unravelled is equation (5.57).

Lets summarize our procedure for lattice discretization via the FEM. Suppose that we have some differential equation for $\phi(t)$. Then we carry out the following procedure:

- (i) Choose a suitable family of basis functions $b_i(t)$ whose span is the space $CPL_a([0, T])$.
- (ii) Expand our function $\phi(t)$ in this basis as $\phi(t) = \sum_{i=0}^N \phi_i b_i(t)$.
- (iii) Plug this expansion of $\phi(t)$ into the equation for weak solutions of our differential equation, and do the same for the test function $\psi(t)$. This reduces to a discrete system of equations which comprises the discretization of the continuum equations.

Equivalently,

- If we have a continuum action $S[\phi(t)]$ whose Euler-Lagrange equations are our differential equation, then we can simply let $\phi(t) = \sum_{i=0}^N \phi_i b_i(t)$ to obtain a discrete action $S_{lattice}[\{\phi_i\}]$, and compute the new Euler-Lagrange equations which are our discretized equations of motion.

The advantage of the FEM approach, besides its conceptual clarity and the compact formulation of discretization can be seen when we turn from $0 + 1$ dimensions to $1 + 1$ dimensions. Before doing so, we will prepare the $0 + 1$ case for the $1 + 1$ generalization. The basis functions $\{b_i(t)\}_{i=0}^N$ are associated to a single lattice site and they overlap, as we saw in the computation of equation (5.57). There is a slightly different organization which fruitfully generalizes to the $1 + 1$ setting. Defining

$$b_{L,j}(t) := b_L(t - (j+1)a), \quad b_{R,j}(t) := b_R(t - ja) \quad \text{for } j = 0, \dots, N-1, \quad (5.60)$$

we can associate $b_{L,j}(t)$ and $b_{R,j}(t)$ with the 1-dimensional edge connecting $t = ja$ to $t = (j+1)a$. It is simple to observe that $b_L(t) + b_R(t) = b(t)$. In fact, $\{b_{L,j}(t), b_{R,j}(t)\}_{j=0}^{N-1}$ comprises a basis for $CPL_a([0, T])$, where we have two functions related with each edge of the temporal lattice. In this notation, the expansion of the field ϕ into the basis $\{b_{L,j}(t), b_{R,j}(t)\}_{j=0}^{N-1}$ takes the form

$$\phi(t) = \sum_{j=0}^{N-1} \phi_{j+1} b_{L,j}(t) + \sum_{j=0}^{N-1} \phi_j b_{R,j}(t). \quad (5.61)$$

Next we examine the $1 + 1$ massless Klein-Gordon equation, with action $S[\phi(t)] = -\frac{1}{2} \int d^2x \partial_\mu \phi \partial^\mu \phi$. Although $\phi(t, x)$ naturally lives in $L^2(\mathbb{R}^2)$, we would like to approximate it by an appropriate family of continuous, piecewise linear function on \mathbb{R}^2 , *i.e.*, the (t, x) plane). To specify this family, we can consider various lattice discretizations of \mathbb{R}^2 . The most obvious is the FDM's approach of a rectangular lattice with spacings $\delta t, \delta x$ but as we saw in sec. 5.1 it fails in our case. Instead, we will opt for the most flexible lattice of all: a triangular lattice. Indeed, any planar lattice can be refined into a triangular lattice by adding more edges [67]. There is enormous freedom in choosing a triangulation; for hyperbolic PDE's such as wave equations, we should be careful that our triangulation is in compliance with the CFL condition [21] which affords numerical stability of the lattice approximation in the continuum limit.

We will express our lattice $\mathcal{L} = \{\Delta_i\}$ as a collection of triangular plaquettes Δ_i , and to each plaquette Δ_i we associate an ordered list of its vertices in \mathbb{R}^2 , namely $(v_{i,1}, v_{i,2}, v_{i,3}) = ((x_{i,1}, y_{i,1}), (x_{i,2}, y_{i,2}), (x_{i,3}, y_{i,3}))$. Next we define our family of basis functions for \mathcal{L} . Let $\chi_\Delta(t, x)$ be the characteristic function for the interior of the 'standard' triangle Δ in \mathbb{R}^2 with vertices $(0, 0)$, $(1, 0)$ and $(0, 1)$. We can write $\chi_\Delta(t, x)$ explicitly in terms of a product of Heaviside step functions as $\chi_\Delta(t, x) = \theta(1-t-x)\theta(t)\theta(x)$. Then we define the three functions

$$B_\Delta^{(1)} := (1-t-x)\chi_\Delta(t, x), \quad B_\Delta^{(2)}(t, x) := t\chi_\Delta(t, x), \quad B_\Delta^{(3)}(t, x) := x\chi_\Delta(t, x). \quad (5.62)$$

We can map the 'standard' triangle Δ to any triangle in \mathbb{R}^2 via an affine transformation, see Fig. 5.4. In particular, if we want to map $((0, 0), (1, 0), (0, 1))$ to $((x_1, y_1), (x_2, y_2), (x_3, y_3))$,

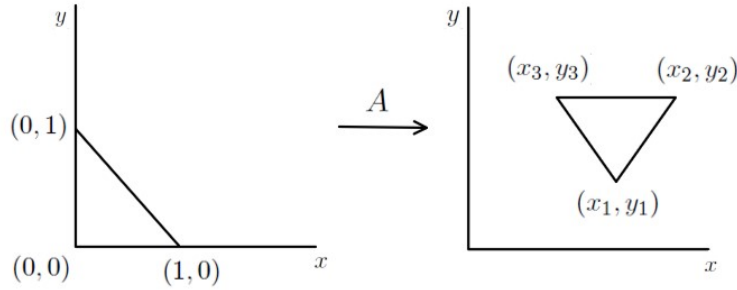


FIGURE 5.4: Affine transformation A from the 'standard' triangle to a random triangle.

then we can leverage the affine transformation

$$A : \begin{bmatrix} x \\ y \end{bmatrix} \mapsto \begin{bmatrix} -x_1 + x_2 & -x_1 + x_3 \\ -y_1 + y_2 & -y_1 + y_3 \end{bmatrix} \begin{bmatrix} x \\ y \end{bmatrix} + \begin{bmatrix} x_1 \\ y_1 \end{bmatrix} \quad (5.63)$$

and transform the $B_{\Delta}^{(j)}(t, x)$ functions to $B_{\Delta}^{(j)}(A^{-1}(t, x))$ accordingly. Note that this is an active transformation where the edges of the triangle transform with respect to the coordinate system. We should be careful to map between triangles with the same orientation in the plane. Let $B_{\Delta_i}^{(j)}(t, x)$ with $j = 1, 2, 3$ correspond to the basis functions above, affinely transformed so that their vertices match the vertices of the plaquette Δ_i . Then we take our family of basis functions to be

$$\left\{ B_{\Delta_i}^{(1)}(t, x), B_{\Delta_i}^{(2)}(t, x), B_{\Delta_i}^{(3)}(t, x) \right\}_{\Delta_i \in \mathcal{L}} \quad (5.64)$$

and denote its real-valued span by the family of functions $CPL_{\mathcal{L}}(R^2)$. We can accordingly expand $\phi(t, x)$ in this basis as

$$\begin{aligned} \phi(t, x) &= \sum_i \left(\phi_{v_{i,1}} B_{\Delta_i}^{(1)}(t, x) + \phi_{v_{i,2}} B_{\Delta_i}^{(2)}(t, x) + \phi_{v_{i,3}} B_{\Delta_i}^{(3)}(t, x) \right) \\ &= \sum_i \sum_{j=1}^3 \left(\phi_{v_{i,j}} B_{\Delta_i}^{(j)}(t, x) \right) \end{aligned} \quad (5.65)$$

Plugging this into the continuum free action, we obtain a lattice action

$$S_{lattice}[\{\phi_v\}] = \sum_{v, v' \in V(\mathcal{L})} \phi_v Q_{v, v'} \phi_{v'} \quad (5.66)$$

for a corresponding stiffness matrix $Q_{v, v'}$, where $V(\mathcal{L})$ is the set of vertices of \mathcal{L} .

Having triangular plaquettes comes with many advantages. The first advantage of triangular plaquettes is that we can accommodate arbitrarily-shaped spacetime boundaries without making a saw-tooth approximation. That is, we can approximate spacetime boundaries in a piecewise-linear fashion that appropriately converge to smooth boundaries in the continuum limit, *i.e.* as we consider a sequence of progressively finer triangulations. This will preclude the divergence of the energy flux from the moving boundary which was a pathology of the saw-tooth approximation, see Fig 5.5. The second, advantage is that we have a more flexible framework for coupling our fields to a curved background, as will become more obvious in the

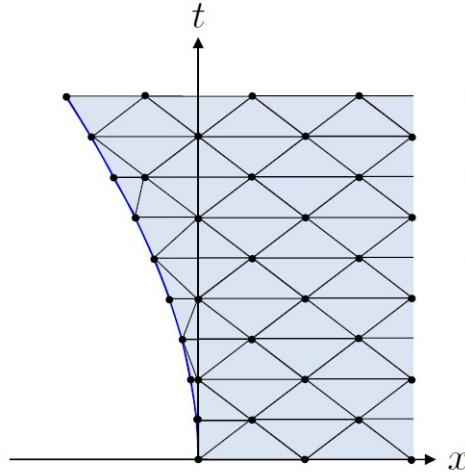


FIGURE 5.5: A triangular FEM lattice regularization of a 1 + 1 scalar field in a spacetime with a moving boundary. The moving boundary is piecewise-linear-approximated by the lattice discretization, which is continuous for any cutoff scale; this is in contrast to the FDM sawtooth approximation of Fig 5.1. Note that the number of lattice sites on each Cauchy slice is increasing with time. The figure was taken from [19].

next section. The third advantage is that we can more readily incorporate a changing number of lattice sites on spacelike Cauchy slices, *i.e.* when the spatial volume is changing as a function of time.

5.2.2 Geometric approach to FEM

In this section we are going to work on Euclidean spacetime to make the geometric illustration more prominent ; see [11] for an overview. One can Wick-rotate back to Minkowski spacetime to match with our previous results of ssec. 5.2.1. The Euclidean action of a free massless scalar field is,

$$I = \frac{1}{2} \int d^2x \delta^{\mu\nu} \partial_\mu \phi(x) \partial_\nu \phi(x), \quad (5.67)$$

where x is used to denote the collection of spacetime coordinates (t_E, x) . We will proceed in three steps,

- **Topology:** The 2D Minkowski \mathcal{M} manifold will be replaced by a triangulated manifold \mathcal{M}_σ composed of 2D triangles, which is homeomorphic to the Minkowski manifold.
- **Geometry:** The metric on Minkowski spacetime (\mathcal{M}, δ) is approxiamted on the triangulated manifold $(\mathcal{M}_\sigma, g_\sigma)$ by assigning lengths l_{ij} on links and extending the metric into the interior of each triangle.
- **Hilbert Space:** The Hilbert space of continuum fields, $\phi(x)$, is truncated by expanding in a finite element basis on each triangle, $\phi_\sigma(x) = \sum_{i=0}^2 E^i(x) \phi_i$.

This approach can be easily generalized in curved manifolds of more dimensions [11]. In flat spacetime, the first step is trivial [67] but was included for the shake of completeness. We will carry on with the following two steps.

The interior of a random triangle in flat spacetime can be parametrized as

$$\vec{y} = \sum_{i=0}^2 \zeta^i \vec{r}_i = \sum_{i=1}^2 \zeta^i \vec{l}_{i0} + \vec{r}_0, \quad (5.68)$$

using barycentric coordinates, $0 \leq \zeta^i \leq 1$, with the constraint $\sum_{i=0}^2 \zeta^i = 1$. The vectors on the edges of the triangle are $\vec{l}_{i0} = \vec{r}_i - \vec{r}_0$. To pick a unique coordinate system on \mathcal{M}_σ , we can arbitrarily eliminate ζ^0 , introducing the differentials,

$$d\vec{y} = \frac{\partial \vec{y}}{\partial \zeta^i} d\zeta^i = \vec{l}_{i0} d\zeta^i, \quad (5.69)$$

where \vec{l}_{i0} are the components of this one form in the basis $d\zeta^i$ with $i = 1, 2, 3$ and dual tangent vectors,

$$\vec{\nabla} = \vec{\nabla}_{\zeta^i} \partial_i = \vec{n}^i \partial_i, \quad (5.70)$$

with components, $\vec{n}^i = \vec{\nabla}_{\zeta^i}$ in the basis ∂_i . The metric on each triangle is

$$ds^2 = d\vec{y} \cdot d\vec{y} = g_{ij} d\zeta^i d\zeta^j, \quad g_{ij} = \vec{l}_{i0} \cdot \vec{l}_{j0} = \frac{1}{2}(l_{i0}^2 + l_{j0}^2 - l_{ij}^2). \quad (5.71)$$

The standard relations for raising and lowering indices by the metric tensor (g_{ij}) and its inverse are

$$g^{ij} = \vec{n}^i \cdot \vec{n}^j \quad \text{or} \quad \vec{n}^i \cdot \vec{l}_{j0} = \delta_j^i, \quad (5.72)$$

applies within each simplex. Not since we are in flat spacetime we choose the notation \vec{l}_{i0} and \vec{n}^i ,

$$\vec{l}_{i0} \rightarrow l_{i0}^\alpha = \frac{\partial y^\alpha}{\partial \zeta^i} \quad \text{and} \quad n_\alpha^i = \frac{\partial \zeta^i}{\partial y^\alpha}, \quad (5.73)$$

for both upper and lower indices.

Now the new action for a massless field ϕ on the triangulated Minkowski spacetime ($\mathcal{M}_\sigma, g_\sigma$) is again determined by equation (5.67) using the metric (5.71). It is given by a sum over all the triangles σ ,

$$\begin{aligned} I_{lattice} &= \frac{1}{2} \sum_\sigma \int d^2 y [\vec{\nabla} \phi_\sigma(y) \cdot \vec{\nabla} \phi_\sigma(y)] \\ &= \frac{1}{2} \sum_\sigma \int d^2 \zeta \sqrt{g_\sigma} [g_\sigma^{ij} \partial_i \phi_\sigma(\zeta) \partial_j \phi_\sigma(\zeta)]. \end{aligned} \quad (5.74)$$

where $\sqrt{g_\sigma}/2$ is the area of each triangle. Finally, we expand $\phi_\sigma(y)$ in a finite element basis on each triangle,

$$\phi_\sigma(y) = E^0(y)\phi_0 + E^1(y)\phi_1 + E^2(y)\phi_2, \quad (5.75)$$

where $E^i(r_j) = \delta_j^i$ so that $\phi_i = \phi(y = r_i)$. We also impose the sum rule, $\sum_i E^i(y) = 1$, so that the constant field is preserved. For simplicity, our subscript σ implies a restriction to a single triangle. The expansion of the field over the entire manifold ($\mathcal{M}_\sigma, g_\sigma$) is given by a sum over all sites,

$$\phi(y) = \sum_\sigma (E_\sigma^0(y)\phi_0 + E_\sigma^1(y)\phi_1 + E_\sigma^2(y)\phi_2). \quad (5.76)$$

Once the elements $E^i(y)$ are chosen, explicit integration for the triangulated action

(5.74) can be carried out leading to a quadratic form for the free massless field action on the values of ϕ_i .

The simplest choice is the *linear* FEM,

$$E^i(\xi) = \xi^i, \quad i = 0, 1, 2. \quad (5.77)$$

Since $E^0 + E^1 + E^2 = 1$ we have,

$$\phi(\xi) = \sum_{i=1}^2 (\phi_i - \phi_0) \xi^i + \phi_0. \quad (5.78)$$

Plugging into the action (5.74),

$$\begin{aligned} I_{lattice} &= \frac{1}{2} \int d^2 \xi \sqrt{g_\sigma} g_\sigma^{ij} \partial_i \left(\sum_{i=1}^2 (\phi_i - \phi_0) \xi^i + \phi_0 \right) \partial_j \left(\sum_{i=1}^2 (\phi_j - \phi_0) \xi^j + \phi_0 \right) \\ &= \frac{1}{4} \sum_{i,j=1}^2 \sqrt{g_\sigma} g_\sigma^{ij} (\phi_i - \phi_0) (\phi_j - \phi_0), \end{aligned} \quad (5.79)$$

where we used the fact that the integration gives us the area of the triangle. Recall that the area is equal to $\sqrt{g_\sigma}/2$.

5.2.3 Analysis vs Geometric

The functional analysis and the geometric approach of FEM arrive at the same result which is the finite element discretization of spacetime, see Table 5.1. In the functional analysis approach, the discretization takes place essentially at the level of the equations of motion. While in the geometric approach, the discretization is applied in the Euclidean metric which is then can become Minkowskian by Wick-rotation.

| | Analysis FEM | Geometric FEM |
|---------------------|------------------------------------------------------------------------------------|--------------------------------------------------------------------------------------------------------------|
| Spacetime Signature | Minkowskian | Euclidean |
| Coordinates | (t, x) | (ξ_1, ξ_2) |
| Basis Functions | $B_{\Delta_i}^{(j)}(t, x)$ | ξ^i |
| Field Expansion | $\phi(t, x) = \sum_i \sum_{j=1}^3 (\phi_{v_{ij}} B_{\Delta_i}^{(j)}(t, x))$ | $\phi(\xi) = \sum_{i=1}^2 (\phi_i - \phi_0) \xi^i + \phi_0$ |
| Discretized Action | $S_{lattice}[\{\phi_v\}] \sum_{v,v' \in V(\mathcal{L})} \phi_v Q_{v,v'} \phi_{v'}$ | $I_{lattice} = \frac{1}{4} \sum_{i,j=1}^2 \sqrt{g_\sigma} g_\sigma^{ij} (\phi_i - \phi_0) (\phi_j - \phi_0)$ |

TABLE 5.1: Comparison between the functional analysis approach of FEM and the geometric one.

Both methods are illuminating and choosing one or the other depends on the preference of the reader. In calculations, there is a slight advantage in the geometric approach since the coordinates change from the (t_E, x) -cartesian coordinates to (ξ_1, ξ_2) -barycentric coordinates absorbs the Heaviside step functions that appear in basis functions $\{B_{\Delta_i}^{(j)}(t, x)\}$ of the functional approach. Moreover, the procedure of the geometric approach is easily generalized to curved manifolds, but this thesis is not about curved manifolds. We remark that in the Euclidean setting, the FEM has been recently leveraged to great effect for lattice simulation of quantum field theories on curved back ground [11, 10, 12]; see [13] for an overview.

Chapter 6

FEM in Scalar Field Theory

Here we will examine scalar field theory on a FEM lattice. Firstly, in sec. 6.1 we will compute the classical discretized action of the scalar field. Next, in sec. 6.2 we will proceed to the quantization of the classical scalar field theory using the path integral formulation, there has been related work using canonical quantization in [28, 43, 23]. Lastly, our main focus in sec. 6.3 will be to understand how the Lorentzian evolution is instantiated by the path integral in a quantum manner, in particular since the number of lattice sites on a Cauchy slice will be growing with time for our examples of interest.

6.1 Classical Considerations

Both the analysis and geometric methods of ssec. 5.2 will be utilized for the calculation of the classical discretized FEM action.

6.1.1 Analysis Approach to Scalar FEM on a Triangle

We will explore the FEM discretizations of classical field equations of motion for the scalar field theory in a triangle with three vertices as seen in Fig. 6.1. We will call the triangle $\tilde{\Delta}$, with vertices $(t, x) = (0, 0)$, $(\delta t, -\delta x)$ and $(\delta t, \delta x)$. We need to find a FEM basis $\{B_{\tilde{\Delta}}^{(j)}(t, x)\}$ for $j = 0, 1, 2$ in order to expand $\phi(t, x)$ as

$$\phi(t, x) = \phi_0 B_{\tilde{\Delta}}^{(0)}(t, x) + \phi_1 B_{\tilde{\Delta}}^{(1)}(t, x) + \phi_2 B_{\tilde{\Delta}}^{(2)}(t, x), \quad (6.1)$$

and the plug this into $S[\phi(t, x)] = -\frac{1}{2} \int d^2x \partial_\mu \phi \partial^\mu \phi$ to obtain a lattice action. The new basis can be found by an affine transformation (5.63) from the 'standard' triangle Δ

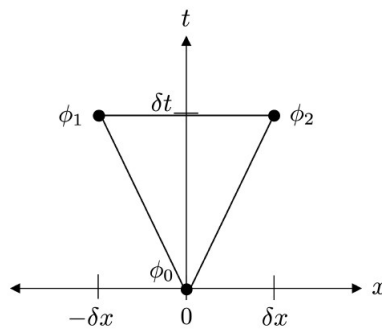


FIGURE 6.1: The triangle $\tilde{\Delta}$ in R^2 with vertices $(t, x) = (0, 0)$, $(\delta t, -\delta x)$ and $(\delta t, \delta x)$. We have labeled the vertices by their corresponding field values ϕ_0, ϕ_1, ϕ_2 .

to the triangle $\tilde{\Delta}$ of the form

$$A = \begin{bmatrix} \delta t & \delta x \\ -\delta x & \delta x \end{bmatrix}, \quad (6.2)$$

with an inverse,

$$A^{-1} = \begin{bmatrix} \frac{1}{2\delta t} & -\frac{1}{2\delta x} \\ \frac{1}{2\delta t} & \frac{1}{2\delta x} \end{bmatrix}. \quad (6.3)$$

Note that the matrix A^{-1} when it is applied to the vector $[t \ x]^T$ results in

$$A^{-1} \begin{bmatrix} t \\ x \end{bmatrix} = \begin{bmatrix} \frac{t}{2\delta t} - \frac{x}{2\delta x} \\ \frac{t}{2\delta t} + \frac{x}{2\delta x} \end{bmatrix}. \quad (6.4)$$

Hence, the mapping between (t, x) and $A^{-1}(t, x)$ is

$$t \mapsto \frac{t}{2\delta t} - \frac{x}{2\delta x}, \quad x \mapsto \frac{t}{2\delta t} + \frac{x}{2\delta x}. \quad (6.5)$$

Then we actively transform $B_{\Delta}^{(j)}(t, x)$ to $B_{\tilde{\Delta}}^{(j)}(t, x) \equiv B_{\Delta}^{(j)}(A^{-1}(t, x))$ accordingly. That is,

$$B_{\tilde{\Delta}}^{(0)}(t, x) = \left(1 - \frac{t}{\delta t}\right) \chi_{\tilde{\Delta}}(t, x), \quad (6.6)$$

$$B_{\tilde{\Delta}}^{(1)}(t, x) = \left(\frac{t}{2\delta t} - \frac{x}{2\delta x}\right) \chi_{\tilde{\Delta}}(t, x), \quad (6.7)$$

$$B_{\tilde{\Delta}}^{(2)}(t, x) = \left(\frac{t}{2\delta t} + \frac{x}{\delta x}\right) \chi_{\tilde{\Delta}}(t, x), \quad (6.8)$$

where $\chi_{\tilde{\Delta}}(t, x) = \theta\left(1 - \frac{t}{\delta t}\right)\theta\left(\frac{t}{2\delta t} - \frac{x}{2\delta x}\right)\theta\left(\frac{t}{2\delta t} + \frac{x}{\delta x}\right)$. Plugging (6.1) into the action and using a computational software, *i.e.* Mathematica, we get

$$S_{\tilde{\Delta}}[\{\phi_0, \phi_1, \phi_2\}] = \frac{\delta x}{\delta t} \cdot \frac{1}{8} (2\phi_0 - (\phi_1 + \phi_2))^2 - \frac{\delta t}{\delta x} \cdot \frac{1}{8} (\phi_1 - \phi_2)^2, \quad (6.9)$$

which is the FEM discretization of the action for a massless free scalar field in the triangle $\tilde{\Delta}$.

6.1.2 Geometric Approach to Scalar FEM on a Triangle

We will calculate the discretized action with the geometric method of FEM. The interior of the triangle $\tilde{\Delta}$ is parametrized by, see Fig. 6.2,

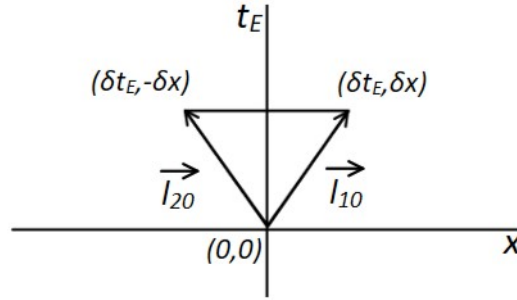
$$\vec{y} = \zeta^1 \vec{l}_{10} + \zeta^2 \vec{l}_{20}, \quad \vec{l}_{10} = \vec{r}_1 = (\delta t_E, \delta x), \quad \vec{l}_{20} = \vec{r}_2 = (\delta t_E, -\delta x), \quad (6.10)$$

where ζ^1, ζ^2 are the barycentric coordinates. In order to find the action (5.79) we will need to calculate the metric (5.71). For our triangle that is

$$\begin{aligned} g_{11} &= \vec{l}_{10} \cdot \vec{l}_{10} = \delta t^2 + \delta x^2, \\ g_{12} &= g_{21} = \vec{l}_{10} \cdot \vec{l}_{20} = \delta t^2 - \delta x^2, \\ g_{22} &= \vec{l}_{20} \cdot \vec{l}_{20} = \delta t^2 + \delta x^2. \end{aligned}$$

In matrix form,

$$g_{\tilde{\Delta}} \equiv [g_{ij}] = \begin{bmatrix} \delta t_E^2 + \delta x^2 & \delta t_E^2 - \delta x^2 \\ \delta t_E^2 - \delta x^2 & \delta t_E^2 + \delta x^2 \end{bmatrix}. \quad (6.11)$$

FIGURE 6.2: The triangle $\tilde{\Delta}$ parametrized by $\vec{l}_{10}, \vec{l}_{20}$.

From this we can compute the inverse of the metric which is

$$g_{\tilde{\Delta}}^{-1} \equiv [g^{ij}] = \begin{bmatrix} \frac{1}{4\delta t_E^2} + \frac{1}{4\delta x^2} & \frac{1}{4\delta t_E^2} - \frac{1}{4\delta x^2} \\ \frac{1}{4\delta t_E^2} - \frac{1}{4\delta x^2} & \frac{1}{4\delta t_E^2} + \frac{1}{4\delta x^2} \end{bmatrix}. \quad (6.12)$$

Plugging into equation (5.79) and using the fact that $\sqrt{g_{\tilde{\Delta}}} = 2\delta x \delta t_E$ we get

$$I_{\tilde{\Delta}}[\{\phi_0, \phi_1, \phi_2\}] = \frac{\delta x}{\delta t_E} \cdot \frac{1}{8} (2\phi_0 - (\phi_1 + \phi_2))^2 + \frac{\delta t_E}{\delta x} \cdot \frac{1}{8} (\phi_1 - \phi_2)^2, \quad (6.13)$$

which the Euclidean discretized FEM action for a free massless scalar field. Observe that by Wick-rotating $t_E \mapsto it$ we get,

$$-I_{\tilde{\Delta}}[\{\phi_0, \phi_1, \phi_2\}] = iS_{\tilde{\Delta}}[\{\phi_0, \phi_1, \phi_2\}]. \quad (6.14)$$

6.2 Quantum Considerations

So far we have discretized classical scalar fields which converge to the desired continuum equations in an appropriate limit. In order to proceed to quantum theory we will perform a path integral quantization of a free massless scalar field on the triangle $\tilde{\Delta}$. Our desired path integral is simply, see ssec 2.4.3, the propagator from $t = 0$ to $t = 1$

$$K(\phi_1, \phi_2; \phi_0) = C e^{iS_{\tilde{\Delta}}[\{\phi_0, \phi_1, \phi_2\}]}. \quad (6.15)$$

Our system is described at time $t = 0$ by a wavefunction $\Psi(\phi_0)$ in \mathcal{H}_0 and at time $t = 1$ by a wavefunction $\Psi(\phi_1, \phi_2)$ in $\mathcal{H}_1 \otimes \mathcal{H}_2$. Thus our forward time evolution which is generated by the propagator $K(\phi_1, \phi_2; \phi_0)$ must map $\mathcal{H}_0 \rightarrow \mathcal{H}_1 \otimes \mathcal{H}_2$,

$$\Psi(\phi_1, \phi_2) = \int d\phi_0 K(\phi_1, \phi_2; \phi_0) \Psi(\phi_0), \quad (6.16)$$

and our backward time evolution which is generated by the conjugate of the propagator $K^*(\phi_1, \phi_2; \phi_0)$ must map $\mathcal{H}_1 \otimes \mathcal{H}_2 \rightarrow \mathcal{H}_0$,

$$\Psi(\phi'_0) = \int d\phi_1 d\phi_2 K^*(\phi_1, \phi_2; \phi'_0) \Psi(\phi_1, \phi_2). \quad (6.17)$$

In operator language equations (8.15, 8.16) is equivalent to

$$|\Psi_{1,2}\rangle = \mathcal{K} |\Psi_0\rangle, \quad |\Psi_0\rangle = \mathcal{K}^\dagger |\Psi_{1,2}\rangle, \quad (6.18)$$

where we call the operator \mathcal{K} kernel and it has matrix elements $\langle \phi_1, \phi_2 | \mathcal{K} | \phi_0 \rangle = K(\phi_1, \phi_2; \phi_0)$. In ssec. 2.4.3 we saw that this map is unitary in the case of equally dimensional Hilbert spaces but this is not the case here. So, an immediate question arises: is our path integral, *aka* the propagator, unitary? What happens if we evolve from $t = 0$ to $t = 1$, and then back to $t = 0$? This is expressed by

$$\begin{aligned} PI &:= \int d\phi_1 d\phi_2 K^*(\phi_1, \phi_2; \phi'_0) K(\phi_1, \phi_2; \phi_0) = |C|^2 \int d\phi_1 d\phi_2 e^{iS_{\Delta}[\{\phi_0, \phi_1, \phi_2\}] - iS_{\Delta}^*[\{\phi'_0, \phi_1, \phi_2\}]} \\ &= |C|^2 e^{\frac{i\delta x}{2\delta t}(\phi_0^2 - \phi_0'^2)} \int d\phi_1 e^{\frac{i}{2} \frac{\delta x}{\delta t}(\phi'_0 - \phi_0)\phi_1} \int d\phi_2 e^{\frac{i}{2} \frac{\delta x}{\delta t}(\phi'_0 - \phi_0)\phi_2}. \end{aligned} \quad (6.19)$$

As you can see the integral does not converge. In order to make it converge we will need an $i\epsilon$ -prescription. We will try to find one by examining the pathologies of the previous integral. Let us make a coordinate change of the form,

$$u = \phi_1 - \phi_2, \quad (6.20)$$

$$v = \phi_1 + \phi_2. \quad (6.21)$$

In this coordinates the action (6.9) takes the form

$$S_{\Delta}[\{\phi_0, v, u\}] = \frac{\delta x}{\delta t} \cdot \frac{1}{8} (2\phi_0 - v)^2 - \frac{\delta t}{\delta x} \cdot \frac{1}{8} u^2. \quad (6.22)$$

A useful equation that we will need down the road is

$$\begin{aligned} iS_{\Delta}[\{\phi_0, v, u\}] - iS_{\Delta}^*[\{\phi_0, v, u\}] &= \frac{i\delta x}{8\delta t} ((2\phi_0 - v)^2 - (2\phi'_0 - v)^2) \\ &\quad + \frac{i\delta t}{8\delta x} u^2 - \frac{i\delta t}{8\delta x} u^2. \end{aligned} \quad (6.23)$$

The pathological integral becomes

$$\begin{aligned} \int d\phi_1 d\phi_2 K^*(\phi_1, \phi_2; \phi'_0) K(\phi_1, \phi_2; \phi_0) &= \frac{|C|^2}{2} \int dudv e^{iS_{\Delta}[\{\phi_0, v, u\}] - iS_{\Delta}^*[\{\phi'_0, v, u\}]} \\ &= \frac{|C|^2}{2} e^{\frac{i\delta x}{2\delta t}(\phi_0^2 - \phi_0'^2)} \int dudv e^{\frac{i}{2} \frac{\delta x}{\delta t}(\phi'_0 - \phi_0)v}, \end{aligned} \quad (6.24)$$

where in the second equality we used equation (7.24). In order for the integral (6.24) to converge we will need terms like $e^{-\epsilon u^2}$ and $e^{-\epsilon v^2}$ which will make the integral to be Gaussian. Observe that these terms can emerge in equation (7.24) with a flip of a sign from $-$ to $+$. For that reason we will prescribe the following $i\epsilon$ -prescription

$$\begin{aligned} iS_{\Delta}[\{\phi_0, v, u\}] - iS_{\Delta}^*[\{\phi_0, v, u\}] &= \frac{i\delta x}{8\delta t} ((2\phi_0 - v)^2 - (2\phi'_0 - v)^2) \\ &\quad - \epsilon \frac{\delta x}{8\delta t} ((2\phi_0 - v)^2 + (2\phi'_0 - v)^2) \\ &\quad + \frac{i\delta t}{8\delta x} u^2 - \frac{i\delta t}{8\delta x} u^2 \\ &\quad - \epsilon \left(\frac{\delta t}{8\delta x} u^2 + \frac{\delta t}{8\delta x} u^2 \right). \end{aligned} \quad (6.25)$$

That comes from an action of the form,

$$\begin{aligned} S_{\bar{\Delta}}[\{\phi_0, \phi_1, \phi_2\}; \epsilon] &= \frac{\delta x}{\delta t} \cdot \frac{1+i\epsilon}{8} (2\phi_0 - v)^2 - \frac{\delta t}{\delta x} \cdot \frac{1-i\epsilon}{8} u^2 \\ &= \frac{\delta x}{\delta t} \cdot \frac{1+i\epsilon}{8} (2\phi_0 - (\phi_1 + \phi_2))^2 - \frac{\delta t}{\delta x} \cdot \frac{1-i\epsilon}{8} (\phi_1 - \phi_2)^2, \end{aligned} \quad (6.26)$$

which in the continuum limit is

$$S_{\bar{\Delta}}[\{\phi_0, \phi_1, \phi_2\}; \epsilon] = -\frac{1}{2} \int d^2x \eta^{\mu\nu} \partial_\mu \phi \partial_\nu \phi + i\epsilon \cdot \frac{1}{2} \int dx^2 \delta^{\mu\nu} \partial_\mu \phi \partial_\nu \phi, \quad (6.27)$$

with the property that $\lim_{\epsilon \rightarrow 0} S_{\bar{\Delta}}[\{\phi_0, \phi_1, \phi_2\}; \epsilon] = S_{\bar{\Delta}}[\{\phi_0, \phi_1, \phi_2\}]$. Notice that the delta metric $\delta^{\mu\nu}$ flips the necessary signs that we need for convergence. Moreover, the second term of our action (6.27) is negative semi-definite when it is multiplied with i in the path integral. Since we are examining a scalar field, our path integral may converge. As a result the divergent integral (6.24) becomes

$$\begin{aligned} PI_\epsilon &:= \frac{|C|^2}{2} e^{\frac{i\delta x}{2\delta t}(\phi_0^2 - \phi_0'^2) - \frac{\epsilon\delta x}{2\delta t}(\phi_0^2 + \phi_0'^2)} \int dv e^{-\frac{\epsilon\delta x}{4\delta t}v^2 + \frac{\delta x}{2\delta t}(\epsilon(\phi_0 + \phi_0') + i(\phi_0' - \phi_0))v} \int du \left(-\frac{\epsilon\delta t}{4\delta x}u^2 \right) \\ &= \frac{|C|^2}{2} e^{\frac{i\delta x}{2\delta t}(\phi_0^2 - \phi_0'^2) - \frac{\epsilon\delta x}{2\delta t}(\phi_0^2 + \phi_0'^2)} e^{\frac{1}{4\epsilon} \frac{\delta x}{\delta t} (\epsilon(\phi_0' + \phi_0) + i(\phi_0' - \phi_0))^2} \sqrt{\frac{4\pi\delta t}{\epsilon\delta x}} \sqrt{\frac{4\pi\delta x}{\epsilon\delta t}} \\ &= |C|^2 \frac{2\pi}{\epsilon} e^{-\frac{\delta x}{\delta t} \frac{1+\epsilon^2}{4\epsilon} (\phi_0' - \phi_0)^2}, \end{aligned} \quad (6.28)$$

where in the second equality we completed the square,

$$\begin{aligned} -\frac{\epsilon\delta x}{4\delta t}v^2 + \frac{\delta x}{2\delta t}(\epsilon(\phi_0 + \phi_0') + i(\phi_0' - \phi_0))v &= -\frac{\epsilon\delta x}{4\delta t} \left(v + \frac{\epsilon(\phi_0' + \phi_0) + i(\phi_0' - \phi_0)}{\epsilon} \right)^2 \\ &\quad + \frac{1}{4\epsilon} \frac{\delta x}{\delta t} (\epsilon(\phi_0' + \phi_0) + i(\phi_0' - \phi_0))^2, \end{aligned} \quad (6.29)$$

and used $\int e^{\frac{1}{2}ax^2} = \sqrt{\frac{2\pi}{a}}$. From equation (2.66) of ssec 2.4.3 we see that the path integral should result in a delta function giving us a condition for the measure C . The definition of the delta function as a limit is

$$\lim_{\epsilon \rightarrow 0} \delta(\phi_0' - \phi_0) = \sqrt{\frac{\delta x}{\delta t} \frac{1}{4\pi\epsilon}} e^{-\frac{\delta x}{\delta t} \frac{(\phi_0' - \phi_0)^2}{4\epsilon}}. \quad (6.30)$$

As $\epsilon \rightarrow 0$, the path integral (6.29) tends to $|C|^2 4 \sqrt{\frac{\delta t}{\delta x} \frac{\pi^3}{\epsilon}} \delta(\phi_0' - \phi_0)$, and so we should set

$$C = \frac{1}{2} \left(\frac{\delta x}{\delta t} \frac{\epsilon}{\pi^3} \right)^{1/4}, \quad (6.31)$$

to obtain,

$$PI_{\epsilon \rightarrow 0} = \lim_{\epsilon \rightarrow 0} \int d\phi_1 d\phi_2 K^*(\phi_1, \phi_2; \phi_0'; \epsilon) K(\phi_1, \phi_2; \phi_0; \epsilon) = \delta(\phi_0' - \phi_0). \quad (6.32)$$

The $i\epsilon$ -prescription might seemed random or that it was pure luck that everything worked out correctly. The issue is that our choice of $i\epsilon$ is non-unique. One could have arrived at the same result with a different prescription, if only she follows the

rules

- (i) The path integral $\int d\phi_1 d\phi_2 K^*(\phi_1, \phi_2; \phi'_0; \epsilon) K(\phi_1, \phi_2; \phi_0; \epsilon)$ is convergent.
- (ii) The evolution $t = 0 \rightarrow t = 1 \rightarrow t = 0$ results in a delta function, $\int d\phi_1 d\phi_2 K^*(\phi_1, \phi_2; \phi'_0; \epsilon) K(\phi_1, \phi_2; \phi_0; \epsilon) = \delta(\phi'_0 - \phi_0)$.

6.2.1 Function Spaces Accommodating the $i\epsilon$ -prescription

The $i\epsilon$ plays a more dramatic role in our analyses than in ordinary quantum field theory. Consider the evolution of a normalizable wavefunction $\Psi(\phi_0)$ on the vertex ϕ_0 and evolve it by the propagator,

$$\begin{aligned} \Psi(\phi_1, \phi_2; \epsilon) &= \int d\phi_0 K(\phi_1, \phi_2; \phi_0; \epsilon) \Psi(\phi_0) \\ &= \frac{1}{2} \left(\frac{\delta x}{\delta t} \frac{\epsilon}{\pi^3} \right)^{1/4} e^{-\frac{\delta t}{\delta x} \frac{\epsilon+i}{8} (\phi_1 - \phi_2)^2} \int d\phi_0 e^{-\frac{\delta x}{\delta t} \frac{\epsilon-i}{8} (2\phi_0 - (\phi_1 + \phi_2))^2} \Psi(\phi_0). \end{aligned} \quad (6.33)$$

Using the coordinate change (6.20,6.21) we can rewrite the above as

$$\Psi(v, u; \epsilon) = \tilde{\Psi}_1(u; \epsilon) \cdot \tilde{\Psi}_2(v; \epsilon) \quad (6.34)$$

where we have defined the wavefunctions $\tilde{\Psi}_1, \tilde{\Psi}_2$ as

$$\tilde{\Psi}_1(u; \epsilon) = \frac{1}{\sqrt{2}} \left(\frac{\delta t}{\delta x} \frac{\epsilon}{\pi} \right)^{1/4} e^{-\frac{\delta t}{\delta x} \frac{\epsilon+i}{8} u^2} \quad (6.35)$$

$$\tilde{\Psi}_2(v; \epsilon) = \frac{1}{\sqrt{2}} \int d\phi_0 e^{-\frac{\delta x}{\delta t} \frac{\epsilon-i}{8} (2\phi_0 - v)^2} \Psi(\phi_0). \quad (6.36)$$

Observe that $\tilde{\Psi}_2$ is an L^2 -normalized wavefunction since

$$\int du |\tilde{\Psi}_1(u; \epsilon)|^2 = \frac{1}{2} \sqrt{\frac{\delta t}{\delta x} \frac{\epsilon}{\pi}} e^{-\frac{1}{2} \frac{\delta t}{\delta x} \frac{\epsilon}{4} u^2} = 1. \quad (6.37)$$

Moreover, $\Psi(v, u; \epsilon)$ is an L^2 -normalized wavefunction, see equation (2.69) of ssec. 2.4.3 and that results in $\tilde{\Psi}_2(v; \epsilon)$ being one too. A peculiar feature is that (6.34) vanishes in the $\epsilon \rightarrow 0$ limit, although if we take its L^2 norm for finite ϵ and then take the limit $\epsilon \rightarrow 0$ we get 1. Apparently, the order of limits matters here: we should compute the norm before taking the limit $\epsilon \rightarrow 0$.

We will consider an illuminating example, let

$$\Psi(\phi_0) = \frac{1}{(2\pi)^{1/4}} e^{-\frac{1}{4}\phi_0^2}, \quad (6.38)$$

so that (6.33) becomes

$$\Psi(\phi_1, \phi_2; \epsilon) = \frac{\left(\frac{\delta t}{\delta x} \frac{\epsilon}{2\pi^2} \right)^{1/4}}{\sqrt{\frac{\delta t}{\delta x} + 2(\epsilon - i)}} e^{-\frac{1}{8 \left(\frac{\delta t}{\delta x} + 2(\epsilon - i) \right)} \left[\left(\frac{\delta t^2}{\delta x^2} (\epsilon + i) + 2 \frac{\delta t}{\delta x} (1 + \epsilon^2) \right) (\phi_1 - \phi_2)^2 + (\epsilon - i) (\phi_1 + \phi_2)^2 \right]}. \quad (6.39)$$

Easily you can check that

$$\lim_{\epsilon \rightarrow 0^+} \int d\phi_1 d\phi_2 \Psi^*(\phi_1, \phi_2; \epsilon) \Psi(\phi_1, \phi_2; \epsilon) = 1, \quad (6.40)$$

while

$$\int d\phi_1 d\phi_2 \left(\lim_{\epsilon \rightarrow 0^+} \Psi^*(\phi_1, \phi_2; \epsilon) \right) \left(\lim_{\epsilon \rightarrow 0^+} \Psi(\phi_1, \phi_2; \epsilon) \right) = 0. \quad (6.41)$$

Indeed, the order of limits is important and in particular $\lim_{\epsilon \rightarrow 0^+} \Psi(\phi_1, \phi_2; \epsilon) = 0$ is not a normalizable wavefunction.

Clearly this dependence on ϵ augments what we mean by a quantum wavefunction in the present setting. In order to treat this we need to understand the nature of the Hilbert spaces \mathcal{H}_i .

In single particle quantum mechanics, we usually think of the Hilbert space as being $L^2(R)$, but a more refined approach is to consider a rigged Hilbert space [51]. A note on semantics. The word "rigged" has nothing to do with any "fixing" or pre-determining a result. A more faithful translation would be "equipped Hilbert space". To rig a Hilbert space means simply to equip that Hilbert space with distribution theory. So, it is not a replacement but an enlargement of the Hilbert space. We will briefly explain the construction of such a function space.

The problem with the single-particle quantum mechanics Hilbert space being $L^2(R)$ is that the \hat{x} and \hat{p} operators and polynomials thereof do not map $L^2(R)$ to itself. For instance, $\psi(x) = \frac{1}{\sqrt{\pi}} \frac{1}{\sqrt{1+x^2}}$ is in $L^2(R)$ since

$$\int dx |\psi(x)|^2 = \frac{1}{\pi} \arctan x|_{-\infty}^{\infty} = 1. \quad (6.42)$$

But acting \hat{x} on the state gives us $x\psi(x)$ which is not in $L^2(R)$.

To ameliorate this issue, we consider Schwartz class functions $\mathcal{S}(R)$ which are a subset of $L^2(R)$ with the property that any operator which is a finite order polynomial in \hat{x} 's and \hat{p} 's maps $\mathcal{S}(R)$ to itself. We can then say that physical wavefunctions live in $\mathcal{S}(R)$. However, eigenfunctions of \hat{x}, \hat{p} and polynomial combination of them need not be in either $\mathcal{S}(R)$ or the larger space $L^2(R)$. An example of this kind of functions is $\delta(x)$ or e^{ipx} . To accommodate these wavefunctions, we consider $\mathcal{S}^\times(R)$ which is the space of antilinear functionals over $\mathcal{S}(R)$ since we want a space of kets. Then our rigged Hilbert space is

$$\mathcal{S}(R) \subset L^2(R) \subset \mathcal{S}^\times(R). \quad (6.43)$$

Our kernel operator \mathcal{K} maps $\mathcal{S}(R)$ to Schwartz class functions from $R^2 \rightarrow C$ which also have a dependence on ϵ . The notation for this space is $\mathcal{S}(R^2, C)$ which denotes Schwartz class functions with domain R^2 and codomain C . We need to expand our codomain space C to accommodate ϵ -dependence, we call this augmented space $*C$. So then we can write

$$\mathcal{K} : \mathcal{S}(R, *C) \rightarrow \mathcal{S}(R^2, *C). \quad (6.44)$$

The notation $*C$ denotes the hypercomplex number **ref** which is a central object in the theory of non-standard analysis. Non-standard analysis is an extension of analysis which includes infinitesimals and infinite number. The only notation we will need, besides the $*C$ symbol, is 'st'. This denotes the 'standard' part of a real number for instance $\text{st}(x + \epsilon y) = x$, and for a smooth function $f(x, y)$ we have $\text{st}(f(x, \epsilon)) = \lim_{\epsilon \rightarrow 0^+} f(x, \epsilon)$. See for [54, 50] a complete discussion.

In this set up the inner product for $L^2(R, *C)$ or $L^2(R^2, *C)$, which induces an inner product on $\mathcal{S}(R, *C)$ or $\mathcal{S}(R^2, *C)$, is chosen as a semi-inner product. For two

functions $\psi(x; \epsilon), \psi'(x; \epsilon) \in L^2(\mathcal{R}, *C)$ that is

$$\langle \psi, \psi' \rangle := \text{st} \int dx \psi^*(x; \epsilon) \psi'(x; \epsilon), \quad (6.45)$$

and we have analogous inner products on the other function spaces. We used the prefix 'semi' since the ϵ part of a wavefunction will essentially be taken to zero when we compute the inner product. The limit $\epsilon \rightarrow 0^+$ is on the outside, which is in agreement with our previous discussion.

The above considerations suggest that we should work with the augmented rigged Hilbert spaces

$$\mathcal{S}(\mathcal{R}, *C) \subset L^2(\mathcal{R}, *C) \subset \mathcal{S}^\times(\mathcal{R}, *C), \quad \mathcal{S}(\mathcal{R}^2, *C) \subset L^2(\mathcal{R}^2, *C) \subset \mathcal{S}^\times(\mathcal{R}^2, C), \quad (6.46)$$

and our kernel may be viewed as implementing the maps

$$\mathcal{K} : \mathcal{S}(\mathcal{R}, *C) \rightarrow \mathcal{S}^\times(\mathcal{R}^2, *C), \quad \mathcal{K}^\dagger : \mathcal{S}(\mathcal{R}^2, *C) \rightarrow \mathcal{S}^\times(\mathcal{R}^2, C). \quad (6.47)$$

In summary, the most interesting output of this discussion is the proposal that we should allow some physics states to have ϵ dependence (i.e. a 'non-standard' part), and in doing so we should leverage the inner product in (6.45).

6.3 Nonunitary Isometric Quantum Evolution

The condition (6.32) can be expressed more algebraically. We have $\mathcal{K} : \mathcal{H}_0 \rightarrow \mathcal{H}_1 \otimes \mathcal{H}_2$, and the condition tells us that

$$\mathcal{K}^\dagger \mathcal{K} = \mathbb{1}_{\mathcal{H}_0}. \quad (6.48)$$

That is, if we evolve from $t = 0$ to $t = 1$ and then back, we find the identity operator on the $t = 0$ Hilbert space \mathcal{H}_0 .

This condition (6.48) tells us that \mathcal{K} is a Hilbert space isometry. That is, if we take any two states $|\Phi\rangle$ and $|\Phi'\rangle$ in \mathcal{H}_0 at the initial time $t = 0$ and evolve them via \mathcal{K} , then their inner product is preserved:

$$\langle \Phi' | \mathcal{K}^\dagger \mathcal{K} | \Phi \rangle = \langle \Phi' | \Phi \rangle. \quad (6.49)$$

Note that $\mathcal{K}|\Phi\rangle$ and $\mathcal{K}|\Phi'\rangle$ are each states in $\mathcal{H}_1 \otimes \mathcal{H}_2$ at time $t = 1$. We also have that $\mathcal{K}^\dagger : \mathcal{H}_1 \otimes \mathcal{H}_2 \rightarrow \mathcal{H}_0$; in fact, the condition (6.48) constrains the possibilities for $\mathcal{K}\mathcal{K}^\dagger$ which is a map from $\mathcal{H}_1 \otimes \mathcal{H}_2 \rightarrow \mathcal{H}_1 \otimes \mathcal{H}_2$. In particular,

$$(\mathcal{K}\mathcal{K}^\dagger)(\mathcal{K}\mathcal{K}^\dagger) = \mathcal{K}\mathcal{K}^\dagger, \quad (6.50)$$

which means that $\mathcal{K}\mathcal{K}^\dagger$ is idempotent, (i.e. if you apply it to itself it gives back itself), and since it is also Hermitian we conclude that $(\mathcal{K}\mathcal{K}^\dagger)$ is a projector. In the case of finite dimensional Hilbert spaces we would have

$$\begin{aligned} \text{rank}[\mathcal{K}\mathcal{K}^\dagger] &= \text{tr}[\mathcal{K}\mathcal{K}^\dagger] = \sum_i (\mathcal{K}\mathcal{K}^\dagger)_{ii} = \sum_i \sum_j \mathcal{K}_{ij} \mathcal{K}_{ji}^\dagger = \sum_j \sum_i \mathcal{K}_{ji}^\dagger \mathcal{K}_{ij} \\ &= \sum_j (\mathcal{K}\mathcal{K}^\dagger)_{jj} = \text{tr}[\mathcal{K}^\dagger \mathcal{K}] = \text{rank}[\mathcal{K}^\dagger \mathcal{K}] = \text{rank}[\mathbb{1}_{\mathcal{H}_0}] \end{aligned} \quad (6.51)$$

and since $\dim(\mathcal{H}_0) = \dim(\mathbb{I}_{\mathcal{H}_0}) \neq \dim(\mathbb{I}_{\mathcal{H}_1 \otimes \mathcal{H}_2}) = \dim(\mathcal{H}_1 \otimes \mathcal{H}_2) < \infty$, we would get $\mathcal{K}\mathcal{K}^\dagger \neq \mathbb{I}_{\mathcal{H}_1 \otimes \mathcal{H}_2}$ meaning that the isometry is not unitary. We denoted by $[\mathcal{K}_{ij}]$ a matrix representation of the kernel \mathcal{K} (and thereof the other kernels $\mathcal{K}\mathcal{K}^\dagger, \mathcal{K}^\dagger\mathcal{K}$). But since the rank of $\mathcal{L}_{\mathcal{H}_0}$ is infinite we do not learn much about the rank of the projector. We will show that $\mathcal{K}\mathcal{K}^\dagger$ has a non-trivial nullspace, which definitively establishes that \mathcal{K} is not unitary and is instead merely an isometry. When we speak of the nullspace of $\mathcal{K}\mathcal{K}^\dagger$, what we operationally mean is the space of vectors which are mapped to zero norm states in the sense of (6.45).

We will consider the evolution of the system from $t = 1$ to $t = 0$, and then back to $t = 1$. Returning to the position-space representation $\mathcal{K}\mathcal{K}^\dagger$ corresponds to

$$\int d\phi_0 K(\phi_1, \phi_2; \phi_0; \epsilon) K^*(\phi'_1, \phi'_2; \phi_0; \epsilon) = \int d\phi_0 e^{iS_\Delta[\{\phi_1, \phi_2; \phi_0\}] - iS_\Delta^*[\{\phi'_1, \phi'_2; \phi_0\}]}, \quad (6.52)$$

where, (with the help of (6.20,6.21)),

$$\begin{aligned} iS_\Delta[\{v, u; \phi_0\}; \epsilon] - iS_\Delta^*[\{v', u'; \phi_0\}; \epsilon] &= \frac{i\delta x}{8\delta t}(v' - v)(4\phi_0 - v - v') \\ &\quad - \frac{\epsilon\delta x}{8\delta t}((2\phi_0 - v)^2 - (2\phi_0 - v')^2) \\ &\quad - \frac{\delta t}{\delta x} \frac{i + \epsilon}{8} u^2 - \frac{\delta t}{\delta x} \frac{-i + \epsilon}{8} u'^2. \end{aligned} \quad (6.53)$$

Plugging into the integral, and performing Gaussian integrations and square completments with respect to ϕ_0 , we get

$$\begin{aligned} \int d\phi_0 K(v, u; \phi_0; \epsilon) K^*(v', u'; \phi_0; \epsilon) &= \frac{1}{4\pi} \exp\left(-\frac{1}{16\epsilon} \frac{\delta x}{\delta t} (v' - v)^2\right. \\ &\quad \left. - \frac{i\delta t}{8\delta x} (u^2 - u'^2) - \epsilon f(v, u, v', u')\right) \end{aligned} \quad (6.54)$$

where

$$f(v, u, v', u') = \frac{1}{16} \left(\frac{\delta x}{\delta t} (v - v')^2 + 2 \frac{\delta t}{\delta x} (u^2 - u'^2) \right). \quad (6.55)$$

In the limit of small ϵ which we will denote by $' \sim '$ we have

$$\int d\phi_0 K(v, u; \phi_0; \epsilon) K^*(v', u'; \phi_0; \epsilon) \sim \sqrt{\frac{\delta t}{\delta x} \frac{\epsilon}{\pi}} \delta(v - v') e^{-\frac{i}{8} \frac{\delta t}{\delta x} (u^2 - u'^2) - \epsilon f(v, u, v', u')}. \quad (6.56)$$

To interpret (6.56) let us integrate our kernel against a normalizable wavefunction $\Psi(v, u)$. Since we are working in v, u coordinates the measure will pick up a factor of $\frac{1}{2}$ due to the Jacobian from $(\phi_1, \phi_2) \rightarrow (v, u)$. Since the same transformation applies to the wave function $\Psi(\phi_1, \phi_2) \rightarrow \Psi(v, u)$ and we want it to be L^2 -normalizable with respect to the $dv' du'$ measure, we multiply by an extra $\frac{1}{\sqrt{2}}$. That is:

$$\sqrt{\frac{\delta t}{\delta x} \frac{\epsilon}{8\pi}} \int dv du \delta(v - v') e^{\frac{i}{8} \frac{\delta t}{\delta x} (u^2 - u'^2) - \epsilon f(v, u, v', u')} \Psi(v, u). \quad (6.57)$$

Performing the v integral, we obtain

$$\sqrt{\frac{\delta t}{\delta x} \frac{\epsilon}{8\pi}} e^{-\frac{\epsilon - i}{8} \frac{\delta t}{\delta x} u'^2} \int du e^{-\frac{\epsilon + i}{8} \frac{\delta t}{\delta x} u^2} \Psi(v', u). \quad (6.58)$$

Interestingly, there is an entire subspace of Ψ 's for which the right-hand side vanishes in the $\epsilon \rightarrow 0$ limit. For instance,

$$\Psi(v, u) = \frac{1}{\sqrt{2\pi}} \exp\left(-\frac{1}{4}v^2 - \frac{1}{4}u^2\right) \quad (6.59)$$

is giving us

$$\lim_{\epsilon \rightarrow 0} \left(\sqrt{\frac{\delta t}{\delta x} \frac{\epsilon}{16\pi^2}} e^{-\frac{\epsilon-i}{8} \frac{\delta t}{\delta x} u^2 - \frac{1}{4}v^2} \sqrt{\frac{8\pi}{(\epsilon+i) \frac{\delta t}{\delta x} + 2}} \right) = 0. \quad (6.60)$$

So, our wavefunction has the property

$$\mathcal{K}\mathcal{K}^\dagger|\Psi\rangle = 0. \quad (6.61)$$

This establishes that $\mathcal{K}\mathcal{K}^\dagger$ has a non-trivial nullspace, and accordingly \mathcal{K} is an isometry which is not unitary.

We can now graduate to a full-fledged field theory with an arbitrary number of lattice sites. Suppose we choose a triangular lattice \mathcal{L} of the 2-dimensional flat spacetime, and we consider the propagator between two adjacent Cauchy slices. Let the field variables on the 'past' Cauchy slice be denoted by the vector $\vec{\phi}_P$ with $|P|$ components, and the field variables on the 'future' Cauchy slice by $\vec{\phi}$ with $|F|$ components. We will suppose that $|F| > |P|$, namely that there are a greater number of lattice points on the future Cauchy slice than on the past Cauchy slice. Then for a free scalar field theory, the most general action will be of the form

$$S[\{\vec{\phi}_F; \vec{\phi}_P\}; \epsilon] = \vec{\phi}_P^\top \cdot Q \cdot \vec{\phi}_P + \vec{\phi}_F^\top \cdot R \cdot \vec{\phi}_P + \vec{\phi}_F^\top \cdot S \cdot \vec{\phi}_F \\ + i\epsilon \vec{\phi}_P^\top \cdot M \cdot \vec{\phi}_P + i\epsilon \vec{\phi}_F^\top \cdot L \cdot \vec{\phi}_P + i\epsilon \vec{\phi}_F^\top \cdot W \cdot \vec{\phi}_F. \quad (6.62)$$

Our propagator (6.15) becomes

$$K(\vec{\phi}_F; \vec{\phi}_P; \epsilon) = C e^{i(\vec{\phi}_P^\top \cdot Q \cdot \vec{\phi}_P + \vec{\phi}_F^\top \cdot R \cdot \vec{\phi}_P + \vec{\phi}_F^\top \cdot S \cdot \vec{\phi}_F) - \epsilon(\vec{\phi}_P^\top \cdot M \cdot \vec{\phi}_P + \vec{\phi}_F^\top \cdot L \cdot \vec{\phi}_P + \vec{\phi}_F^\top \cdot W \cdot \vec{\phi}_F)}. \quad (6.63)$$

Let us compute the path integral that propagates the system from past to future to past. This is

$$\int d\vec{\phi}_F K^*(\vec{\phi}_F; \vec{\phi}'_P; \epsilon) K(\vec{\phi}_F; \vec{\phi}_P; \epsilon) \\ = |C|^2 e^{i(\vec{\phi}'_P^\top \cdot Q \cdot \vec{\phi}_P - \vec{\phi}'_P^\top \cdot Q \cdot \vec{\phi}'_P + \vec{\phi}_F^\top \cdot R \cdot (\vec{\phi}_P - \vec{\phi}'_P)) - \epsilon(\vec{\phi}'_P^\top \cdot M \cdot \vec{\phi}_P - \epsilon \vec{\phi}'_P^\top \cdot M \cdot \vec{\phi}'_P - \epsilon \vec{\phi}_F^\top \cdot L \cdot (\vec{\phi}_P + \vec{\phi}'_P) - 2\epsilon \vec{\phi}_F^\top \cdot W \cdot \vec{\phi}_F)}. \quad (6.64)$$

We will calculate this integral schematically. Every constant or unimportant term will be denoted by $\#$. Let us begin by rearranging the path integral (7.19),

$$\int d\vec{\phi}_F K^*(\vec{\phi}_F; \vec{\phi}'_P; \epsilon) K(\vec{\phi}_F; \vec{\phi}_P; \epsilon) = |C|^2 \# \int d\vec{\phi}_F e^{-\epsilon \vec{\phi}_F^\top \cdot W \cdot \vec{\phi}_F + \vec{\phi}_F^\top \cdot (iR \cdot (\vec{\phi}_P - \vec{\phi}'_P) - \epsilon L \cdot (\vec{\phi}_P + \vec{\phi}'_P))} \\ = |C|^2 \# \int d\phi_F |_1 \cdots d\phi_F |_{|F|} e^{-\epsilon \sum_{i=1}^{|F|} \sum_{j=1}^{|F|} \phi_F |_i W_{ij} \phi_F |_j + \sum_{i=1}^{|F|} \sum_{j=1}^{|P|} \phi_F |_i (iR_{ij} (\phi_P - \phi'_P) |_j - \epsilon L_{ij} (\phi_P + \phi'_P) |_j)} \\ = |C|^2 \frac{\#}{\epsilon^{\frac{|F|}{2}}} e^{\frac{\#}{\epsilon} (i(\vec{\phi}_P - \vec{\phi}'_P)^\top \cdot R^\top - \epsilon(\vec{\phi}_P + \vec{\phi}'_P)^\top \cdot L^\top) \cdot W^{-1} (iR \cdot (\vec{\phi}_P - \vec{\phi}'_P) - \epsilon L \cdot (\vec{\phi}_P + \vec{\phi}'_P))}, \quad (6.65)$$

where we used the identity $\int d\vec{x} e^{-\frac{\epsilon}{2}x^T \cdot A \cdot x + x^T \cdot J} = \left(\left(\frac{2\pi}{\epsilon} \right)^N \frac{1}{\det[A]} \right)^{\frac{1}{2}} e^{\frac{1}{2\epsilon} J^T \cdot A^{-1} \cdot J}$ for Gaussian integrals of dimension N . For small ϵ the above integral becomes

$$\int d\vec{\phi}_F K^*(\vec{\phi}_F; \vec{\phi}'_P; \epsilon) K(\vec{\phi}_F; \vec{\phi}_P; \epsilon) = |C|^2 \frac{\#}{\epsilon^{\frac{|F|}{2}}} e^{-\frac{\#}{\epsilon} (\vec{\phi}_P - \vec{\phi}'_P)^T \cdot R^T \cdot W^{-1} \cdot R \cdot (\vec{\phi}_P - \vec{\phi}'_P)}. \quad (6.66)$$

Notice that $R^T \cdot W^{-1} \cdot R$ is a $|P| \times |P|$ matrix, so a better reorganization of the above result is

$$\int d\vec{\phi}_F K^*(\vec{\phi}_F; \vec{\phi}'_P; \epsilon) K(\vec{\phi}_F; \vec{\phi}_P; \epsilon) = |C|^2 \frac{\#}{\epsilon^{\frac{|F|}{2} - \frac{|P|}{2}}} \frac{1}{\epsilon^{\frac{|P|}{2}}} e^{-\frac{\#}{\epsilon} (\vec{\phi}_P - \vec{\phi}'_P)^T \cdot R^T \cdot W^{-1} \cdot R \cdot (\vec{\phi}_P - \vec{\phi}'_P)}. \quad (6.67)$$

Compare the previous result with the generalization of the delta function (6.30),

$$\lim_{\epsilon \rightarrow 0} \delta^{(N)}(\vec{\phi} - \vec{\phi}') \sim \frac{\#}{\epsilon^{\frac{N}{2}}} e^{-\frac{\#}{\epsilon} (\vec{\phi} - \vec{\phi}')^T \cdot (\vec{\phi} - \vec{\phi}')}, \quad (6.68)$$

which has the property $\delta^{(N)}(A \cdot (\vec{\phi} - \vec{\phi}')) = \frac{1}{|\det[A]|} \delta^{(N)}(\vec{\phi} - \vec{\phi}')$ ¹ meaning that,

$$\lim_{\epsilon \rightarrow 0} \delta^{(N)}(A \cdot (\vec{\phi} - \vec{\phi}')) \sim \frac{\#}{\epsilon^{\frac{N}{2}}} e^{-\frac{\#}{\epsilon} (\vec{\phi} - \vec{\phi}')^T \cdot A^T \cdot A \cdot (\vec{\phi} - \vec{\phi}')} \sim \lim_{\epsilon \rightarrow 0} \delta^{(N)}(\vec{\phi} - \vec{\phi}'), \quad (6.69)$$

for a $N \times N$ matrix A . So, in the limit of $\epsilon \rightarrow 0$ equation (6.67) becomes

$$\lim_{\epsilon \rightarrow 0} \int d\vec{\phi}_F K^*(\vec{\phi}_F; \vec{\phi}'_P; \epsilon) K(\vec{\phi}_F; \vec{\phi}_P; \epsilon) = |C|^2 \frac{\#}{\epsilon^{\frac{|F|}{2} - \frac{|P|}{2}}} \delta^{(|P|)}(\vec{\phi}_P - \vec{\phi}'_P). \quad (6.70)$$

Letting $C = \epsilon^{\frac{|F| - |P|}{4}} / \#^{1/2}$, we are left with

$$\lim_{\epsilon \rightarrow 0} \int d\vec{\phi}_F K^*(\vec{\phi}_F; \vec{\phi}'_P; \epsilon) K(\vec{\phi}_F; \vec{\phi}_P; \epsilon) = \delta^{(|P|)}(\vec{\phi}_P - \vec{\phi}'_P), \quad (6.71)$$

and so $\mathcal{K}^\dagger \mathcal{K}$ is the identity. Hence \mathcal{K} is a Hilbert space isometry. Similarly, if we examine future to past to future propagation we find

$$\begin{aligned} & \int d\vec{\phi}_P K^*(\vec{\phi}'_F; \vec{\phi}_P; \epsilon) K(\vec{\phi}_F; \vec{\phi}_P; \epsilon) \\ &= |C|^2 \int d\vec{\phi}_P e^{i(\vec{\phi}'_F \cdot S \cdot \vec{\phi}_F - \vec{\phi}'_F \cdot S \cdot \vec{\phi}'_F + (\vec{\phi}_F - \vec{\phi}'_F)^T \cdot R \cdot \vec{\phi}_P) - 2\epsilon \vec{\phi}'_P \cdot K \cdot \vec{\phi}_P - \epsilon (\vec{\phi}_F + \vec{\phi}'_F)^T \cdot L \cdot \vec{\phi}_P - \epsilon \vec{\phi}'_F \cdot W \cdot \vec{\phi}_F - \epsilon \vec{\phi}'_F \cdot W \cdot \vec{\phi}'_F} \\ &= |C|^2 \# \int d\vec{\phi}_P e^{-\# \epsilon \vec{\phi}'_P \cdot M \cdot \vec{\phi}_P + (i(\vec{\phi}_F - \vec{\phi}'_F)^T \cdot R - \epsilon (\vec{\phi}_F + \vec{\phi}'_F)^T \cdot L) \cdot \vec{\phi}_P} \\ &= |C|^2 \frac{\#}{\epsilon^{\frac{|P|}{2}}} e^{\frac{\#}{\epsilon} (i(\vec{\phi}_F - \vec{\phi}'_F)^T \cdot R - \epsilon (\vec{\phi}_F + \vec{\phi}'_F)^T \cdot L) \cdot M^{-1} \cdot (iR^T \cdot (\vec{\phi}_F - \vec{\phi}'_F) - \epsilon L^T \cdot (\vec{\phi}_F + \vec{\phi}'_F))} \\ &= \frac{\#}{\epsilon^{\frac{|P|}{2}}} e^{-\frac{\#}{\epsilon} (\vec{\phi}_F - \vec{\phi}'_F)^T \cdot R \cdot M^{-1} \cdot R^T \cdot (\vec{\phi}_F - \vec{\phi}'_F)}, \end{aligned} \quad (6.72)$$

where we used the identity $\int d\vec{x} e^{-\frac{\epsilon}{2}x^T \cdot A \cdot x + J^T \cdot x} = \left(\left(\frac{2\pi}{\epsilon} \right)^N \frac{1}{\det[A]} \right)^{\frac{1}{2}} e^{\frac{1}{2\epsilon} J^T \cdot A^{-1} \cdot J}$ for Gaussian integrals of dimension N and the last equality holds for small ϵ . Observe that $R \cdot M^{-1} \cdot R^T$ is an $|F| \times |F|$ matrix. It seems that in the $\epsilon \rightarrow 0$ limit we would obtain $\sim \delta^{(|F|)}(\vec{\phi}_F - \vec{\phi}'_F)$ by comparing with equation (6.69) and with a reshuffling of

¹Properties of the dirac delta function with a matrix argument can be found in the paper [69] of L. Zhang.

the power of the ϵ term in front. In that case our kernel $\mathcal{K}\mathcal{K}^\dagger$ would be the identity, hence \mathcal{K} would be unitary. But this is too quick and contradicts the previous results of our toy model for a scalar field on a triangle. We need to take into account the fact that R is a $|F| \times |P|$ matrix for $|F| > |P|$. This means that the rank of the matrix R is $|P|$. Hence, the integral cannot possibly equal $\delta^{(|F|)}(\vec{\phi}_F - \vec{\phi}'_F)$, and so $\mathcal{K}\mathcal{K}^\dagger$ is not the identity. We again conclude that \mathcal{K} is not unitary and is instead just an isometry.

In an expanding spacetime, we have a sequence of Cauchy slices such that the number of lattice sites per Cauchy slice is increasing with time. If $\mathcal{K}_{2 \leftarrow 1}$ is the propagator from the first to second Cauchy slice, $\mathcal{K}_{3 \leftarrow 2}$ from the second to third, and so on, then our analysis above establishes that each $\mathcal{K}_{i+1 \leftarrow i}$ is a Hilbert space isometry. Then it is readily checked that for $i < j$,

$$\mathcal{K}_{j \leftarrow i} := \mathcal{K}_{j \leftarrow j-1} \cdots \mathcal{K}_{i+2 \leftarrow i+1} \mathcal{K}_{i+1 \leftarrow i}, \quad (6.73)$$

is also Hilbert space isometry, since $\mathcal{K}_{i \rightarrow j}^\dagger \mathcal{K}_{i \rightarrow j}$ is the identity on the Hilbert space corresponding to the i th Cauchy slice, and $\mathcal{K}_{i \rightarrow j} \mathcal{K}_{i \rightarrow j}^\dagger$ is a non-identity projection.

Chapter 7

FEM in Fermionic Field Theory

In the previous chapter we applied the FEM method on scalar field theory where we showed that quantum mechanical time evolution is isometric. In sec. 6.3 it was noted that for a case of finite dimensional Hilbert spaces the isometry of the evolution operator \mathcal{K} would have been obvious without the need of dealing with the null space of the $\mathcal{K}\mathcal{K}^\dagger$ projector. That prompted us to apply the FEM method in fermionic field theory where the Hilbert spaces are finite dimensional, in hope of getting more intuition for the evolution of quantum states in our lattice field theory.

One anticipates that for fermions the whole procedure will be simplified due to the grassmannian nature of the fields. For example, the problems of convergence of the path integral that we faced in the scalar field theory are supposed to be easily solvable. It turns out that this is not the case. For free fermions, even in flat space-time, there are additional difficulties that are not addressed in the FEM literature to our knowledge. It is pointed out a long time ago in [29] that a non-regular, *aka* FDM, latticization is unclear with fermions. Even nowadays the only two references that rigorously study fermions on a FEM lattice are [13] and [11] but there is no mention about quantum mechanical time evolution. Their analysis is about the energy spectrum of the field on a curved manifold without time evolution.

The organization of the chapter goes as follows. In sec. 7.1 we will discretize our classical action using the FEM method. In section 7.2 we describe the problems that arise in the quantization of the discretized FEM field. Finally, in section 7.3 there is a discussion for the nourishment of those problems.

7.1 Classical Considerations

Similarly with the scalar field case both the analysis and geometric methods of ssec (5.2.1,5.2.2) will be utilized for the calculation of the classical discretized fermionic FEM action.

7.1.1 Analysis Approach to Fermionic FEM on a Triangle

We will explore the FEM discretizations of classical field equations of motion for the fermionic theory in the same 2 dimensional triangle lattice $\tilde{\Delta}$ as for the scalar field, see Fig. 7.1. The FEM basis $\{B_{\tilde{\Delta}}^{(j)}(t,x)\}$ for $j = 0,1,2$ is given by equations

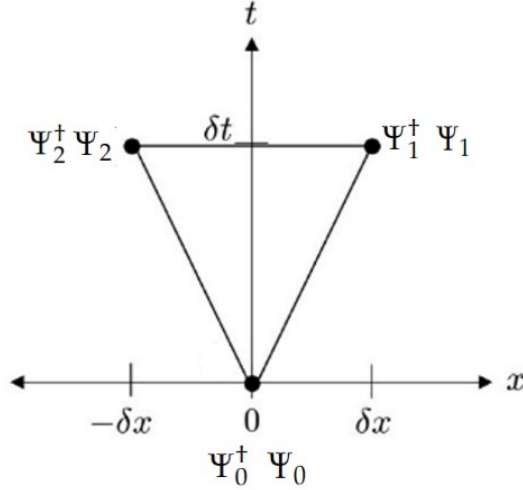


FIGURE 7.1: The triangle $\tilde{\Delta}$ in R^2 with vertices $(t, x) = (0, 0)$, $(\delta t, -\delta x)$ and $(\delta t, \delta x)$. We have labeled the vertices by their corresponding field values $\Psi_0 - \Psi_0^\dagger$, $\Psi_1 - \Psi_1^\dagger$, $\Psi_2 - \Psi_2^\dagger$.

(6.33,6.7,6.8) in ssec. 6.1.1. We present them below for the convenience of the reader,

$$B_{\tilde{\Delta}}^{(0)}(t, x) = \left(1 - \frac{t}{\delta t}\right) \chi_{\tilde{\Delta}}(t, x), \quad (7.1)$$

$$B_{\tilde{\Delta}}^{(1)}(t, x) = \left(\frac{t}{2\delta t} - \frac{x}{2\delta x}\right) \chi_{\tilde{\Delta}}(t, x), \quad (7.2)$$

$$B_{\tilde{\Delta}}^{(2)}(t, x) = \left(\frac{t}{2\delta t} + \frac{x}{\delta x}\right) \chi_{\tilde{\Delta}}(t, x). \quad (7.3)$$

The expansion of the fermion field in this basis is

$$\Psi(t, x) = \Psi_0 B_{\tilde{\Delta}}^{(0)}(t, x) + \Psi_1 B_{\tilde{\Delta}}^{(1)}(t, x) + \Psi_2 B_{\tilde{\Delta}}^{(2)}(t, x), \quad (7.4)$$

where Ψ takes values in a complex vector space described concretely as \mathbb{C}^2 . The components of a representation of the fields Ψ_i in the \mathbb{C}^2 space are denoted by,

$$\Psi_i = \begin{bmatrix} \Psi_{i0} \\ \Psi_{i1} \end{bmatrix}, \quad (7.5)$$

with $i = 0, 1, 2$. Our goal is to FEM discretize the Dirac action for a massless fermion in 2-dimensions which is

$$S = \int dx^2 \bar{\Psi} (i\gamma^\mu \partial_\mu \Psi), \quad (7.6)$$

where $\bar{\Psi} = \Psi^\dagger \gamma^0$ and the gamma matrices γ^μ with $\mu = 0, 1$ have the defining property $\{\gamma^\mu, \gamma^\nu\} = \gamma^\mu \gamma^\nu + \gamma^\nu \gamma^\mu = -2\eta^{\mu\nu} I_2$ to generate a Clifford algebra. We choose the following representation for the gamma's

$$\gamma^0 = \begin{bmatrix} 1 & 0 \\ 0 & -1 \end{bmatrix}, \quad \gamma^1 = \begin{bmatrix} 0 & 1 \\ -1 & 0 \end{bmatrix}, \quad \gamma^0 \gamma^1 = \begin{bmatrix} 0 & 1 \\ 1 & 0 \end{bmatrix}. \quad (7.7)$$

In order for Hermiticity of the discretized action to be enforced, one must use the freedom of the continuum Dirac action with respect to the boundary. This results in

an action of the form,

$$S = \int dx^2 \left(\frac{i}{2} \bar{\Psi} \gamma^\mu \partial_\mu \Psi - \frac{i}{2} (\partial_\mu \bar{\Psi}) \gamma^\mu \Psi \right). \quad (7.8)$$

Plugging the field expansion (7.4) into the action (7.8) and using Mathematica, we get

$$\begin{aligned} S_{\tilde{\Delta}}[\{\Psi_0, \Psi_0^\dagger, \Psi_1, \Psi_1^\dagger, \Psi_2, \Psi_2^\dagger\}] &= -\frac{idx}{12} (\Psi_0^\dagger + \Psi_1^\dagger + \Psi_2^\dagger) (2\Psi_0 - \Psi_1 - \Psi_2) \\ &\quad + \frac{idx}{12} (2\Psi_0^\dagger - \Psi_1^\dagger - \Psi_2^\dagger) (\Psi_0 + \Psi_1 + \Psi_2) \\ &\quad + \frac{idt}{12} (\Psi_0^\dagger + \Psi_1^\dagger + \Psi_2^\dagger) \begin{bmatrix} 0 & 1 \\ 1 & 0 \end{bmatrix} (\Psi_2 - \Psi_1) \\ &\quad - \frac{idt}{12} (\Psi_2^\dagger - \Psi_1^\dagger) \begin{bmatrix} 0 & 1 \\ 1 & 0 \end{bmatrix} (\Psi_0 + \Psi_1 + \Psi_2) \\ &= +\frac{i\delta x}{4} \Psi_0^\dagger (\Psi_1 + \Psi_2) - \frac{i\delta x}{4} (\Psi_1^\dagger + \Psi_2^\dagger) \Psi_0 \\ &\quad + \frac{i\delta t}{12} \Psi_0^\dagger \begin{bmatrix} 0 & 1 \\ 1 & 0 \end{bmatrix} (\Psi_2 - \Psi_1) - \frac{i\delta t}{12} (\Psi_2^\dagger - \Psi_1^\dagger) \begin{bmatrix} 0 & 1 \\ 1 & 0 \end{bmatrix} \Psi_0 \\ &\quad + \frac{i\delta t}{12} (\Psi_1^\dagger + \Psi_2^\dagger) \begin{bmatrix} 0 & 1 \\ 1 & 0 \end{bmatrix} (\Psi_2 - \Psi_1) \\ &\quad - \frac{i\delta t}{12} (\Psi_2^\dagger - \Psi_1^\dagger) \begin{bmatrix} 0 & 1 \\ 1 & 0 \end{bmatrix} (\Psi_1 + \Psi_2) \end{aligned} \quad (7.9)$$

which is the FEM discretization of the action for a massless fermion field in the triangle $\tilde{\Delta}$. One can easily verify that the action is indeed Hermitian $S_{\tilde{\Delta}}^\dagger = S_{\tilde{\Delta}}$.

7.1.2 Geometric Approach to Fermionic FEM on a Triangle

The Euclidean continuum Dirac action is of the form,

$$I_{\tilde{\Delta}} = \int_{\tilde{\Delta}} dt_E dx \left(\frac{1}{2} \bar{\Psi}(t_E, x) \vec{\gamma}_E \cdot \vec{\nabla} \Psi(t_E, x) - \frac{1}{2} (\vec{\nabla} \bar{\Psi}(t_E, x)) \cdot \vec{\gamma}_E \Psi(t_E, x) \right), \quad (7.10)$$

where this time anti-Hermiticity is being enforced. This is due to the fact that the Dirac operator is anti-Hermitian in Euclidean signature. The Euclidean gamma matrices are related to the Minkowskian by the equations

$$\gamma_E^0 = \gamma^0, \quad \gamma_E^1 = i\gamma^1. \quad (7.11)$$

and are defined by the property $\{\gamma_E^\mu, \gamma_E^\nu\} = \gamma_E^\mu \gamma_E^\nu + \gamma_E^\nu \gamma_E^\mu = 2\delta^{\mu\nu} I_2$.

A more appealing geometric form than the one that was used for the scalar field in ssec 5.2.2 can be found. Moreover, it will be more suited for the fermionic action which only has first order derivatives. A convenient way to derive this is to relax the constraint $\xi_0 + \xi_1 + \xi_2 = 1$ and introduce an overcomplete set of 2 + 1 dual vectors, $\vec{n}^k = \vec{\nabla} \xi^k$ with $k = 0, 1, 2$, that are perpendicular to the face opposite the vertex k and normalized relative to the edge vectors by

$$\vec{n}^k \cdot \vec{l}_{ij} = \delta_i^k - \delta_j^k. \quad (7.12)$$

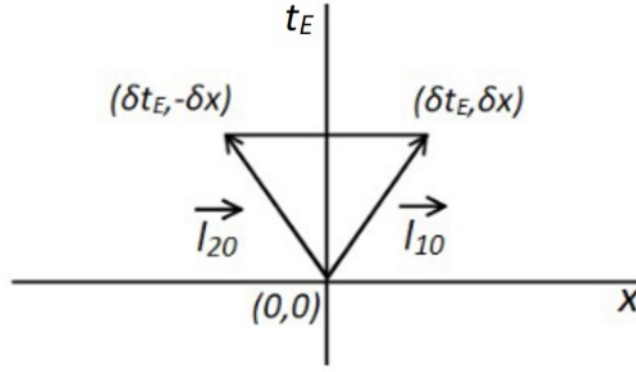


FIGURE 7.2: The triangle $\tilde{\Delta}$ parametrized by $\vec{l}_{10}, \vec{l}_{20}$ with the addition of the vector \vec{l}_{21} .

For our triangle $\tilde{\Delta}$ we have, see Fig. 7.2,

$$\vec{l}_{10} = (\delta t_E, \delta x), \quad \vec{l}_{20} = (\delta t_E, -\delta x), \quad \vec{l}_{21} = \vec{l}_{20} - \vec{l}_{10} = (0, -2\delta x) \quad (7.13)$$

which translates into a $\{\vec{n}^k\}_{k=0,1,2}$ basis as,

$$\vec{n}^0 = \left(-\frac{1}{\delta t_E}, 0\right), \quad \vec{n}^1 = \left(\frac{1}{2\delta t_E}, \frac{1}{2\delta x}\right), \quad \vec{n}^2 = \left(\frac{1}{2\delta t_E}, -\frac{1}{2\delta x}\right). \quad (7.14)$$

In this over-complete basis, the gradient is $\vec{\nabla}\Psi = \vec{n}^0\Psi_0 + \vec{n}^1\Psi_1 + \vec{n}^2\Psi_2$. Expanding $\Psi(\xi) = \Psi_0\xi^0 + \Psi_1\xi^1 + \Psi_2\xi^2$ into the linear FEM basis and plugging into the action (7.10) we get

$$\begin{aligned} I_{\tilde{\Delta}}[\{\Psi_0, \Psi_0^\dagger, \Psi_1, \Psi_1^\dagger, \Psi_2, \Psi_2^\dagger\}] &= \frac{\delta t_E \delta x}{6} \sum_{i,j=0}^2 \bar{\Psi}_i (\vec{n}^j - \vec{n}^i) \cdot \gamma_E \Psi_j \\ &= +\frac{\delta x}{4} \Psi_0^\dagger (\gamma_E^0)^2 (\Psi_1 + \Psi_2) - \frac{\delta x}{4} (\Psi_1^\dagger + \Psi_2^\dagger) (\gamma_E^0)^2 \Psi_0 \\ &\quad + \frac{\delta t_E}{12} (\Psi_2^\dagger - \Psi_1^\dagger) \gamma_E^0 \gamma_E^1 \Psi_0 - \frac{\delta t_E}{12} \Psi_0^\dagger \gamma_E^0 \gamma_E^1 (\Psi_2 - \Psi_1) \\ &\quad + \frac{\delta t_E}{12} (\Psi_2^\dagger - \Psi_1^\dagger) \gamma_E^0 \gamma_E^1 (\Psi_1 + \Psi_2) \\ &\quad - \frac{\delta t_E}{12} (\Psi_1^\dagger + \Psi_2^\dagger) \gamma_E^0 \gamma_E^1 (\Psi_2 - \Psi_1) \end{aligned} \quad (7.15)$$

where we used the identity of the barycentric coordinates $\int dt_E dx \xi^i(t_E, x) = \int d\xi^1 d\xi^2 \sqrt{g_{\tilde{\Delta}}} \xi^i = \frac{\sqrt{g_{\tilde{\Delta}}}}{(1+2)!}$ for $i = 1, 2$ with $\sqrt{g_{\tilde{\Delta}}} = 2\delta t_E \delta x$; see [62]. Wick-rotating back to Minkowski time,

$t_E \rightarrow it$, we get

$$\begin{aligned}
I_{\tilde{\Delta}}[\{\Psi_0, \Psi_0^\dagger, \Psi_1, \Psi_1^\dagger, \Psi_2, \Psi_2^\dagger\}] &= + \frac{\delta x}{4} \Psi_0^\dagger (\Psi_1 + \Psi_2) - \frac{\delta x}{4} (\Psi_1^\dagger + \Psi_2^\dagger) \Psi_0 \\
&\quad - \frac{\delta t}{12} (\Psi_2^\dagger - \Psi_1^\dagger) \begin{bmatrix} 0 & 1 \\ 1 & 0 \end{bmatrix} \Psi_0 + \frac{\delta t}{12} \Psi_0^\dagger \begin{bmatrix} 0 & 1 \\ 1 & 0 \end{bmatrix} (\Psi_2 - \Psi_1) \\
&\quad - \frac{\delta t_E}{12} (\Psi_2^\dagger - \Psi_1^\dagger) \begin{bmatrix} 0 & 1 \\ 1 & 0 \end{bmatrix} (\Psi_1 + \Psi_2) \\
&\quad + \frac{\delta t_E}{12} (\Psi_1^\dagger + \Psi_2^\dagger) \begin{bmatrix} 0 & 1 \\ 1 & 0 \end{bmatrix} (\Psi_2 - \Psi_1), \tag{7.16}
\end{aligned}$$

which is equivalent, see equation (7.9), to

$$-I_{\tilde{\Delta}}[\{\Psi_0, \Psi_0^\dagger, \Psi_1, \Psi_1^\dagger, \Psi_2, \Psi_2^\dagger\}] = iS_{\tilde{\Delta}}[\{\Psi_0, \Psi_0^\dagger, \Psi_1, \Psi_1^\dagger, \Psi_2, \Psi_2^\dagger\}]. \tag{7.17}$$

7.2 Quantum Considerations and Isometric Evolution

In order to proceed to quantum theory we will again perform a path integral quantization of the free massless fermion field on the triangle $\tilde{\Delta}$. The propagator from $t = 0$ to $t = 1$ is

$$K(\Psi_1, \Psi_1^\dagger, \Psi_2, \Psi_2^\dagger; \Psi_0, \Psi_0^\dagger) = C e^{iS_{\tilde{\Delta}}[\{\Psi_0, \Psi_0^\dagger, \Psi_1, \Psi_1^\dagger, \Psi_2, \Psi_2^\dagger\}]}. \tag{7.18}$$

We will examine the evolution of the system from $t = 0$ to $t = 1$ back to $t = 0$. This is expressed by the path integral

$$\begin{aligned}
PI &:= \int d\Psi_1 d\Psi_1^\dagger d\Psi_2 d\Psi_2^\dagger K^\dagger(\Psi_1, \Psi_1^\dagger, \Psi_2, \Psi_2^\dagger; \Psi'_0, \Psi'_0) K(\Psi_1, \Psi_1^\dagger, \Psi_2, \Psi_2^\dagger; \Psi_0, \Psi_0^\dagger) \\
&= |C|^2 \int d\Psi_1 d\Psi_1^\dagger d\Psi_2 d\Psi_2^\dagger e^{iS_{\tilde{\Delta}}[\{\Psi_0, \Psi_0^\dagger, \Psi_1, \Psi_1^\dagger, \Psi_2, \Psi_2^\dagger\}] - iS_{\tilde{\Delta}}[\{\Psi'_0, \Psi'_0, \Psi_1, \Psi_1^\dagger, \Psi_2, \Psi_2^\dagger\}]}, \tag{7.19}
\end{aligned}$$

where,

$$\begin{aligned}
iS_{\tilde{\Delta}}[\{\Psi_0, \Psi_0^\dagger, \Psi_1, \Psi_1^\dagger, \Psi_2, \Psi_2^\dagger\}] - iS_{\tilde{\Delta}}^\dagger[\{\Psi'_0, \Psi'_0, \Psi_1, \Psi_1^\dagger, \Psi_2, \Psi_2^\dagger\}] &= \\
&= + \frac{\delta x}{4} (\Psi'_0 - \Psi_0^\dagger) (\Psi_1 + \Psi_2) - \frac{\delta x}{4} (\Psi_1^\dagger + \Psi_2^\dagger) \\
&\quad + \frac{\delta t}{12} (\Psi'_0 - \Psi_0^\dagger) \begin{bmatrix} 0 & 1 \\ 1 & 0 \end{bmatrix} (\Psi_2 - \Psi_1) \\
&\quad - \frac{\delta t}{12} (\Psi_2^\dagger - \Psi_1^\dagger) \begin{bmatrix} 0 & 1 \\ 1 & 0 \end{bmatrix} (\Psi'_0 - \Psi_0^\dagger). \tag{7.20}
\end{aligned}$$

We will use a coordinate transformation of the form.

$$u = \Psi_2 - \Psi_1 \tag{7.21}$$

$$v = \Psi_2 + \Psi_1 \tag{7.22}$$

$$a = \Psi'_0 - \Psi_0 \tag{7.23}$$

Unravelling equation (7.20) in these coordinates yields,

$$\begin{aligned}
& (iS_{\bar{\Delta}} - iS_{\bar{\Delta}}^{\dagger}) [\{a_i, a_i^*, v_i, v_i^*, u_i, u_i^*\}_{i=0,1}] = \\
& = -\frac{\delta x}{4} v_0 a_0^* - \frac{\delta x}{4} v_0^* a_0 - \frac{\delta x}{4} v_1 a_1^* - \frac{\delta x}{4} v_1^* a_1 \\
& \quad - \frac{\delta t}{12} u_0 a_1^* - \frac{\delta t}{12} u_0^* a_1 - \frac{\delta t}{12} u_1 a_0^* - \frac{\delta t}{12} u_1^* a_0. \tag{7.24}
\end{aligned}$$

Plugging into the path integral (7.19) we get,

$$\begin{aligned}
PI &= 16|C|^2 \int dv_0 dv_1 dv_0^* dv_1^* du_0 du_1 du_0^* du_1^* e^{(iS_{\bar{\Delta}} - iS_{\bar{\Delta}}^{\dagger}) [\{a_i, a_i^*, v_i, v_i^*, u_i, u_i^*\}_{i=0,1}]} \\
&= 16|C|^2 \left(\frac{\delta x}{4}\right)^4 \left(\frac{\delta t}{12}\right)^4 a_0^* a_0 a_1^* a_1 a_1^* a_1 a_0^* a_0 \\
&= 0, \tag{7.25}
\end{aligned}$$

where the factor of 16 comes for the inverse of the determinant of the coordinate transformation since we are working with Grassmann numbers. As you can see we end up with a pathological result which means that there is no time propagation of the states from $t = 0$ to $t = 1$ to $t = 0$. Ideally we would like the path integral to result in a delta function of the form,

$$\delta(a_0, a_0^*, a_1, a_1^*) = a_0 a_0^* a_1 a_1^*. \tag{7.26}$$

We speculated that for this to happen we need an ϵ^1 -prescription. There were many failed attempts. The only prescription that seemed to work, but it is highly problematic, is the following

$$\begin{aligned}
& S_{\bar{\Delta}}[\{\Psi_0, \Psi_0^{\dagger}, \Psi_1, \Psi_1^{\dagger}, \Psi_2, \Psi_2^{\dagger}\}; E, E^{\dagger}] = \\
& = +\frac{i\delta x}{4} \Psi_0^{\dagger} (\Psi_1 + \Psi_2) - \frac{i\delta x}{4} (\Psi_1^{\dagger} + \Psi_2^{\dagger}) \Psi_0 \\
& \quad + \frac{i\delta t}{12} \Psi_0^{\dagger} \begin{bmatrix} 0 & 1 \\ 1 & 0 \end{bmatrix} (\Psi_2 - \Psi_1) - \frac{i\delta t}{12} (\Psi_2^{\dagger} - \Psi_1^{\dagger}) \begin{bmatrix} 0 & 1 \\ 1 & 0 \end{bmatrix} \Psi_0 \\
& \quad + \frac{i\delta t}{12} (\Psi_1^{\dagger} + \Psi_2^{\dagger}) \begin{bmatrix} 0 & 1 \\ 1 & 0 \end{bmatrix} (\Psi_2 - \Psi_1) \\
& \quad - \frac{i\delta t}{12} (\Psi_2^{\dagger} - \Psi_1^{\dagger}) \begin{bmatrix} 0 & 1 \\ 1 & 0 \end{bmatrix} (\Psi_1 + \Psi_2) \\
& \quad + \frac{\delta x}{8} E^{\dagger} (\Psi_1 + \Psi_2) - \frac{\delta x}{8} (\Psi_1^{\dagger} + \Psi_2^{\dagger}) E \\
& \quad + \frac{\delta t}{24} E^{\dagger} \begin{bmatrix} 0 & 1 \\ 1 & 0 \end{bmatrix} (\Psi_2 - \Psi_1) - \frac{\delta t}{24} (\Psi_2^{\dagger} - \Psi_1^{\dagger}) \begin{bmatrix} 0 & 1 \\ 1 & 0 \end{bmatrix} E, \tag{7.27}
\end{aligned}$$

where,

$$E = \begin{bmatrix} \epsilon \\ \epsilon \end{bmatrix}, \tag{7.28}$$

¹Typically, we use an $i\epsilon$ -prescription. In our case, the integrated parameters take values in the complex numbers so the prescription should not necessarily be imaginary. In standard QFT, the $i\epsilon$ -prescription is used in the calculation of the propagator where the integration parameter is real *i.e.* the 0-momentum component. In that case, there is a reason to be made for an imaginary prescription. Nevertheless, one could attempt the usual $i\epsilon$ -prescription but since our work with fermions, as you will shortly see, is highly problematic that attempt is left to the reader.

with ϵ being a real number and not a Grassman variable. In this setting and using coordinates (7.21,7.22,7.23) equation (7.24) becomes,

$$\begin{aligned} (iS_{\bar{\Delta}} - iS_{\Delta}^{\dagger})[\{a, a^{\dagger}, v, v^{\dagger}, u, u^{\dagger}\}; E, E^{\dagger}] &= \\ &= + \frac{\delta x}{4}(a^{\dagger} + iE^{\dagger})v - \frac{\delta x}{4}v^{\dagger}(a + iE) \\ &+ \frac{\delta t}{12}(a^{\dagger} + iE^{\dagger}) \begin{bmatrix} 0 & 1 \\ 1 & 0 \end{bmatrix} u - \frac{\delta t}{12}u^{\dagger} \begin{bmatrix} 0 & 1 \\ 1 & 0 \end{bmatrix} (a + iE), \end{aligned} \quad (7.29)$$

which unravelled is equal to,

$$\begin{aligned} (iS_{\bar{\Delta}} - iS_{\Delta}^{\dagger})[\{a_i, a_i^*, v_i, v_i^*, u_i, u_i^*\}_{i=0,1}; \epsilon] &= \\ &= - \frac{\delta x}{4}v_0(a_0^* + i\epsilon) - \frac{\delta x}{4}v_0^*(a_0 + i\epsilon) - \frac{\delta x}{4}v_1(a_1^* + i\epsilon) - \frac{\delta x}{4}v_1^*(a_1 + i\epsilon) \\ &- \frac{\delta t}{12}u_0(a_1^* + i\epsilon) - \frac{\delta t}{12}u_0^*(a_1 + i\epsilon) - \frac{\delta t}{12}u_1(a_0^* + i\epsilon) - \frac{\delta t}{12}u_1^*(a_0 + i\epsilon). \end{aligned} \quad (7.30)$$

Now, the equation (7.25) for the path integral takes the form,

$$\begin{aligned} PI_{\epsilon} &:= 16|C|^2 \int dv_0 dv_1 dv_0^* dv_1^* du_0 du_1 du_0^* du_1^* e^{(iS_{\bar{\Delta}} - iS_{\Delta}^{\dagger})[\{a_i, a_i^*, v_i, v_i^*, u_i, u_i^*\}_{i=0,1}; \epsilon]} \\ &= 16|C|^2 \left(\frac{\delta x}{4}\right)^4 \left(\frac{\delta t}{12}\right)^4 \left((a_0^* + i\epsilon)(a_0 + i\epsilon)(a_1^* + i\epsilon)(a_1 + i\epsilon)\right) \\ &\quad \times \left(a_1^* + i\epsilon)(a_1 + i\epsilon)(a_0^* + i\epsilon)(a_0 + i\epsilon)\right) \\ &= 16|C|^2 \left(\frac{\delta x}{4}\right)^4 \left(\frac{\delta t}{12}\right)^4 (2i\epsilon)^4 a_0 a_0^* a_1 a_1^*. \end{aligned} \quad (7.31)$$

If we set,

$$C = \left(\frac{12}{\delta x \delta t \epsilon}\right)^2 \quad (7.32)$$

we obtain, in the limit of $\epsilon \rightarrow 0$,

$$PI_{\epsilon \rightarrow 0} = \delta(a_0, a_0^*, a_1, a_1^*). \quad (7.33)$$

Returning back to our original coordinates this is equal to,

$$\begin{aligned} PI_{\epsilon \rightarrow 0} &= \lim_{\epsilon \rightarrow 0} \int d\Psi_1 d\Psi_1^{\dagger} d\Psi_2 d\Psi_2^{\dagger} \left(K^{\dagger}(\Psi_1, \Psi_1^{\dagger}, \Psi_2, \Psi_2^{\dagger}; \Psi_0', \Psi_0'^{\dagger}; E, E^{\dagger}) \right. \\ &\quad \left. \times K(\Psi_1, \Psi_1^{\dagger}, \Psi_2, \Psi_2^{\dagger}; \Psi_0, \Psi_0^{\dagger}; E, E^{\dagger}) \right) = \delta(\Psi_0' - \Psi_0, \Psi_0'^{\dagger} - \Psi_0^{\dagger}). \end{aligned} \quad (7.34)$$

As you can see, our ϵ -prescription enables us to arrive in a delta function and thus our kernel \mathcal{K} ends up being an isometry from $\mathcal{H}_1 \rightarrow \mathcal{H}_1 \otimes \mathcal{H}_2$. The isometry is nonunitary since $\text{rank}[\mathcal{K}\mathcal{K}^{\dagger}] = \text{rank}[\mathcal{K}^{\dagger}\mathcal{K}] = \text{rank}[\mathbb{I}_{\mathcal{H}_0}]$ and $\dim(\mathcal{H}_0) = \dim(\mathbb{I}_{\mathcal{H}_0}) \neq \dim(\mathbb{I}_{\mathcal{H}_1 \otimes \mathcal{H}_2}) = \dim(\mathcal{H}_1 \otimes \mathcal{H}_2) < \infty$, meaning $\mathcal{K}\mathcal{K}^{\dagger} \neq \mathbb{I}_{\mathcal{H}_1 \otimes \mathcal{H}_2}$.

We will not proceed further in our work with fermions due to the fact that our way of nourishing the path integral is controversial.

7.3 Discussion

Initially, let us compare the scalar and fermion case in order to get some intuition about the construction of the isometric evolution. For the scalar case the path integral $PI|_{scalar}$ without the ϵ -prescription diverges to infinity,

$$PI|_{scalar} = \int d\phi_1 d\phi_2 K^*(\phi_1, \phi_2; \phi'_0) K(\phi_1, \phi_2; \phi_0) = \infty, \quad (7.35)$$

while in the fermion case the path integral $PI|_{fermion}$ is zero,

$$\begin{aligned} PI|_{fermion} &= \int d\Psi_1 d\Psi_1^\dagger d\Psi_2 d\Psi_2^\dagger K^\dagger(\Psi_1, \Psi_1^\dagger, \Psi_2, \Psi_2^\dagger; \Psi'_0, \Psi_0^\dagger) K(\Psi_1, \Psi_1^\dagger, \Psi_2, \Psi_2^\dagger; \Psi_0, \Psi_0^\dagger) \\ &= 0. \end{aligned} \quad (7.36)$$

This is to be expected since, in general, the path integral construction between scalars and fermions has an inverse relationship.

We nourished this problem by introducing an ϵ -prescription. For the scalar case, we were able to achieve a continuum limit for the prescription which is of the form,

$$i\epsilon \cdot \frac{1}{2} \int dx^2 \delta^{\mu\nu} \partial_\mu \phi \partial_\nu \phi. \quad (7.37)$$

This combined with the fact that we defined the measure of the path integral to be controlled by a constant C in the propagator (6.15) which was,

$$C_{scalar} = \frac{1}{2} \left(\frac{\delta x}{\delta t} \frac{\epsilon}{\pi^3} \right)^{1/4}, \quad (7.38)$$

resulted in a convergent path integral of the form,

$$PI_\epsilon|_{scalar} = \int d\phi_1 d\phi_2 K^*(\phi_1, \phi_2; \phi'_0; \epsilon) K(\phi_1, \phi_2; \phi_0; \epsilon) = \delta(\phi'_0 - \phi_0). \quad (7.39)$$

In the case of the fermion we did not achieved a continuum limit and our prescription was designed only to superficially render the path integral to result in a delta function. The prescription was,

$$\begin{aligned} &+ \frac{\delta x}{8} E^\dagger (\Psi_1 + \Psi_2) - \frac{\delta x}{8} (\Psi_1^\dagger + \Psi_2^\dagger) E \\ &+ \frac{\delta t}{24} E^\dagger \begin{bmatrix} 0 & 1 \\ 1 & 0 \end{bmatrix} (\Psi_2 - \Psi_1) - \frac{\delta t}{24} (\Psi_2^\dagger - \Psi_1^\dagger) \begin{bmatrix} 0 & 1 \\ 1 & 0 \end{bmatrix} E. \end{aligned} \quad (7.40)$$

Including the defining constant of the measure,

$$C_{fermion} = \left(\frac{12}{\delta x \delta t \epsilon} \right)^2, \quad (7.41)$$

it yields a path integral of the form,

$$\begin{aligned}
PI_\epsilon|_{fermion} &= \\
&= \int d\Psi_1 d\Psi_1^\dagger d\Psi_2 d\Psi_2^\dagger K^\dagger(\Psi_1, \Psi_1^\dagger, \Psi_2, \Psi_2^\dagger; \Psi_0', \Psi_0'^\dagger; E, E^\dagger) K(\Psi_1, \Psi_1^\dagger, \Psi_2, \Psi_2^\dagger; \Psi_0, \Psi_0^\dagger; E, E^\dagger) \\
&= \delta(\Psi_0' - \Psi_0, \Psi_0'^\dagger - \Psi_0^\dagger). \tag{7.42}
\end{aligned}$$

Notice that in the limit of $\epsilon \rightarrow 0$ there is also an inverse relationship between the measures since,

$$\lim_{\epsilon \rightarrow 0} C_{scalar} = 0, \quad \lim_{\epsilon \rightarrow 0} C_{fermion} = \infty, \tag{7.43}$$

which probably occurs again due to the nature of the scalar and fermionic path integral. The measure absorbs each divergence by being divergent in the opposite way in order for our path integral to result in a finite answer.

The issue with our prescription, in the fermion case, is that the FEM discretized action contains terms that are Grassmann-odd, *aka* linear fermionic terms. In conventional formulations the action and the Hamiltonian should be Grassmann-even. Grassmann-even numbers commute with each other and they are often called *c*-numbers, while Grassmann-odd anticommute. Since the Hamiltonian is supposed to measure energy, which is an ordinary number, it should contain an even number of Grassmann-odd terms. There might be a case against this, since we discretized time and so there is no Hamiltonian for the above argument to hold. Moreover, our Grassmann-odd terms are part of an ϵ -prescription which at the end of our calculation should vanish, since we are taking the limit $\epsilon \rightarrow 0$.

Looking back in our $PI|_{fermion}$ computation (7.25), we observe that the reason for it to be zero is the emergence of a doubling effect on the a components. We present it below for the convenience of the reader,

$$PI_{fermion} = 16|C|^2 \left(\frac{\delta x}{4}\right)^4 \left(\frac{\delta t}{12}\right)^4 a_0^* a_0 a_1^* a_1 a_0^* a_0, \tag{7.44}$$

where,

$$a_0 = \Psi'_{00} - \Psi_{00}, \quad a_1 = \Psi'_{01} - \Psi_{01}, \quad a_0^* = \Psi'^*_{00} - \Psi^*_{00}, \quad a_1^* = \Psi'^*_{01} - \Psi^*_{01}. \tag{7.45}$$

This observation could lead one to think that the pathology of the path integral is due to the well-known fermion doubling problem. In lattice field theory, even without the FEM discretization, fermion doubling occurs when naively putting the fermionic fields on a lattice, resulting in more fermionic states than expected. It is intractably linked to chiral invariance by the Nielsen-Ninomiya theorem [65]. A naive fermionic lattice action could possess a symmetry that it is not found in the continuum limit. There are many strategies that are used to solve this problem requiring modified fermions which reduce to the Dirac fermion only in the continuum limit.

In our case the FEM discretized action (7.9) is indeed problematic according to [11]. The ansatz of the previous reference for a FEM discretized action, in the Euclidean signature, is of the following form,

$$I_{ansatz} = \frac{1}{2} \sum_{\langle i,j \rangle} \frac{V_{ij}}{l_{ij}^2} (\bar{\Psi}_i \vec{l}_{ij} \cdot \vec{\gamma}_E \Psi_j - \bar{\Psi}_j \vec{l}_{ij} \cdot \vec{\gamma}_E \Psi_i). \tag{7.46}$$

Notice that the only difference with the action (7.16),

$$I_{naive} = \frac{\delta t_E \delta x}{6} \sum_{\langle i,j \rangle} \bar{\Psi}_i (\vec{n}^j - \vec{n}^i) \cdot \vec{\gamma}_E \Psi_j, \quad (7.47)$$

that we used in our computation is the replacement of $(\vec{n}^j - \vec{n}^i) \cdot \vec{\gamma}_E$ with $\frac{V_{ij}}{l_{ij}^2} \vec{l}_{ij} \cdot \vec{\gamma}_E$ where V_{ij} could be thought as a non-zero number². This has implications of spin orientations upon the lattice but does not solve our problem since it only results in a change of the numerical values in front of $a_0^* a_0 a_1^* a_1 a_1^* a_0^* a_0$ in (7.44)³.

Besides a change in the action the fermionic doubling problem could be overcome by the addition of a Wilson term which acts like a mass operator in the action (7.46). That was a potential candidate for an ϵ -prescription. A Wilson term is,

$$I_{Wilson} = \sum_{\langle i,j \rangle} \frac{V_{ij}}{l_{ij}^2} (\bar{\Psi}_i - \bar{\Psi}_j) (\Psi_i - \Psi_j). \quad (7.48)$$

Again this does not solve our problem. If you unravel the summation and try to incorporate the term in the path integral calculation you will once more end up with residual α 's.

One last observation that might be useful is the following. In the scalar case the action is of the form (6.26). That is,

$$S_{\Delta}[\{\phi_0, \phi_1, \phi_2\}; \epsilon] = \frac{\delta x}{\delta t} \cdot \frac{1+i\epsilon}{8} (2\phi_0 - (\phi_1 + \phi_2))^2 - \frac{\delta t}{\delta x} \cdot \frac{1-i\epsilon}{8} (\phi_1 - \phi_2)^2, \quad (7.49)$$

which following a coordinate transformation of the form $u = \phi_1 - \phi_2$, $v = \phi_1 + \phi_2$ becomes,

$$S_{\Delta}[\{\phi_0, v, u\}; \epsilon] = \frac{\delta x}{\delta t} \cdot \frac{1+i\epsilon}{8} (2\phi_0 - v)^2 - \frac{\delta t}{\delta x} \cdot \frac{1-i\epsilon}{8} u^2. \quad (7.50)$$

Notice that the degrees of freedom ϕ_0 and u are uncoupled, while ϕ_0 seems to be coupled with v . That means that the initial degrees of freedom at $t = 0$ do not couple with all the degrees of freedom at $t = 1$.

In the fermion case the action (7.9), combined with the coordinate transformation $u = \Psi_2 - \Psi_1$, $v = \Psi_2 + \Psi_1$, yields,

$$\begin{aligned} S_{\Delta}[\{\Psi_0, \Psi_0^\dagger, v, v^\dagger, u, u^\dagger\}] = & + \frac{i\delta x}{4} \Psi_0^\dagger v - \frac{i\delta x}{4} v^\dagger \Psi_0 \\ & + \frac{i\delta t}{12} \Psi_0^\dagger \begin{bmatrix} 0 & 1 \\ 1 & 0 \end{bmatrix} u - \frac{i\delta t}{12} u^\dagger \begin{bmatrix} 0 & 1 \\ 1 & 0 \end{bmatrix} \Psi_0 \\ & + \frac{i\delta t}{12} v^\dagger \begin{bmatrix} 0 & 1 \\ 1 & 0 \end{bmatrix} u - \frac{i\delta t}{12} u^\dagger \begin{bmatrix} 0 & 1 \\ 1 & 0 \end{bmatrix} v. \end{aligned} \quad (7.51)$$

The initial degrees of freedom Ψ_0^\dagger and Ψ_0 at $t = 0$ are coupled with all the final degrees of freedom v, u and v^\dagger, u^\dagger at $t = 1$, respectively. The same behaviour between the degrees of freedom is observed in the previous attempts (7.46, 7.48) for a possible solution of the problem and it might contribute in the fermion doubling.

²The V_{ij} 's is actually 2-dimensional hybrid volumes for the links between the lattice sites. More information can be found in [11]. For our investigation, only their non-zero nature is needed.

³After a Wick-rotation in the Minkowskian signature.

In conclusion, our FEM discretized action for the fermion is naive but even with corrections does not render the time evolution viable. This possibly comes from the fact that the initial degrees of freedom couple with all the final degrees of freedom resulting in a doubling of the Ψ_0 's in the path integral. Residual symmetries due to discretization is a usual problem in fermionic theories and our situation might belong in this category. Another possibility is that the path integral measure is not a flat one. That would make $C_{fermion}$ a function of fields in our definition (7.18) of the propagator $K(\Psi_1, \Psi_1^\dagger, \Psi_2, \Psi_2^\dagger; \Psi_0, \Psi_0^\dagger)$. Additional information about an ϵ -prescription could come from an examination of the normalization of the wavefunctions, *c.f.* ssec. 6.2.1. Nevertheless, our Grassmann-odd ϵ -prescription (7.40) seems to break this doubling of Ψ_0 's and could act as a hint for future research in this direction.

Chapter 8

Closing Remarks and Future Endeavours

In our final remarks the goal is to illuminate some foggy aspects of our previous work and suggest future research directions. The organization of this chapter goes as follows. In sec. 8.1 we describe the FEM latticization of the continuum moving mirror model that we saw earlier and suggest further research in order to achieve a better understanding of the FEM method on the mirror toy-models. In sec. 8.2 we present how the postulate of unitarity of quantum theory emerges in our setting and complement with comments for further study. Next, in sec. 8.3 and ssec. 8.3.1 we mention the intuitive connection between our isometric time evolution and quantum error correction codes while suggesting further work for the entanglement entropy of a region of de Sitter spacetime. We conclude with a closing statement 8.4.

8.1 FEM in the Moving Mirror

In chapter 3 we dived deep into moving mirrors as a toy model for cosmological expansion. While in sec. 5.2 we argued that FEM discretization is more suitable for spacetimes with a time-dependent boundary. As a matter of fact Fig. 5.5 illustrates how FEM discretization approaches a spacetime with a moving mirror boundary. The boundary corresponds to a uniformly accelerating mirror in $1 + 1$ dimensions. We will proceed in a schematic construction of its action, in order to guide further research into this toy-model.

At first we consider a $1 + 1$ free massless scalar field for $t \geq 0$ without a mirror boundary. We leverage a triangulation of isosceles with width $2\delta x$ and height δt , see Fig. 8.1. In order to satisfy the CFL condition [21] for numerical stability we choose $\frac{\delta t}{\delta x} < 1$. In order to utilize the FEM machinery we label vertices according to



(8.1)

Let $\nabla_{i,j}$ denote a triangular plaquette with its bottom vertex labeled by $\phi_{i,j}$, its upper left vertex labeled by $\phi_{i+1,j}$ and its upper right vertex labeled by $\phi_{i+1,j+1}$. Similarly, let ${}_{i,j}\triangle$ denote a plaquette with its bottom left vertex labeled by $\phi_{i,j}$, its upper vertex labeled by $\phi_{i+1,j+1}$, and its lower right vertex labeled by $\phi_{i,j+1}$. Each of these

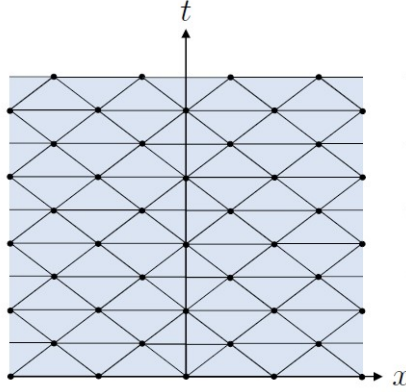


FIGURE 8.1: A triangulation of \mathbb{R}^2 for $t \geq 0$, built out of isosceles triangles. The figure was taken from [19].

plaquettes contributes to the total lattice action as,

$$S[\nabla_{i,j}; \epsilon] = \frac{\delta x}{\delta t} \cdot \frac{1 + i\epsilon}{8} (2\phi_{i,j} - (\phi_{i+1,j+1} + \phi_{i+1,j}))^2 - \frac{\delta t}{\delta x} \cdot \frac{1 - i\epsilon}{8} (\phi_{i+1,j+1} - \phi_{i+1,j})^2, \quad (8.2)$$

$$S[i,j\Delta; \epsilon] = \frac{\delta x}{\delta t} \cdot \frac{1 + i\epsilon}{8} (2\phi_{i+1,j+1} - (\phi_{i,j+1} + \phi_{i,j}))^2 - \frac{\delta t}{\delta x} \cdot \frac{1 - i\epsilon}{8} (\phi_{i,j+1} - \phi_{i,j})^2, \quad (8.3)$$

where we used the action (6.26) for a single triangle lattice. Notice that the triangle $i,j\Delta$ is rotated and translated with respect to the triangle $\nabla_{i,j}$ but the action is unaffected since the metric (5.71) is invariant under rotations and translations¹. The total lattice action can be written as

$$S_{\text{lattice}}[\{\phi_{i,j}\}; \epsilon] = \sum_{i,j} (S[\nabla_{i,j}; \epsilon] + S[i,j\Delta; \epsilon]). \quad (8.4)$$

Next, we generalize our construction to account for a left-moving, accelerating mirror. For a uniform acceleration to the left its worldline is of the form,

$$(t(\tau), x(\tau)) = (\sinh(\tau), 1 - \cosh(\tau)). \quad (8.5)$$

The trajectory of the mirror intersects with our triangulation, see Fig. 8.2. We need to modify the triangulation to accommodate the new boundary.

Observe that most of the triangles in the $x \geq 0$ region are unaltered. For the altered triangles, we need to replace their contribution to the action (8.4). The triangles left of the boundary are removed entirely in our replacement procedure and so do not contribute to the new lattice action at all. The other altered triangles are deformed; for instance, consider triangles of the general form,

$$(8.6)$$

¹The geometric approach to FEM makes the invariance property more apparent.

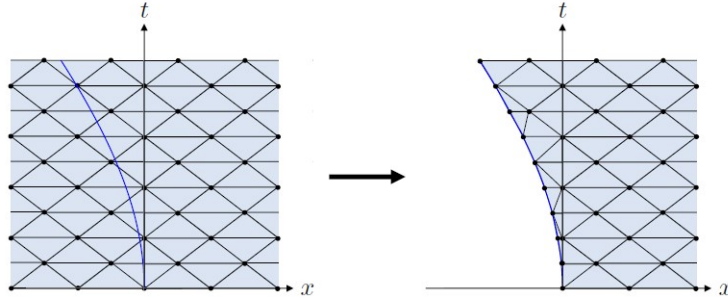


FIGURE 8.2: Triangulation with modified triangles. The figure was taken from [19].

and also,

$$\begin{array}{c}
 \phi_{c+1,d+1} \\
 \delta t' \\
 \phi_{c,d} \quad \delta x' \quad \delta x'' \quad \phi_{c,d+1}
 \end{array}
 \quad (8.7)$$

where labeled field degrees of freedom live upon their vertices. The lattice action for these triangles is, respectively²,

$$\begin{aligned}
 S[\nabla'_{a,b}; \epsilon] = & \frac{1}{\delta t'(\delta x' + \delta x'')} \cdot \frac{1 + i\epsilon}{4} \left(\delta x'' \phi_{a+1,b+1} + \delta x' \phi_{a+1,b} - (\delta x' + \delta x'') \phi_{a,b} \right)^2 \\
 & - \frac{\delta t'}{\delta x' + \delta x''} \cdot \frac{1 - i\epsilon}{4} (\phi_{a+1,b+1} - \phi_{a+1,b})^2, \quad (8.8)
 \end{aligned}$$

$$\begin{aligned}
 S[{}_{c,d}\Delta'; \epsilon] = & \frac{1}{\delta t'(\delta x' + \delta x'')} \cdot \frac{1 + i\epsilon}{4} \left(\delta x'' \phi_{c,d} + \delta x' \phi_{c,d+1} - (\delta x' + \delta x'') \phi_{c+1,d+1} \right)^2 \\
 & - \frac{\delta t'}{\delta x' + \delta x''} \cdot \frac{1 - i\epsilon}{4} (\phi_{c,d+1} - \phi_{c,d})^2. \quad (8.9)
 \end{aligned}$$

The action for the modified triangle is calculated similarly to ssec. 6.1.1 with an active affine transformation of the form,

$$A^{-1} = \begin{bmatrix} \frac{\delta x'}{(\delta x' + \delta x'')\delta t} & -\frac{1}{\delta x' + \delta x''} \\ \frac{\delta x''}{(\delta x' + \delta x'')\delta t} & \frac{1}{\delta x' + \delta x''} \end{bmatrix}, \quad (8.10)$$

in the FEM basis $\{B^{(j)}(t, x)\}$.

Our original triangles are a special case of the modified ones with $\delta x' = \delta x'' = \delta x$. The desired lattice action comes from a summation over all the triangles in our modified triangulation $\{\nabla'_{a,b,c,d} \Delta'\}$. To impose Dirichlet boundary conditions on the mirror, we simply set the field elements along the mirror boundary equal to zero. In total, the lattice action for the moving mirror model becomes,

$$S_{lattice}^{mirror}[\{\phi_{i,j}\}; \epsilon] = \left(\sum_{\nabla'_{a,b}} S[\nabla'_{a,b}; \epsilon] + \sum_{c,d\Delta'} S[{}_{c,d}\Delta'; \epsilon] \right) \Big|_{\text{boundary } \phi'_s=0}. \quad (8.11)$$

²Again, the rotated and translated triangle leaves the form of the action unchanged.

Notice the triangulation on the right-hand side of Fig. 8.2, we see that the corresponding lattice action propagators from the past to the future will instantiate Hilbert space isometries, since the degrees of freedom upon each Cauchy slice increases.

In fact this isometric evolution is in accordance with the continuum observation of ssec. 3.3.3 where any finite resolution detector will not see unitary evolution. Future research should aim in the precise calculation of the lattice action. Furthermore, there is a need in understanding the continuum limit of this FEM discretization in enough detail to reproduce the numerical value (3.104) of the entanglement entropy produced by an accelerating mirror.

8.2 The Physical Subspace and the Recovery of Unitarity

In sec. 6.2 we proposed that time evolution of a free massless scalar field in $1 + 1$ dimensions is instantiated by an isometry which is not unitary. There are indications, in sec. 7.2, that the same holds true for a free massless fermionic field. The fermionic case came with a bunch of problems that were discussed in sec 7.3, so further research should aim in their nourishment. Nevertheless, both cases seem to point towards isometric quantum mechanical time evolution in the setting of cosmological expansion. Here we discuss some physical consequences of this proposal. We will work with finite dimensional Hilbert space since it is more illuminating.

Suppose we have a sequence of Hilbert spaces $\mathcal{H}_{t_0}, \mathcal{H}_{t_1}, \mathcal{H}_{t_2}, \dots$ with increasing dimensions $d_0 < d_1 < d_2 < \dots$. The time evolution is instantiated by an isometric but non-unitary propagator $\mathcal{K}_{j \leftarrow i}$ which maps $\mathcal{H}_{t_i} \rightarrow \mathcal{H}_{t_j}$ for $i < j$. We identify \mathcal{H}_{t_0} with the ‘physical’ Hilbert space $\mathcal{H}_{\text{phys}}$, for reasons that will become apparent shortly.

Imagine an initial state $|\Psi_0\rangle$ in $\mathcal{H}_{\text{phys}}$. If we evolve it via $\mathcal{K}_{j \leftarrow 0}$, then $|\Psi_j\rangle := \mathcal{K}_{j \leftarrow 0}|\Psi_0\rangle$ is in \mathcal{H}_j . Suppose that there is another state $|\Psi'_j\rangle$ in \mathcal{H}_j . A state like this could emerge from an operator O_j which takes \mathcal{H}_j to itself; that is, $|\Psi'_j\rangle = O_j|\Psi_j\rangle$. A question immediately arises: is there an alternative initial state $|\Psi_0'\rangle$ in $\mathcal{H}_{\text{phys}}$ such that $|\Psi'_j\rangle = \mathcal{K}_{j \leftarrow 0}|\Psi_0'\rangle$? This is equivalent to asking if there are any initial conditions which could have evolved into $|\Psi'_j\rangle$.

Let $\mathcal{H}_{\text{phys}, t_j}$ denote the image of $\mathcal{H}_{\text{phys}}$ under evolution by the propagator $\mathcal{K}_{j \rightarrow 0}$. It is obvious that $\mathcal{H}_{\text{phys}, t_j}$ is a proper subspace of \mathcal{H}_{t_j} with dimension d_0 . Then the answer to the above question is that there exists such a $|\Psi_0'\rangle$ if and only if $|\Psi'_j\rangle$ is in $\mathcal{H}_{\text{phys}, t_j}$. It is apparent that most states $|\Psi'_j\rangle$ do not have antecedent states $|\Psi_0'\rangle$.

Essentially there is a sequence of bijections,

$$\mathcal{H}_{\text{phys}} \xrightarrow{\mathcal{K}_{1 \leftarrow 0}} \mathcal{H}_{\text{phys}, t_1} \xrightarrow{\mathcal{K}_{2 \leftarrow 1}} \mathcal{H}_{\text{phys}, t_2} \xrightarrow{\mathcal{K}_{3 \leftarrow 2}} \dots, \quad (8.12)$$

that comprises the physical evolution of physical states. From this point of view, the evolution restricted to the physical subspaces is completely unitary. Even though \mathcal{H}_{t_j} is larger in dimension than \mathcal{H}_{t_0} , this is in effect illusory since the only physically accessible states in \mathcal{H}_{t_j} are those in $\mathcal{H}_{\text{phys}, t_j}$. A consequence is that the physical algebra of observables on \mathcal{H}_{t_j} is composed of precisely those observables that map $\mathcal{H}_{\text{phys}, t_j}$ to itself.

8.2.1 Comments

In the context of effective field theory, the Hilbert space of states increases in an expanding universe. As pointed out a long time ago in [63], this is due to the fact that

in order to maintain a fixed physical scale for the UV cutoff there need to be a continuous production of modes. So, it appears that the Hilbert space is time-dependent. Conceptually, time evolution is being instantiated by isometries in expanding universes since the volume of the space grows as a function of time but the Planck length, and as a result the UV cutoff, stays fixed.

There is a holographic analog of this for universes in which the horizon of each observer is expanding, such as our own universe in its present phase. If an observer identify the area of his cosmological horizon with the number of degrees of freedom which describe the universe; suppose that it increases for all observers, then the numbers of degrees of freedom is increasing with time. Thus even a holographic perspective appears to necessitate some form of isometric but non-unitary time evolution.

Furthermore, most early universe models are based on an effective field theory analysis. A scalar matter field is introduced to yield the cosmological background evolution desired. In the case of inflation [33], the unitarity problem for effective field theory models was discussed a number of years ago under the name *Trans-Planckian Problem* (TPP) for cosmological perturbations [52] where it was pointed out that, if the wavelength corresponding to the mode whose current wavelength is equal to the current Hubble radius is smaller than the Planck length at the beginning of inflation, then new physics should be revoked; see [8] for a complete discussion.

Recently, Bedroya and Vafa [5] formulated the *Trans-Planckian Censorship Conjecture* (TCC) which states that in no consistent quantum theory of gravity the situation will arise that some mode with initial wavelength smaller than the Planck length becomes super-Hubble.

A question arises about contracting geometries: How should we examine them? There is not much to say. One is driven out of the region of validity of effective field theory since the modes are blueshifted above the UV cutoff. If we ignore this and naively time reverse the propagator 6.15 the isometry becomes a projection. Perhaps the forward arrow of time is correlated with the isometric direction so that we always perceive geometries as expanding. This could leads to a multi-history picture as in [31] or a final state projection as in [41]; see also [20]. This concept could be examined in future research.

The general picture is that even for a scalar field coupled to gravity in the continuum limit not all states of the quantum field in the far future will correspond to antecedent states in the far past. For instance, many configurations when evolved backwards will lead to singularities at finite time, past which we cannot evolve back further. One might conclude some of these late-time states could be ruled out once a suitable definition of the physical subspace is understood in this setting. But this could be too hasty: an alternate possibility is that the scalar effective field theory breaks down and more degrees of freedom are needed. In an analogous AdS setting this line of reasoning leads to the inclusion of black holes [56] rather than constrains on the boundary Hilbert space.

Finally, narrowing the conversation about unitarity down in the context of two-dimensional toy models of gravity. Cotler and Jensen [18] studied time evolution in two simple models of de Sitter quantum gravity, Jackiw-Teitelboim (JT) gravity and a minisuperspace approximation to Einstein gravity with a positive cosmological constant. In de Sitter JT gravity they found that time evolution is isometric while there were suggestions that the same holds true for Einstein gravity.

8.3 Apparent Degrees of Freedom (Fact or Fiction?)

Our perspective of restricting to physical subspaces recovers unitarity, but allows for the number of ‘apparent’ degrees of freedom to increase in time. A valid question arises: what is the role of the total ambient Hilbert space, which increases in size as time advances?

An analogy with gauge theory may be appropriate. A gauge theory possesses gauge-invariance which is not a physical symmetry but an artifact of how we formulate our theories. Two configurations related by a gauge transformation, are physically equivalent and our description of the physics thus has redundancies. Since gauge-invariance is not physical, the theory can be described in terms of physical gauge-invariant objects which are the Wilson loops. Thus, the physical states only lie in the gauge-invariant (physical) subspace. Moreover, the Wilson loops are non-local objects. In order to render the theory as local we choose a redundant description with gauge fields. In other words we embed the theory in a larger ambient Hilbert space.

Turning back to theories in expanding universes, we need a progressively larger ambient Hilbert space as time advances to keep rendering the theory local. Similarly with the gauge theory, we could choose to describe an expanding universe solely in terms of unitary evolution of the physical subspace. In that case the dynamics may be non-local. We can render the dynamics local by requiring a larger ambient Hilbert space whose size increases with time, and as such need isometric evolution. On the one hand, if we describe evolution as unitary we lose locality. On the other hand, if we describe it as local we lose unitarity. This suggests a possible tension between unitarity and locality in cosmological expansion.

Besides gauge theory, there are parallels between the above and the ‘code subspace’ in the error correction interpretation of AdS/CFT bulk reconstruction [3, 56]. That could further illuminate the need of apparent degrees of freedom in the description of quantum states in expanding cosmologies. However, we have no argument that our isometries in our FEM field discretization need to be ones which comprise a quantum error correction code robust to spatially local errors. In the quantum error correction scheme that we will describe below there is a need of both the apparent and physical degrees of freedom.

8.3.1 Quantum Error Correction

Quantum error correction is a scheme where a small message made from quantum states is redundantly encoded inside a bigger system. Say Alice wants to send Bob a quantum state of k qubits in the mail, but she is worried that some of the qubits might get lost on the way. Quantum error correction is a procedure that allows her to embed this state into $n > k$ qubits in such a way that even if some qubits are lost, Bob can still recover it. More can be found on section 4 of [34]. Here we will use just an illuminating example to make a connection with our previous discussion and motivate the need for apparent degrees of freedom.

The simplest example of quantum error correction uses three-state qutrits to send a single-qutrit message [3].

Say Alice wishes to send the state

$$|\psi\rangle = \sum_{i=0}^2 a_i |i\rangle. \quad (8.13)$$

The idea is to instead send the state

$$|\tilde{\psi}\rangle = \sum_{i=0}^2 a_i |\tilde{i}\rangle, \quad (8.14)$$

where

$$|\tilde{0}\rangle = \frac{1}{\sqrt{3}}(|000\rangle + |111\rangle + |222\rangle) \quad (8.15)$$

$$|\tilde{1}\rangle = \frac{1}{\sqrt{3}}(|012\rangle + |120\rangle + |201\rangle) \quad (8.16)$$

$$|\tilde{2}\rangle = \frac{1}{\sqrt{3}}(|021\rangle + |102\rangle + |210\rangle). \quad (8.17)$$

This protocol has two remarkable properties. First of all for any state $|\tilde{\psi}\rangle$, the reduced density matrix on any one of the qubits is maximally mixed. Thus no single qutrit can be used to acquire any information about the state. Secondly, from any two of the qutrits Bob can reconstruct the state. For example, say he has access to only the first two qutrits. He can make use of the fact that there exists a unitary transformation U_{12} acting only on the first two qutrits that implements,

$$(U_{12} \otimes I_3)|\tilde{i}\rangle = |i\rangle \otimes \frac{1}{\sqrt{3}}(|00\rangle + |11\rangle + |22\rangle). \quad (8.18)$$

Acting with this on the encoded message, we see that Bob can recover the state $|\psi\rangle$,

$$(U_{12} \otimes I_3)|\tilde{\psi}\rangle = |\psi\rangle \otimes \frac{1}{\sqrt{3}}(|00\rangle + |11\rangle + |22\rangle). \quad (8.19)$$

Explicitly U_{12} is a permutation that acts as

$$\begin{array}{lll} |00\rangle \rightarrow |00\rangle & |11\rangle \rightarrow |01\rangle & |22\rangle \rightarrow |02\rangle \\ |01\rangle \rightarrow |12\rangle & |12\rangle \rightarrow |10\rangle & |20\rangle \rightarrow |11\rangle \\ |02\rangle \rightarrow |21\rangle & |10\rangle \rightarrow |22\rangle & |21\rangle \rightarrow |20\rangle \end{array} \quad (8.20)$$

Clearly by the symmetry of (8.15,8.16,8.17) a similar construction is also possible if Bob has access only to the second and third, or first and third qutrits. Thus Bob can correct for the loss of any one of the qutrits. The subspace spanned by (8.15,8.16,8.17) is called the *code subspace*³.

Turning back to our expanding universes, the initial encoded state (8.13) by Alice, can be thought as a state in our physical subspace $\mathcal{H}_{phys} \approx \mathcal{H}_{t_0}$ at $t = 0$ while the state (8.14) can be thought as a state in the total ambient Hilbert space \mathcal{H}_{t_1} at $t = 1$. So, to describe a state at that Hilbert space there need to be apparent degrees of freedom that consist the code subspace. The Hilbert spaces \mathcal{H}_{phys} with $\dim(\mathcal{H}_{phys}) = 3$ and \mathcal{H}_{t_1} with $\dim(\mathcal{H}_{t_1}) = 3^3$ are connected with an isometry $\mathcal{H}_{phys} \rightarrow \mathcal{H}_{t_1}$ which is a perfect tensor; see [56] for an interesting analysis about perfect tensors and isometries. Note that as we already stated we have no argument that our isometries in our FEM field discretization are necessarily ones that comprise a quantum error correction code. The parallelism above is that this might be the case and there are indications that we might need the apparent degrees of freedom in our regime.

All in all, this analysis points out to interesting structures of encodings provided

³The entanglement of the states in the code subspace is essential for the functioning of the protocol.

by isometric time evolution in quantum field theory and hypothetically in quantum gravity. Understanding the precise information-theoretic properties of these encodings should be a future pursuit.

Comments

As we stated earlier, the holographic structure of AdS itself is captured by a quantum error-correcting code [56]. One can use the fact that quantum gravity in de Sitter space can be holographically realized by embedding it as an RS-type braneworld near the boundary of AdS [39], to connect the de Sitter space with the quantum error-correcting code of the Anti-de Sitter space. One therefore could reproduce the result (4.33) for the entanglement entropy of a region of de Sitter space. We leave this to future study. This work will broadly suggest that toy tensor network models of de Sitter with isometric time evolution [48, 4, 53, 55] should be taken more seriously as capturing properties of time evolution in the real world.

8.4 Closing Statement

Throughout this thesis, our research indicated that quantum mechanical time evolution is isometric in expanding cosmologies. This coupled with encodings of quantum information theory, possibly points to interesting structures in quantum gravity. Understanding the precise mechanism of the above appears to be an interesting avenue for future pursuit.

Appendix A

Introduction to Conformal Field Theory

The purpose of this section is to get comfortable with the basic language of conformal field theory. We will only cover the material that is needed for the thesis. Much of the material covered in this section was first described by Belavin, Polyakov and Zamalodchikov [6]. The canonical reference for learning conformal field theory is the excellent review by Ginsparg [32].

A.1 Conformal Algebra in 2-dimensional Euclidean Space

We will work in Euclidean space since it is much simpler and elegant. Everything we do could also be formulated in Minkowski space. Consider the space \mathbb{R}^2 with flat metric $g_{\mu\nu} = \delta_{\mu\nu}$ and line element $ds^2 = g_{\mu\nu}dx^\mu dx^\nu$. Under a change of coordinates, $x \rightarrow x'$, we have $g_{\mu\nu} \rightarrow g'_{\mu\nu}(x') = \frac{\partial x^\alpha}{\partial x'^\mu} \frac{\partial x^\beta}{\partial x'^\nu} g_{\alpha\beta}(x)$. By definition, the conformal group is the subgroup of coordinate transformations that leaves the metric invariant up to a scale change

$$g_{\mu\nu} \rightarrow g'_{\mu\nu}(x') = \Omega(x)g_{\mu\nu}(x). \quad (\text{A.1})$$

These are coordinate transformations that preserve the angles. Invariance under the transformation (A.1) can only hold if the theory has no preferred length scale. But this means that there can be nothing in the theory like a mass or a Compton wavelength.

The infinitesimal generators of the conformal algebra can be determined by considering the infinitesimal coordinate transformation $x^\mu \rightarrow x^\mu + \epsilon^\mu$, under which

$$ds^2 \rightarrow ds^2 + (\partial_\mu \epsilon_\nu + \partial_\nu \epsilon_\mu) dx^\mu dx^\nu \quad (\text{A.2})$$

To satisfy (A.1) we must require $\partial_\mu \epsilon_\nu + \partial_\nu \epsilon_\mu$ to be proportional to $g_{\mu\nu}$,

$$\partial_\mu \epsilon_\nu + \partial_\nu \epsilon_\mu = (\partial \cdot \epsilon) g_{\mu\nu}, \quad (\text{A.3})$$

where the constant of proportionality is fixed by tracing both sides with $g_{\mu\nu}$. It can be easily seen that (A.3) becomes the Cauchy-Riemann equations

$$\partial_1 \epsilon_1 = \partial_2 \epsilon_2, \quad \partial_1 \epsilon_2 = -\partial_2 \epsilon_1 \quad (\text{A.4})$$

It is then natural to move in the complex plane \mathbb{C} and write $\epsilon(z) = \epsilon^1 + i\epsilon^2$ and $\bar{\epsilon}(\bar{z}) = \epsilon^1 - i\epsilon^2$, in the complex coordinates $z, \bar{z} = x^1 \pm ix^2$. Two dimensional conformal transformations thus coincide with the analytic coordinate transformations

$$z \rightarrow f(z), \quad \bar{z} \rightarrow \bar{f}(\bar{z}), \quad (\text{A.5})$$

the local algebra of which is infinite dimensional. In complex coordinates we write

$$ds^2 = (dx^1)^2 + (dx^2)^2 = dzd\bar{z} \rightarrow \left| \frac{\partial f}{\partial z} \right|^2 dzd\bar{z} \quad (\text{A.6})$$

and have $\Omega = |\partial f / \partial z|^2$. Note that we have an infinite number of conformal transformations — in fact, a whole functions worth $f(z)$. This is special to conformal field theories in two dimensions. In higher dimensions, the space of conformal transformations is a finite dimensional group. For theories defined on $\mathbb{R}^{p,q}$, the conformal group is $SO(p+1, q+1)$ when $p+q > 2$.

A.2 Constraints of Conformal Invariance in 2-dimensions

Recall from (A.6) that the line element $ds^2 = dzd\bar{z}$ transforms under $z \rightarrow f(z)$ as

$$ds^2 \rightarrow \left(\frac{\partial f}{\partial z} \right) \left(\frac{\partial \bar{f}}{\partial \bar{z}} \right) ds^2. \quad (\text{A.7})$$

We shall generalize this transformation law to the form

$$\Phi(z, \bar{z}) \rightarrow \left(\frac{\partial f}{\partial z} \right)^h \left(\frac{\partial \bar{f}}{\partial \bar{z}} \right)^{\bar{h}} \Phi(f(z), \bar{f}(\bar{z})) \quad (\text{A.8})$$

where h and \bar{h} are real-valued¹.

The transformation (A.8) defines what is known as a primary field Φ of conformal weight (h, \bar{h}) . Some comments:

- In a unitary CFT, all operators have $h, \bar{h} \geq 0$ (add ref)
- The weights tell us how operators transform under rotations and scalings. The eigenvalue under rotation is the *spin*, s and is given in terms of the weights as $s = h - \bar{h}$. Meanwhile, the *scaling dimension* Δ of an operator is $\Delta = h + \bar{h}$.

Infinitesimally, under $z \rightarrow z + \epsilon(z)$, $\bar{z} \rightarrow \bar{z} + \bar{\epsilon}(\bar{z})$, we have from (A.8)

$$\delta_{\epsilon, \bar{\epsilon}} \Phi(z, \bar{z}) = ((h\partial\epsilon + \epsilon\partial) + (\bar{h}\bar{\partial}\bar{\epsilon} + \bar{\epsilon}\bar{\partial})) \Phi(z, \bar{z}), \quad (\text{A.9})$$

where $\bar{\partial} \equiv \partial_{\bar{z}}$.

Now the 2-point function $G^{(2)}(z_i, \bar{z}_i) = \langle \Phi_1(z_1, \bar{z}_1) \Phi_2(z_2, \bar{z}_2) \rangle$ is defined to satisfy

$$\langle \Phi_1(z_1, \bar{z}_1) \Phi_2(z_1, \bar{z}_2) \rangle = \left| \frac{\partial z'_1}{\partial z_1} \right|^{h_1} \left| \frac{\partial z'_2}{\partial z_2} \right|^{h_2} \left| \frac{\partial \bar{z}'_1}{\partial \bar{z}_1} \right|^{\bar{h}_1} \left| \frac{\partial \bar{z}'_2}{\partial \bar{z}_2} \right|^{\bar{h}_2} \langle \Phi_1(z'_1, \bar{z}'_1) \Phi_2(z'_2, \bar{z}'_2) \rangle, \quad (\text{A.10})$$

which infinitesimally takes the form,

$$\delta_{\epsilon, \bar{\epsilon}} G^{(2)}(z_i, \bar{z}_i) = \langle \delta_{\epsilon, \bar{\epsilon}} \Phi_1, \Phi_2 \rangle + \langle \Phi_1, \delta_{\epsilon, \bar{\epsilon}} \Phi_2 \rangle = 0, \quad (\text{A.11})$$

giving the partial equation

$$\begin{aligned} & \left((\epsilon(z_1)\partial_{z_1} + h_1\partial\epsilon(z_1)) + (\epsilon(z_2)\partial_{z_2} + h_2\partial\epsilon(z_2)) \right. \\ & \left. + (\bar{\epsilon}(\bar{z}_1)\partial_{\bar{z}_1} + \bar{h}_1\partial\bar{\epsilon}(\bar{z}_1)) + (\bar{\epsilon}(\bar{z}_2)\partial_{\bar{z}_2} + \bar{h}_2\partial\bar{\epsilon}(\bar{z}_2)) \right) G^{(2)}(z_i, \bar{z}_i) = 0. \end{aligned} \quad (\text{A.12})$$

¹ \bar{h} does not indicate the complex conjugate of h .

By using $\epsilon(z) = \bar{\epsilon}(\bar{z}) = 1$ we can observe that $G^{(2)}$ depends only on $z_{12} = z_1 - z_2$, $\bar{z}_{12} = \bar{z}_1 - \bar{z}_2$; then use $\epsilon(z) = z$ and $\bar{\epsilon}(\bar{z}) = \bar{z}$ to require $G^{(2)} = C_{12}/(z_{12}^{(h_1+h_2)}\bar{z}_{12}^{\bar{h}_1+\bar{h}_2})$; and finally $\epsilon(z) = z^2$ and $\bar{\epsilon}(\bar{z}) = \bar{z}^2$ to require $h_1 = h_2 = h$, $\bar{h}_1 = \bar{h}_2 = \bar{h}$. The result is that the 2-point function is constrained to take the form

$$G^{(2)}(z_i, \bar{z}_i) = \frac{C_{12}}{z_{12}^{2h}\bar{z}_{12}^{2\bar{h}}}. \quad (\text{A.13})$$

If we consider bosonic fields with spin $s = h - \bar{h} = 0$, (A.13) is equivalent to

$$G^{(2)}(z_i, \bar{z}_i) = \frac{C_{12}}{|z_{12}|^{2\Delta}}. \quad (\text{A.14})$$

A.3 The Stress-Energy Tensor

Symmetry generators in general can be constructed via the Noether prescription. A $1+1$ quantum theory with an exact symmetry has an associated conserved current j^μ , satisfying $\partial_\mu j^\mu = 0$. The conserved charge $Q = \int dx^0 j_0(x)$, constructed by integrating over a fixed-time slice, generates, according to $\delta_\epsilon A = \epsilon[Q, A]$, the infinitesimal symmetry variation in any field A . In particular, local coordinate transformations are generated by charges constructed from the stress-energy tensor $T_{\mu\nu}$. We define the stress-energy tensor to be

$$T_{\mu\nu} = -\frac{4\pi}{\sqrt{g}} \frac{\partial S}{\partial g^{\mu\nu}}. \quad (\text{A.15})$$

In conformal theories, $T_{\mu\nu}$ is traceless. To see this, vary the action with respect to a scale transformation $\delta g_{\mu\nu} = \epsilon g_{\mu\nu}$. Then we have $0 = \delta S = \int dx^2 \frac{\partial S}{\partial g_{\mu\nu}} \delta g_{\mu\nu} = -\frac{1}{4\pi} \int dx^2 \sqrt{g} \epsilon T_\mu^\mu$ which gives $T_\mu^\mu = 0$. In our case, we will work with flat Euclidean "space" and "time" coordinates x^1 and x^0 , so $g_{\mu\nu} = \delta_{\mu\nu}$. In Minkowski space, the standard light-cone coordinates would be $x^0 \pm x^1$. In Euclidean space the analogs are instead complex coordinates $\zeta, \bar{\zeta} = x^0 \pm ix^1$. The two dimensional Minkowski space notions of left- and right-moving massless fields become Euclidean fields that have purely holomorphic or anti-holomorphic dependence on the coordinates. Occasionally, we call the holomorphic and anti-holomorphic fields left and right-movers respectively.

We introduce the necessary complex tensor analysis since we will be working on the complex plane. In complex coordinates $z = x^0 + ix^1$, the line element is $ds^2 = (dx^0)^2 + (dx^1)^2 = dzd\bar{z}$. The components of the Euclidean metric are thus $\delta_{zz} = \delta_{\bar{z}\bar{z}} = 0$ and $\delta_{z\bar{z}} = \delta_{\bar{z}z} = \frac{1}{2}$, and the components of the stress-energy tensor are $T_{zz} = \frac{1}{4}(T_{00} - 2iT_{10} - T_{11})$, $T_{\bar{z}\bar{z}} = \frac{1}{4} = \frac{1}{4}(T_{00} + 2iT_{10} - T_{11})$ and $T_{z\bar{z}} = T_{\bar{z}z} = \frac{1}{4}(T_{00} + T_{11}) = \frac{1}{4}T_\mu^\mu$. The conservation law $\delta^{\alpha\mu}\partial_\alpha T_{\mu\nu} = 0$ gives two relations, $\partial_{\bar{z}}T_{zz} + \partial_z T_{\bar{z}\bar{z}} = 0$ and $\partial_z T_{z\bar{z}} + \partial_{\bar{z}} T_{\bar{z}z} = 0$. Using the traceless condition $T_{zz} = T_{\bar{z}\bar{z}} = 0$, these imply

$$\partial_{\bar{z}}T_{zz} = 0 \quad \text{and} \quad \partial_z T_{\bar{z}\bar{z}} = 0. \quad (\text{A.16})$$

Thus we only have holomorphic and anti-holomorphic dependences

$$T(z) \equiv T_{zz}(z) \quad \text{and} \quad \bar{T}(\bar{z}) = T_{\bar{z}\bar{z}}(\bar{z}). \quad (\text{A.17})$$

A.4 Quantum Aspects

So far our discussion has been entirely classical. We now turn to quantum theory. To eliminate any infrared divergences, we compactify the space coordinate, $x^1 \equiv x^1 + 2\pi$. This defines a cylinder in the x^1, x^0 coordinates. Next we consider the conformal map $\zeta \rightarrow z = \exp\zeta = \exp(x^0 + ix^1)$ that maps the cylinder to the complex plane coordinatized by z , see Fig. A.1. To build up a quantum theory of conformal fields on the z -plane, we will need to realize the operators that implement conformal mappings on the plane. The integral of the component of the current orthogonal to an "equal-time" (constant radius) surface becomes $\int j_0(x)dx \rightarrow \int j_r(\theta)d\theta$. Thus we should take

$$Q = \frac{1}{2\pi i} \oint \left(dz T(z) \epsilon(z) + d\bar{z} \bar{T}(\bar{z}) \bar{\epsilon}(\bar{z}) \right) \quad (\text{A.18})$$

as the conserved charge.

The variation of any field is given by the "equal-time" commutator with the charge (A.18),

$$\delta_{\epsilon, \bar{\epsilon}} \Phi(w, \bar{w}) = \frac{1}{2\pi i} \oint \left[dz T(z), \Phi(w, \bar{w}) \right] + \left[d\bar{z} \bar{T}(\bar{z}) \bar{\epsilon}(\bar{z}), \Phi(w, \bar{w}) \right]. \quad (\text{A.19})$$

In parallel with time ordered functional integral formulation we define the radial ordering operation R as

$$R(A(z)B(w)) = \begin{cases} A(z)B(w) & |z| > |w| \\ B(w)A(z) & |w| > |z| \end{cases} \quad (\text{A.20})$$

The equal-time commutator of a local operator A with the spatial integral of an operator B will become the contour integral of the radially ordered product,

$$\left[\int dx B, A \right]_{E.T.} \rightarrow \oint dz R(B(z)A(w)). \quad (\text{A.21})$$

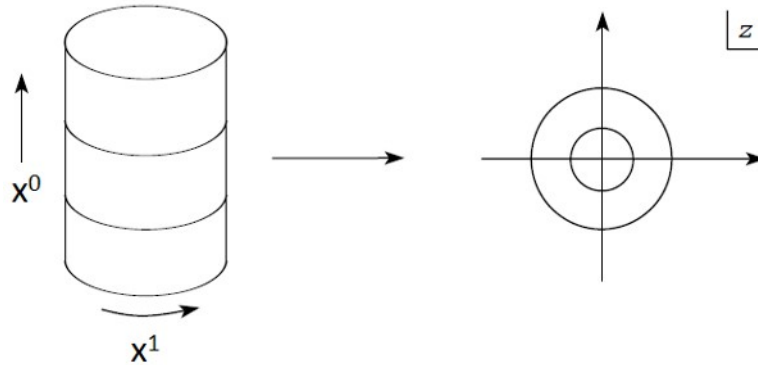


FIGURE A.1: Map of the cylinder to the plane

We may thus rewrite (A.19) in the form

$$\begin{aligned}
\delta_{\epsilon, \bar{\epsilon}} \Phi(w, \bar{w}) &= \frac{1}{2\pi i} \left(\oint_{|z| > |w|} - \oint_{|z| < |w|} \right) \left(dz \epsilon(z) R(T(z) \Phi(w, \bar{w})) \right. \\
&\quad \left. + d\bar{z} \bar{\epsilon}(\bar{z}) R(\bar{T}(\bar{z}) \Phi(w, \bar{w})) \right) \\
&= \frac{1}{2\pi i} \oint \left(dz \epsilon(z) R(T(z) \Phi(w, \bar{w})) + d\bar{z} \bar{\epsilon}(\bar{z}) R(\bar{T}(\bar{z}) \Phi(w, \bar{w})) \right) \\
&= h \partial \epsilon(w) \Phi(w, \bar{w}) + \epsilon(w) \partial \Phi(w, \bar{w}) + \bar{h} \bar{\partial} \bar{\epsilon}(\bar{w}) \Phi(w, \bar{w}) \\
&\quad + \bar{\epsilon}(\bar{w}) \bar{\partial} \Phi(w, \bar{w}),
\end{aligned} \tag{A.22}$$

where in the last line we have substituted the desired result, i.e. the result of the transformation (A.8) in the case of infinitesimal $f(z) = z + \epsilon(z)$. In order that the charge (A.18) induce the correct infinitesimal conformal transformations, we infer that the short distance singularities of T and \bar{T} with Φ should be

$$\begin{aligned}
R(T(z) \Phi(w, \bar{w})) &= \frac{h}{(z-w)^2} \Phi(w, \bar{w}) + \frac{1}{z-w} \partial_w \Phi(w, \bar{w}) + \dots \\
R(\bar{T}(\bar{z}) \Phi(w, \bar{w})) &= \frac{\bar{h}}{(\bar{z}-\bar{w})^2} \Phi(w, \bar{w}) + \frac{1}{\bar{z}-\bar{w}} \partial_{\bar{w}} \Phi(w, \bar{w}) + \dots
\end{aligned} \tag{A.23}$$

From now on we shall drop R symbol and remember that we are working with radially ordered products. The above equations encodes the conformal transformation properties of a primary field Φ . They are equivalent to canonical commutators of the modes of the fields, for further research look at ref.

A.5 Conformal Ward Identities

Ward identities are generally identities satisfied by correlation functions as a reflection of symmetries possessed by a theory.

We consider insertions of operators at points w_1 and w_2 as in Fig. A.2, and perform a conformal transformation in the interior of the region bounded by the z contour by line integrating $\epsilon(z)T(z)$ ² around it. The result is thus

$$\begin{aligned}
&\left\langle \oint \frac{dz}{2\pi i} \epsilon(z) T(z) \Phi_1(w_1, \bar{w}_1) \Phi_n(w_n, \bar{w}_n) \right\rangle \\
&= \left\langle \oint \frac{dz}{2\pi i} \epsilon(z) T(z) \Phi_1(w_2, \bar{w}_2) \Phi_2 \right\rangle + \left\langle \Phi_1(w_1, \bar{w}_1) \oint \frac{dz}{2\pi i} \epsilon(z) T(z) \Phi_2 \right\rangle \\
&= \langle \delta_\epsilon \Phi_1(w_1, \bar{w}_1) \Phi(w_2, \bar{w}_2) \rangle + \langle \Phi_1(w_1, \bar{w}_1) \delta_\epsilon \Phi(w_2, \bar{w}_2) \rangle.
\end{aligned} \tag{A.24}$$

In the last line we have used the infinitesimal transformation property

$$\delta_\epsilon \Phi = \oint \frac{dz}{2\pi i} \epsilon(z) T(z) \Phi(w, \bar{w}) = (\epsilon(w) \partial + h \partial \epsilon(w)) \Phi(w, \bar{w}), \tag{A.25}$$

encoded in the operator product expansion (A.23).

²The same applies for $\bar{\epsilon}(\bar{z})\bar{T}(\bar{z})$ since the right and left movers can be treated as independent.

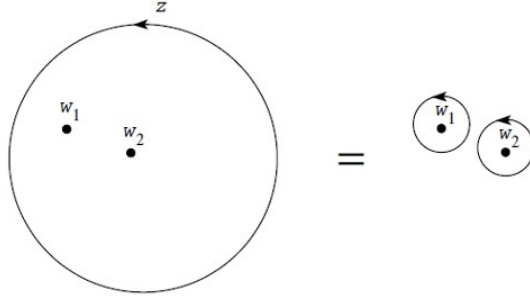


FIGURE A.2: Caption

Since (A.24) is true for arbitrary $\epsilon(z)$ and $\oint d\bar{z}T(z) = 0$, we can write an unintegrated form of the conformal Ward identities,

$$\begin{aligned} & \langle T(z)\Phi_1(w_1, \bar{w}_1)\Phi_2(w_2, \bar{w}_2) \rangle \\ &= \sum_{j=1}^2 \left(\frac{h_j}{(z-w_j)^2} + \frac{1}{z-w_j} \frac{\partial}{\partial w_j} \right) \langle \Phi_1(w_1, \bar{w}_1)\Phi_2(w_2, \bar{w}_2) \rangle. \end{aligned} \quad (\text{A.26})$$

A.6 The Central Charge

Not all fields satisfy the simple transformation property (A.8) under conformal transformations. A secondary field is any field that has higher than the double pole singularity (A.23) in its operator product expansion with T or \bar{T} . An example of such kind of a field is the stress-energy tensor itself.

For any CFT, T has weight $(h, \bar{h}) = (2, 0)$. The reason for this is simple: $T_{\mu\nu}$ has dimension $\Delta = 2$ because we obtain the energy by integrating over space. It has spin $s = 2$ because it is a symmetric 2-tensor. But these two pieces of information are equivalent to the statement that T is an operator of weight $(2, 0)$. Similarly, \bar{T} has weight $(0, 2)$. This means that

$$T(z)T(w) = \dots + \frac{2T}{(z-w)^2} + \frac{\partial T}{z-w} + \dots \quad (\text{A.27})$$

and similar for $\bar{T}\bar{T}$. Moreover, each term has dimension $\Delta = 4$, any operators that appear on the right-hand-side must be of the form $\mathcal{O}_n/(z-w)^n$ where $\Delta[\mathcal{O}_n] = 4 - n$. But, in a unitary CFT there are no operator with $h, \bar{h} < 0$. So the most singular term that we can have is of order $(z-w)^{-4}$. Such a term must be multiplied by a constant. We write³,

$$T(z)T(w) = \frac{c/2}{(z-w)^4} + \frac{2T}{(z-w)^2} + \frac{\partial T}{z-w} + \dots \quad (\text{A.28})$$

and similarly for $\bar{T}(\bar{z})\bar{T}(\bar{w})$ with constant \bar{c} .

The constants c and \bar{c} are called the *central charges*. Sometimes they are referred to as left-moving and right-moving central charges. They somehow measure

³We did not include a $(z-w)^{-3}$ term due to the fact that the operator expansion product should be invariant under $z \leftrightarrow w$. These operator equations are taken to be radially(time)-ordered $T(z)T(w) = T(w)T(z)$.

the number of degrees of freedom in the CFT. For example, if we consider D non-interacting free scalar fields, we would get $c = \bar{c} = D$.

In general, the infinitesimal transformation law for $T(z)$ ⁴ induced by (A.28) is

$$\delta_\epsilon T(z) = \epsilon(z)\partial T(z) + 2\partial\epsilon(z)T(z) + \frac{c}{12}\partial^3\epsilon(z) \quad (\text{A.29})$$

It can be integrated to give

$$T(z) \rightarrow (\partial f)^2 T(f(z)) + \frac{c}{12} S(f, z) \quad (\text{A.30})$$

under $z \rightarrow f(z)$, where the quantity

$$S(f, z) = \frac{\partial_z f \partial_z^3 f - \frac{3}{2}(\partial_z^2 f)^2}{(\partial_z f)^2} \quad (\text{A.31})$$

is known as the Schwarzian derivative.

⁴This can be seen by performing the procedure of paragraph A.4 but in reverse.

Bibliography

- [1] Ibrahim Akal et al. “Holographic moving mirrors”. In: *Classical and Quantum Gravity* 38.22 (2021), p. 224001. DOI: [10.1088/1361-6382/ac2c1b](https://doi.org/10.1088/1361-6382/ac2c1b). URL: <https://doi.org/10.1088/1361-6382/ac2c1b>.
- [2] Ibrahim Akal et al. “Zoo of holographic moving mirrors”. In: *Journal of High Energy Physics* 2022.8 (2022). DOI: [10.1007/jhep08\(2022\)296](https://doi.org/10.1007/jhep08(2022)296). URL: [https://doi.org/10.1007/jhep08\(2022\)296](https://doi.org/10.1007/jhep08(2022)296).
- [3] Ahmed Almheiri, Xi Dong, and Daniel Harlow. “Bulk locality and quantum error correction in AdS/CFT”. In: *Journal of High Energy Physics* 2015.4 (2015). DOI: [10.1007/jhep04\(2015\)163](https://doi.org/10.1007/jhep04(2015)163). URL: [https://doi.org/10.1007/jhep04\(2015\)163](https://doi.org/10.1007/jhep04(2015)163).
- [4] Ning Bao et al. “de Sitter space as a tensor network: Cosmic no-hair, complementarity, and complexity”. In: *Physical Review D* 96.12 (2017). DOI: [10.1103/PhysRevD.96.123536](https://doi.org/10.1103/PhysRevD.96.123536). URL: <https://doi.org/10.1103/PhysRevD.96.123536>.
- [5] Alek Bedroya and Cumrun Vafa. “Trans-Planckian Censorship and the Swampland”. In: *Journal of High Energy Physics* 2020.9 (2020). DOI: [10.1007/jhep09\(2020\)123](https://doi.org/10.1007/jhep09(2020)123). URL: [https://doi.org/10.1007/jhep09\(2020\)123](https://doi.org/10.1007/jhep09(2020)123).
- [6] A. A. Belavin, Alexander M. Polyakov, and A. B. Zamolodchikov. “Infinite Conformal Symmetry in Two-Dimensional Quantum Field Theory”. In: *Nucl. Phys. B* 241 (1984). Ed. by I. M. Khalatnikov and V. P. Mineev, pp. 333–380. DOI: [10.1016/0550-3213\(84\)90052-X](https://doi.org/10.1016/0550-3213(84)90052-X).
- [7] Eugenio Bianchi and Matteo Smerlak. “Entanglement entropy and negative energy in two dimensions”. In: *Physical Review D* 90.4 (2014). DOI: [10.1103/PhysRevD.90.041904](https://doi.org/10.1103/PhysRevD.90.041904). URL: <https://doi.org/10.1103/PhysRevD.90.041904>.
- [8] Robert Brandenberger and Vahid Kamali. “Unitarity problems for an effective field theory description of early universe cosmology”. In: *Eur. Phys. J. C* 82.9 (2022), p. 818. DOI: [10.1140/epjc/s10052-022-10783-2](https://doi.org/10.1140/epjc/s10052-022-10783-2). arXiv: [2203.11548](https://arxiv.org/abs/2203.11548) [hep-th].
- [9] Susanne C. Brenner and L. Ridgway. *The Mathematical Theory of Finite Element Methods*. Springer New York, NY, 2010. DOI: <https://doi.org/10.1007/978-0-387-75934-0>.
- [10] Richard Brower et al. “Lattice 4 field theory on Riemann manifolds: Numerical tests for the 2D Ising CFT on S²”. In: *Physical Review D* 98 (July 2018). DOI: [10.1103/PhysRevD.98.014502](https://doi.org/10.1103/PhysRevD.98.014502).
- [11] Richard C. Brower et al. “Lattice Dirac fermions on a simplicial Riemannian manifold”. In: *Physical Review D* 95.11 (2017). DOI: [10.1103/PhysRevD.95.114510](https://doi.org/10.1103/PhysRevD.95.114510). URL: <https://doi.org/10.1103/PhysRevD.95.114510>.

- [12] Richard C. Brower et al. “Lattice setup for quantum field theory in AdS₂”. In: *Physical Review D* 103.9 (2021). DOI: [10.1103/physrevd.103.094507](https://doi.org/10.1103/physrevd.103.094507). URL: <https://doi.org/10.1103%2Fphysrevd.103.094507>.
- [13] Richard C. Brower et al. *Quantum Finite Elements for Lattice Field Theory*. 2016. arXiv: [1601.01367](https://arxiv.org/abs/1601.01367) [hep-lat].
- [14] JAMES A. CADZOW. “Discrete calculus of variations”. In: *International Journal of Control* 11.3 (1970), pp. 393–407. DOI: [10.1080/00207177008905922](https://doi.org/10.1080/00207177008905922). eprint: <https://doi.org/10.1080/00207177008905922>. URL: <https://doi.org/10.1080/00207177008905922>.
- [15] Pasquale Calabrese and John Cardy. “Entanglement entropy and conformal field theory”. In: *Journal of Physics A: Mathematical and Theoretical* 42.50 (2009), p. 504005. DOI: [10.1088/1751-8113/42/50/504005](https://doi.org/10.1088/1751-8113/42/50/504005). URL: <https://doi.org/10.1088%2F1751-8113%2F42%2F50%2F504005>.
- [16] Robert D. Carlitz and Raymond S. Willey. “Reflections on moving mirrors”. In: *Phys. Rev. D* 36 (8 1987), pp. 2327–2335. DOI: [10.1103/PhysRevD.36.2327](https://doi.org/10.1103/PhysRevD.36.2327). URL: <https://link.aps.org/doi/10.1103/PhysRevD.36.2327>.
- [17] Sean Carroll. *Spacetime and Geometry: An Introduction to General Relativity*. Benjamin Cummings, 2003. ISBN: 0805387323. URL: <http://www.amazon.com/Spacetime-Geometry-Introduction-General-Relativity/dp/0805387323>.
- [18] Jordan Cotler and Kristan Jensen. *Isometric evolution in de Sitter quantum gravity*. 2023. arXiv: [2302.06603](https://arxiv.org/abs/2302.06603) [hep-th].
- [19] Jordan Cotler and Andrew Strominger. *The Universe as a Quantum Encoder*. 2022. arXiv: [2201.11658](https://arxiv.org/abs/2201.11658) [hep-th].
- [20] Jordan Cotler et al. “Quantum causal influence”. In: *Journal of High Energy Physics* 2019.7 (2019). DOI: [10.1007/jhep07\(2019\)042](https://doi.org/10.1007/jhep07(2019)042). URL: <https://doi.org/10.1007%2Fjhep07%282019%29042>.
- [21] Richard Courant, Kurt Otto Friedrichs, and Hans Lewy. “On the Partial Difference Equations, of Mathematical Physics”. In: 2015.
- [22] Michael Creutz. *Quarks, Gluons and Lattices*. Oxford University Press, 1983. ISBN: 978-1-00-929039-5, 978-1-00-929038-8, 978-1-00-929037-1, 978-0-521-31535-7. DOI: [10.1017/9781009290395](https://doi.org/10.1017/9781009290395).
- [23] Bianca Dittrich and Philipp A. Höhn. “Constraint analysis for variational discrete systems”. In: *Journal of Mathematical Physics* 54.9 (2013), p. 093505. DOI: [10.1063/1.4818895](https://doi.org/10.1063/1.4818895). URL: <https://doi.org/10.1063%2F1.4818895>.
- [24] Alexandre Ern and Jean-Luc Guermond. *Theory and Practice of Finite Elements*. Springer New York, NY, 2010. DOI: <https://doi.org/10.1007/978-1-4757-4355-5>.
- [25] Charles Evans. “Quantized scalar fields under the influence of moving mirror and anisotropic curved spacetime”. PhD thesis. University of North Carolina at Chapel Hill, 2011. DOI: <https://doi.org/10.17615/a075-pg88>.
- [26] Lawrence C. Evans. *Partial differential equations*. Providence, R.I.: American Mathematical Society, 2010. ISBN: 9780821849743 0821849743.
- [27] Thomas M. Fiola et al. “Black hole thermodynamics and information loss in two dimensions”. In: *Physical Review D* 50.6 (1994), pp. 3987–4014. DOI: [10.1103/physrevd.50.3987](https://doi.org/10.1103/physrevd.50.3987). URL: <https://doi.org/10.1103%2Fphysrevd.50.3987>.

- [28] Brendan Z Foster and Ted Jacobson. “Quantum field theory on a growing lattice”. In: *Journal of High Energy Physics* 2004.08 (2004), pp. 024–024. DOI: [10.1088/1126-6708/2004/08/024](https://doi.org/10.1088/1126-6708/2004/08/024). URL: <https://doi.org/10.1088/1126-6708/2004/08/024>.
- [29] R. Friedberg, Tsung Dao Lee, and Hai-Cang Ren. “Fermion Field on a Random Lattice”. In: *Progress of Theoretical Physics Supplement* 86 (Jan. 1986), pp. 322–328. ISSN: 0375-9687. DOI: [10.1143/PTPS.86.322](https://doi.org/10.1143/PTPS.86.322). eprint: <https://academic.oup.com/ptps/article-pdf/doi/10.1143/PTPS.86.322/5327977/86-322.pdf>. URL: <https://doi.org/10.1143/PTPS.86.322>.
- [30] S. A. Fulling and P. C. W. Davies. *Radiation from a moving mirror in two dimensional space-time: conformal anomaly*. 1976. DOI: <https://doi.org/10.1098/rspa.1976.0045>.
- [31] Murray Gell-Mann and James B. Hartle. *Time Symmetry and Asymmetry in Quantum Mechanics and Quantum Cosmology*. 2005. arXiv: [gr-qc/9304023](https://arxiv.org/abs/gr-qc/9304023) [gr-qc].
- [32] Paul Ginsparg. *Applied Conformal Field Theory*. 1988. arXiv: [hep-th/9108028](https://arxiv.org/abs/hep-th/9108028) [hep-th].
- [33] Alan H. Guth. “Inflationary universe: A possible solution to the horizon and flatness problems”. In: *Phys. Rev. D* 23 (2 1981), pp. 347–356. DOI: [10.1103/PhysRevD.23.347](https://doi.org/10.1103/PhysRevD.23.347). URL: <https://link.aps.org/doi/10.1103/PhysRevD.23.347>.
- [34] Daniel Harlow and Patrick Hayden. “Quantum computation vs. firewalls”. In: *Journal of High Energy Physics* 2013.6 (2013). DOI: [10.1007/jhep06\(2013\)085](https://doi.org/10.1007/jhep06(2013)085). URL: [https://doi.org/10.1007/jhep06\(2013\)085](https://doi.org/10.1007/jhep06(2013)085).
- [35] J. B. Hartle and S. W. Hawking. “Wave function of the Universe”. In: *Phys. Rev. D* 28 (12 1983), pp. 2960–2975. DOI: [10.1103/PhysRevD.28.2960](https://doi.org/10.1103/PhysRevD.28.2960). URL: <https://link.aps.org/doi/10.1103/PhysRevD.28.2960>.
- [36] Thomas Hartman. *Lectures on Quantum Gravity and Black Holes*. 2015.
- [37] S. W. Hawking. “Breakdown of predictability in gravitational collapse”. In: *Phys. Rev. D* 14 (10 1976), pp. 2460–2473. DOI: [10.1103/PhysRevD.14.2460](https://doi.org/10.1103/PhysRevD.14.2460). URL: <https://link.aps.org/doi/10.1103/PhysRevD.14.2460>.
- [38] S. W. Hawking. “Particle creation by black holes”. In: 43 (1975), pp. 199–220. DOI: <https://doi.org/10.1007/BF02345020>.
- [39] Stephen Hawking, Juan Maldacena, and Andrew Strominger. “DeSitter entropy, quantum entanglement and ADS/CFT”. In: *Journal of High Energy Physics* 2001.05 (2001), pp. 001–001. DOI: [10.1088/1126-6708/2001/05/001](https://doi.org/10.1088/1126-6708/2001/05/001). URL: <https://doi.org/10.1088/1126-6708/2001/05/001>.
- [40] Christoph Holzhey, Finn Larsen, and Frank Wilczek. “Geometric and renormalized entropy in conformal field theory”. In: *Nuclear Physics B* 424.3 (1994), pp. 443–467. DOI: [10.1016/0550-3213\(94\)90402-2](https://doi.org/10.1016/0550-3213(94)90402-2). URL: [https://doi.org/10.1016/0550-3213\(94\)90402-2](https://doi.org/10.1016/0550-3213(94)90402-2).
- [41] Gary T Horowitz and Juan Maldacena. “The black hole final state”. In: *Journal of High Energy Physics* 2004.02 (2004), pp. 008–008. DOI: [10.1088/1126-6708/2004/02/008](https://doi.org/10.1088/1126-6708/2004/02/008). URL: <https://doi.org/10.1088/1126-6708/2004/02/008>.
- [42] Jon Häggblad and Olof Runborg. “Accuracy of staircase approximations in finite-difference methods for wave propagation”. In: *Numerische Mathematik* 128 (Dec. 2014), pp. 741–771. DOI: [10.1007/s00211-014-0625-1](https://doi.org/10.1007/s00211-014-0625-1).

- [43] Philipp A. Höhn. “Quantization of systems with temporally varying discretization. I. Evolving Hilbert spaces”. In: *Journal of Mathematical Physics* 55.8 (2014), p. 083508. DOI: [10.1063/1.4890558](https://doi.org/10.1063/1.4890558). URL: <https://doi.org/10.1063%2F1.4890558>.
- [44] Philipp A. Höhn. “Quantization of systems with temporally varying discretization. II. Local evolution moves”. In: *Journal of Mathematical Physics* 55.10 (2014), p. 103507. DOI: [10.1063/1.4898764](https://doi.org/10.1063/1.4898764). URL: <https://doi.org/10.1063%2F1.4898764>.
- [45] George Jaroszkiewicz and Keith Norton. “Principles of discrete time mechanics: I. Particle systems”. In: *Journal of Physics A: Mathematical and General* 30.9 (1997), pp. 3115–3144. DOI: [10.1088/0305-4470/30/9/022](https://doi.org/10.1088/0305-4470/30/9/022). URL: <https://doi.org/10.1088%2F0305-4470%2F30%2F9%2F022>.
- [46] George Jaroszkiewicz and Keith Norton. “Principles of discrete time mechanics: II. Classical field theory”. In: *Journal of Physics A: Mathematical and General* 30.9 (1997), pp. 3145–3163. DOI: [10.1088/0305-4470/30/9/023](https://doi.org/10.1088/0305-4470/30/9/023). URL: <https://doi.org/10.1088%2F0305-4470%2F30%2F9%2F023>.
- [47] Daniel Kapec, Ana-Maria Raclariu, and Andrew Strominger. “Area, entanglement entropy and supertranslations at null infinity”. In: *Classical and Quantum Gravity* 34.16 (2017), p. 165007. DOI: [10.1088/1361-6382/aa7f12](https://doi.org/10.1088/1361-6382/aa7f12). URL: <https://doi.org/10.1088%2F1361-6382%2Faa7f12>.
- [48] Raj Sinai Kunkolienkar and Kinjal Banerjee. “Towards a dS/MERA correspondence”. In: *International Journal of Modern Physics D* 26.13 (2017), p. 1750143. DOI: [10.1142/s0218271817501437](https://doi.org/10.1142/s0218271817501437). URL: <https://doi.org/10.1142%2Fs0218271817501437>.
- [49] Wing Kam Liu, Shaofan Li, and Harold Park. *Eighty Years of the Finite Element Method: Birth, Evolution, and Future*. 2021. arXiv: [2107.04960](https://arxiv.org/abs/2107.04960) [math.NA].
- [50] Peter A. Loeb and M. P. H. Wolff. “Nonstandard analysis for the working mathematician”. In: 2000.
- [51] Rafael de la Madrid. “The role of the rigged Hilbert space in quantum mechanics”. In: *European Journal of Physics* 26.2 (2005), pp. 287–312. DOI: [10.1088/0143-0807/26/2/008](https://doi.org/10.1088/0143-0807/26/2/008). URL: <https://doi.org/10.1088%2F0143-0807%2F26%2F2%2F008>.
- [52] Jerome Martin and Robert H. Brandenberger. “Trans-Planckian problem of inflationary cosmology”. In: *Physical Review D* 63.12 (2001). DOI: [10.1103/physrevd.63.123501](https://doi.org/10.1103/physrevd.63.123501). URL: <https://doi.org/10.1103%2Fphysrevd.63.123501>.
- [53] Ashley Milsted and Guifre Vidal. *Geometric interpretation of the multi-scale entanglement renormalization ansatz*. 2018. arXiv: [1812.00529](https://arxiv.org/abs/1812.00529) [hep-th].
- [54] Gert Heinz Müller. *Non-Standard Analysis*. Princeton University Press, 1966.
- [55] Laura Niermann and Tobias J. Osborne. “Holographic networks for (1+1)-dimensional de Sitter space-time”. In: *Physical Review D* 105.12 (2022). DOI: [10.1103/physrevd.105.125009](https://doi.org/10.1103/physrevd.105.125009). URL: <https://doi.org/10.1103%2Fphysrevd.105.125009>.
- [56] Fernando Pastawski et al. “Holographic quantum error-correcting codes: toy models for the bulk/boundary correspondence”. In: *Journal of High Energy Physics* 2015.6 (2015). DOI: [10.1007/jhep06\(2015\)149](https://doi.org/10.1007/jhep06(2015)149). URL: <https://doi.org/10.1007%2Fjhep06%282015%29149>.

- [57] Joseph Polchinski. *String Theory and Black Hole Complementarity*. 1995. arXiv: [hep-th/9507094](https://arxiv.org/abs/hep-th/9507094) [[hep-th](#)].
- [58] Mukund Rangamani and Tadashi Takayanagi. *Holographic Entanglement Entropy*.
- [59] Marcus Spradlin, Andrew Strominger, and Anastasia Volovich. *Les Houches Lectures on De Sitter Space*. 2001. arXiv: [hep-th/0110007](https://arxiv.org/abs/hep-th/0110007) [[hep-th](#)].
- [60] Andy Strominger. *Les Houches Lectures on Black Holes*. 1995. arXiv: [hep-th/9501071](https://arxiv.org/abs/hep-th/9501071) [[hep-th](#)].
- [61] Anna-Karin Tornberg and Björn Engquist. “Consistent boundary conditions for the Yee scheme”. In: *Journal of Computational Physics* 227.14 (2008), pp. 6922–6943. ISSN: 0021-9991. DOI: <https://doi.org/10.1016/j.jcp.2008.03.045>. URL: <https://www.sciencedirect.com/science/article/pii/S0021999108002039>.
- [62] Tatiana V. Voitovich and Stefan Vandewalle. “Barycentric Interpolation and Exact Integration Formulas for the Finite Volume Element Method”. In: *AIP Conference Proceedings* 1048.1 (2008), pp. 575–579. DOI: [10.1063/1.2990990](https://doi.org/10.1063/1.2990990). eprint: <https://aip.scitation.org/doi/pdf/10.1063/1.2990990>. URL: <https://aip.scitation.org/doi/abs/10.1063/1.2990990>.
- [63] Nathan Weiss. “Constraints on Hamiltonian Lattice Formulations of Field Theories in an Expanding Universe”. In: 1985.32 (1985). DOI: [10.1103/PhysRevD.32.3228](https://doi.org/10.1103/PhysRevD.32.3228). URL: <https://doi.org/10.1103/PhysRevD.32.3228>.
- [64] Wikipedia contributors. *Cauchy surface* — *Wikipedia, The Free Encyclopedia*. [Online; accessed 9-April-2023]. 2022. URL: https://en.wikipedia.org/w/index.php?title=Cauchy_surface&oldid=1117732519.
- [65] Wikipedia contributors. *Fermion doubling* — *Wikipedia, The Free Encyclopedia*. https://en.wikipedia.org/w/index.php?title=Fermion_doubling&oldid=1146705755. [Online; accessed 10-April-2023]. 2023.
- [66] Wikipedia contributors. *Nikolay Bogolyubov* — *Wikipedia, The Free Encyclopedia*. [Online; accessed 10-April-2023]. 2023. URL: https://en.wikipedia.org/w/index.php?title=Nikolay_Bogolyubov&oldid=1148284982.
- [67] Wikipedia contributors. *Triangulation (topology)* — *Wikipedia, The Free Encyclopedia*. [Online; accessed 9-April-2023]. 2023. URL: [https://en.wikipedia.org/w/index.php?title=Triangulation_\(topology\)&oldid=1145406437](https://en.wikipedia.org/w/index.php?title=Triangulation_(topology)&oldid=1145406437).
- [68] Frank Wilczek. *Quantum Purity at a Small Price: Easing a Black Hole Paradox*. 1993. arXiv: [hep-th/9302096](https://arxiv.org/abs/hep-th/9302096) [[hep-th](#)].
- [69] Lin Zhang. “Dirac Delta Function of Matrix Argument”. In: *International Journal of Theoretical Physics* 60.7 (2020), pp. 2445–2472. DOI: [10.1007/s10773-020-04598-8](https://doi.org/10.1007/s10773-020-04598-8). URL: <https://doi.org/10.1007/s10773-020-04598-8>.